

**Hydrogen Production via a Commercially Ready
Inorganic membrane Reactor**

**Final Technical Report
Reporting Period: October 01, 2003 to June 30, 2007**

**Paul K. T. Liu
Project Director**

October 15, 2007

**PREPARED FOR THE UNITED STATES
DEPARTMENT OF ENERGY
Under Cooperative Agreement
No. DE-FC26-03NT41852**

**By
MEDIA AND PROCESS TECHNOLOGY, INC.
1155 William Pitt Way
Pittsburgh, PA 15238**

Disclaimer

This report was prepared as an account of work sponsored by an agency of the United States Government. Neither the United States Government nor any agency thereof, nor any of their employees, makes any warranty, express or implied, or assumes any legal liability or responsibility for the accuracy, completeness, or usefulness of any information, apparatus, product, or process disclosed, or represents that its use would not infringe privately owned rights. Reference herein to any specific commercial product, process, or service by trade name, trademark, manufacturer, or otherwise does not necessarily constitute or imply its endorsement, recommendation, or favoring by the United States Government or any agency thereof. The views and opinions of authors expressed herein do not necessarily state or reflect those of the United States Government or any agency thereof.

ABSTRACT

It has been known that use of the hydrogen selective membrane as a reactor (MR) could potentially improve the efficiency of the water shift reaction (WGS), one of the least efficient unit operations for production of high purity hydrogen from syngas. However, no membrane reactor technology has been reduced to industrial practice thus far, in particular for a large-scale operation. This implementation and commercialization barrier is attributed to the lack of a commercially viable hydrogen selective membrane with (i) material stability under the application environment and (ii) suitability for large-scale operation. Thus, in this project, we have focused on (i) the deposition of the hydrogen selective carbon molecular sieve (CMS) membrane we have developed on commercially available membranes as substrate, and (ii) the demonstration of the economic viability of the proposed WGS-MR for hydrogen production from coal-based syngas.

The commercial stainless steel (SS) porous substrate (i.e., ZrO₂/SS from Pall Corp.) was evaluated comprehensively as the 1st choice for the deposition of the CMS membrane for hydrogen separation. The CMS membrane synthesis protocol we developed previously for the ceramic substrate was adapted here for the stainless steel substrate. Unfortunately no successful hydrogen selective membranes had been prepared during Yr I of this project. The characterization results indicated two major sources of defect present in the SS substrate, which may have contributed to the poor CMS membrane quality. Near the end of the project period, an improved batch of the SS substrate (as the 2nd generation product) was received from the supplier. Our characterization results confirm that leaking of the crimp boundary no longer exists. However, the thermal stability of the ZrO₂/SS substrate through the CMS membrane preparation condition must be re-evaluated in the future.

In parallel with the SS membrane activity, the preparation of the CMS membranes supported on our commercial ceramic membrane for large-scale applications, such as coal-based power generation/hydrogen production, was also continued. A significant number (i.e., 98) of full-scale membrane tubes have been produced with an on-spec ratio of >76% during the first production trial. In addition, we have verified the functional performance and material stability of this hydrogen selective CMS membrane with a hydrocracker purge gas stream at a refinery pilot testing facility. No change in membrane performance was noted over the >100 hrs of testing conducted in the presence of >30% H₂S, >5,000 ppm NH₃ (estimated), and heavy hydrocarbons on the order of 25%. The excellent stability of our hydrogen selective CMS membrane opens the door for its use in WGS-MR with a significantly reduced requirement of the feedstock pretreatment.

One of the well-known technical barriers for ceramic membranes is its scale up potential. Under this project, we initiated the fabrication of a prototype ceramic membrane module which can be qualified for the proposed application temperature (200-300°C). An innovative full-scale membrane module has been designed, which can potentially deliver >20 to 30 m²/module suitable for large-scale applications. A prototype bundle (3" diameter and 35"L) has been prepared, which passes the temperature stability requirement. It also meets the burst pressure of 500-750 psi. We believe that additional improvement of this prototype module can potentially upgrade its burst pressure to 1000 to 1500 psi range.

Single stage low-temperature-water-gas-shift (WGS-LTS) via a membrane reactor (MR) process using our hydrogen selective CMS membrane was studied through both mathematical simulation and bench-top experimental verification in this project. The results from the experimental study verified satisfactorily the simulation results. According to our simulation of the WGS reaction, the WGS-LTS-MR could require a reactor size that is 10 to >55% smaller than the comparable conventional reactor for a CO conversion of 80 to 90%. In addition, the CO contaminant level in the hydrogen produced via MR ranges from 1,000 to 4,000 ppm vs 40,000 to >70,000 ppm via the conventional reactor. It is obvious that the WGS-MR we proposed offers significantly improved efficiency over existing WGS reactor.

Using the mathematical model which was experimentally verified, we undertook a preliminary process simulation for hydrogen production from coal gasifier off-gas. First of all, since our CMS membrane proved to be stable in the presence of H_2S , NH_3 , and other contaminants at the LTS temperature range, WGS reaction in the presence of sulfur can be accomplished with the proposed MR with the use of the Co/MoS₂ catalyst. This catalyst has been employed industrially as a sour gas shift catalyst. Our process simulation with the Co/MoS₂ catalyst has demonstrated that a nearly complete CO conversion (i.e., 99+%) can be accomplished. We estimate that ~90% of the hydrogen produced from the H_2+CO in the coal gasifier off-gas can be recovered via our proposed WGS-MR process. The produced H_2 purity level ranges from 80 to 92% for membrane H_2/CO_2 selectivities of 10 and 25, respectively. If a H_2 purity of 95% is required, the hydrogen recovery ratio will drop to ~80% for the membrane with $H_2/CO_2=25$. Our process simulation supports the proposed WGS-MR developed with the conventional Zn/Cu catalyst is applicable to the WGS-MR with the Co/MoS₂ catalyst. No cost minimization has been taken into consideration under this project.

The fringe benefit of the use of the proposed WGS-MR is the reduced burden in both pre- and post-treatment for hydrogen production from coal. The pretreatment can be streamlined to the particulate removal only. Since no sulfur removal is required prior to the WGS step, no hot gas clean-up (HGCP) is necessary. Further, no excess water beyond the stoichiometric requirement for CO conversion is necessary; thus, the sensible heat available from the gasifier off-gas can be recovered as much as possible. Finally, operation at this mild temperature (~250°C) offers the advantage of the use of the standard hardware and material for the proposed MR. No post treatment is required for hydrogen production for power generation or as chemicals for sale. Since the delivery of CO to <<10 ppm ready for PEM fuel cell applications is not practical with our technology, post treatment with preferential oxidation (PROX) for the elimination of trace CO is necessary. Further, the CO contaminant level from our WGS-MR is 20-30 ppm; thus, existing technology, such as preferential oxidation (PROX), can be implemented economically and reliably. Finally, hydrogen product separation is integrated into the WGS reactor; no separate hydrogen separation step is required. The CO₂-rich reject stream is available at high pressure and can be sent for sequestration.

In short, besides the improvement of the WGS reaction efficiency, the membrane reactor (MR) we proposed can reduce the capital and operating cost significantly for hydrogen

production from the coal gasifier via process intensification before, during and after the WGS reaction. Using the economics published in the literature as the base case, our proposed WGS-MR with the sulfide catalyst can deliver production economics comparable to existing hydrogen production cost from methane steam reforming. More importantly, our proposed process scheme does not rely on the development of the high temperature advanced membrane technology to justify the production economics as proposed in the literature. Preparation of the proposed hydrogen selective CMS membrane for field testing is recommended as the next step.

TABLE OF CONTENTS

1.	INTRODUCTION	1
2.	EXECUTIVE SUMMARY	3
3.	EXPERIMENTAL.....	6
3.1	Preparation of CMS Membrane on Commercial Stainless Steel Substrate	6
3.2	Full Scale Membrane and Module Preparation	6
3.3	Mathematical Modeling of Water Gas Shift Reaction via Membrane Reactor	7
3.4	Process Simulation for Coal Gasifier Off-gas	8
3.5	Potential Process Schemes Available in Literature for Hydrogen Production from Coal Gasification Process.	8
4	RESULTS AND DISCUSSION.....	10
4.1	Preparation of CMS Membrane on Stainless Steel Substrate.....	10
4.2	Full Scale Membrane and Module Production	14
4.3	Mathematical Modeling of Water Gas Shift Reaction via Membrane Reactor	21
4.4	Effect of Operating Variables on WGS-MR Performance	28
4.5	Process Simulation for Coal Gasifier Off-gas	37
4.6	Benchmarking against Other Hydrogen Production Processes	47
5.	CONCLUSIONS.....	55
6.	REFERENCES	60
7.	ACRONYMS.....	61
APPENDIX I	Mathematical Model for Proposed Membrane Reactor for Water-Gas-Shift Reaction	62
APPENDIX II	Material Balance of the Mathematical Model Developed in this Study	65

List of Graphical Materials

Figures

Figure 1	Illustration of the “Crimped Endseal” Region Where Defect Was Identified with Bubble Test.....	11
Figure 2	SEM Photomicrographs of the Cross Section of Inside Tube Surface of ZrO ₂ /stainless steel substrate including ZrO ₂ layer and M&P Al ₂ O ₃	12
Figure 3	SEM photomicrograph of the Cross Section of the ZrO ₂ /Stainless Steel Substrate Provided by the Supplier as the 2 nd Generation Product.....	13
Figure 4	Picture of CMS Membrane Deposited on SS and Ceramic Tubes	13
Figure 5	H ₂ permeance vs. selectivity of full scale membrane tubes prepared during this project period	16
Figure 6	Gas Stream Compositions and Stage Cut and H ₂ Recovery for the VGO Hydrocracker Pilot Test	17
Figure 7	Candle Filter Ceramic Membrane Bundle and Module (bottom) and Patented High Temperature Packing/Seal Design (top) and a Single Element Pilot Scale Module (middle).....	20
Figure 8	Experimental determination of E _a and A based upon ln(k) vs. 1/RT.....	23
Figure 9	LTS-WGS via Our CMS-Based Membrane Reactor: Experimental vs Simulation Results	25
Figure 10	Experimental vs Predicted CO Conversion using a CMS Membrane as a Reactor	26
Figure 11	Effect of Sweep Ratio (as a fraction of the feed flow rate) on the CO Conversion: Experimental vs Predicted. The feed condition used is the same as the one used for Figure 10.	27
Figure 12	Effect of Feed Pressure on the CO Conversion using a CMS-WGS-MR (the feed pressure as indicated, the rest of the condition is presented in text as the base case)	28
Figure 13	Effect of W/F on the CO Conversion (the W/F used as noted, the rest of the operating condition is presented in the text as the base case).....	30
Figure 14	Effect of Sweep Ratio on the CO Conversion (sweep ratio as a fraction of the feed stream as noted, the rest of the condition is presented in the text as the base case)	31

Figure 15	Effect of Feed pressure on the Hydrogen Recovery Ratio (the feed pressures as noted, the rest of the conditions are presented in the text as the base case)....	32
Figure 16	Effect of W/F on Hydrogen Recovery Ratio (the W/F used as noted, the rest of the conditions are presented in the text as the base case).....	33
Figure 17	Effect of Sweep Ratio on Hydrogen Recovery Ratio (the sweep ratio used as indicated, the rest of the conditions are presented in the text as the base case)...	34
Figure 18	Effect of Feed Pressure on the CO Impurity Level in the Hydrogen Recovered (the feed pressure as noted, the rest of the conditions are presented in the text as the base case).....	35
Figure 19	Preliminary Optimization study on the Proposed WGS-MR at 4 (top), 10 (middle) and 40 (bottom) Bar feed Pressure.....	36
Figure 20	CO conversion for Membrane Reactor vs Packed Bed Reactor with W/F as a Parameter for WGS at 280°C with the Use of Sour Gas Shift Catalyst.	39
Figure 21	Hydrogen Recovery in the Membrane Reactor with W/F as a Parameter.....	40
Figure 22	CO Conversion in a Membrane Reactor with Feed Pressure as a Parameter. The feed and operating condition is listed in Sec. 3.	41
Figure 23	Hydrogen Recovery in a Membrane Reactor with the Feed Side Pressure as a Parameter. The rest of the operating condition is listed in Sec. 3.....	42
Figure 24	Residual CO Concentration in Membrane Reactor vs Packed Bed Reactor. Feed pressure is 80 bar, and W/F=1. Other feed and operating condition is listed in Sec. 2.....	43
Figure 25	Hydrogen Purity and CO Contaminant Level for the WGS-MR with A Nearly Complete Conversion of CO and the Use of Nearly Stoichiometric H ₂ O/CO Ratio.	44
Figure 26	Effect of H ₂ /CO ₂ Selectivity on Hydrogen Purity on WGS-MR with Complete CO Conversion.....	45
Figure 27	Production of Hydrogen using Advanced Gasifier, Gas Cleaning, and Membrane Technologies (Case #3).....	48
Figure 28	Production of Hydrogen based upon Case #3 Incorporating Process Features offered by our Proposed WGS/CMS-MR (indicated in red).	51

Figure 29	Overall Process Scheme for Hydrogen Production from Coal Gasifier Off-gas via WGS-MR with Our Hydrogen Selective CMS Membrane	52
-----------	---	----

List of Graphical Materials

Tables

Table 1	Comparison of Gas Permeation for CMS Membranes Deposited on Stainless Steel vs Ceramic Substrate.....	10
Table 2	Qualitative Description of Defects Observed on CMS Membranes Deposited on Stainless Steel Substrate	11
Table 3	Characterization of Full-scale Hydrogen Selective Membrane (30’’L) Produced During this Project Period.....	15
Table 4	Degradation of the CMS Membrane Challenged by the Dead-end Operation and the Restoration of the Original Permeance via Regeneration.	18
Table 5	Experimental Results for Kinetic Parameter Determination	22
Table 6	Membrane Reactor Performance Prediction based upon Ours vs. Literature Kinetic Parameters	24
Table 7	Processes for Hydrogen Production from Coal discussed in the Literature [Ref. 3]	47
Table 8	Process Features of Two Cases (Cases #3 & 7) involving the use of Membranes	47
Table 9	Economic Analysis for Hydrogen from Existing and Advanced Coal Based Process vs from Steam Methane Reforming.....	49

1. INTRODUCTION

Hydrogen production from abundant domestic supplies of coal is one of the attractive avenues for the transformation from the current fossil fuel-based into a hydrogen-based economy. It is well known that a membrane reactor (MR) technology can improve the production efficiency of thermodynamically limited reactions, such as the water gas shift reaction (WGS) involved in the conversion of CO in syngas to hydrogen. However, MR technology has rarely been reduced to industrial practice thus far, in particular for a large scale operation. This implementation barrier is attributed to the lack of a commercially viable hydrogen selective membrane with (i) material stability under the application environment and (ii) suitability for large scale operation. Thus, in this project, we have focused on (i) the deposition of the carbon molecular sieve (CMS)-based hydrogen selective membrane we developed on commercially viable porous substrates, and (ii) the demonstration of the economic viability of the proposed WGS-MR for hydrogen production from coal-based syngas. Both commercially available stainless steel (SS) and ceramic substrates have been explored for the deposition of the CMS membrane for hydrogen separation at an intermediate temperature (150 to 300°C). In addition, we have conducted membrane manufacturing development, module design and construction, and material stability testing under a sulfur and ammonia containing environment. It has been our objective to establish the technology/know-how to fabricate a field test-ready membrane/module by the end of this project period.

In the conventional WGS process, high temperature shift (HTS) is performed as a first stage reactor to convert a majority of the CO, taking the advantage of the enhanced reaction kinetics at a high temperature (i.e., 350 – 450°C). Then the residual CO is sent to the LTS as a polishing step to reduce CO to the level of $\leq 1\%$. Based upon the enhanced efficiency potentially delivered by the MR via the in-situ removal of the reaction products, it is possible to achieve nearly complete CO conversion via a single stage with a low temperature shift (LTS). Thus, the hydrogen production process can be streamlined substantially, since (i) the HTS reactor is no longer needed, and (ii) the enhanced LTS conversion is sufficient for complete CO conversion. More importantly, the pre- and post-treatment burden for the WGS reaction step can be alleviated significantly as a result of the WGS at a low temperature. Finally, since carbon is chemically inert at this reaction temperature and most likely (as demonstrated by us) sulfur resistant, our CMS-based membrane can open the door for the use of the sulfide catalyst, instead of the conventional Cu/Zn-based catalyst. As a result hot gas clean-up (HGCP) pretreatment can be eliminated. In summary, the introduction of the CMS-based hydrogen selective membrane as a MR could offer tremendous process and economic advantages.

With the successfully completion of the development of a commercially viable membrane and the demonstration of the technical and process viability of the WGS-MR, we then moved our focus to the evaluation of the hydrogen production economics based on the streamlined hydrogen production process. A mathematical model for WGS-MR was developed which was experimentally verified using simulated coal gasifier off-gas. Our simulation demonstrates that a membrane reactor can offer the advantages below for hydrogen production from coal:

- A nearly complete conversion of CO (i.e., >99%) can be achieved; thus, minimal or no post treatment is required to meet the CO contaminant spec for hydrogen products;

- A near stoichiometric steam-to-CO ratio is adequate to achieve nearly complete CO conversion; thus, the power generation efficiency can be maximized with the minimum addition of water/steam.
- Hydrogen product separation can be integrated into the WGS reactor; thus, no separate hydrogen separation step is required;
- After hydrogen separation, CO₂-rich residual stream can be sent for sequestration;
- The thermal management required to deal with the reaction exotherm can be integrated into part of the WGS/MR reactor.

Taking into account the above process advantages on the WGS-MR, and the reduced requirement of the pre- and post-treatment, an economic analysis was performed to compare its production economics against the current hydrogen production via methane steam reforming under this project. Also, our proposed CMS membrane-based process was benchmarked against other emerging hydrogen production processes available in the literature.

2. EXECUTIVE SUMMARY

The commercial stainless steel (SS) substrate (i.e., ZrO₂/SS) was evaluated comprehensively as substrate for the deposition of the CMS membrane for hydrogen separation. The CMS membrane synthesis protocol we developed previously for the ceramic substrate was adapted to this SS substrate. Unfortunately, no successful membranes had been prepared during Yr I of this project. Our characterization results indicated two major sources of defects present in the SS substrate, which contributed to the poor quality of the CMS membrane. They are (i) leaking from the crimp boundary at the porous to non-porous transition (endseal) of the SS substrate, and (ii) the delamination of the ZrO₂ layer deposited on the SS substrate during the preparation of the CMS membranes. Near the end of the project period, a new batch of the SS substrate as the 2nd generation product was received from the supplier. Our characterization results confirmed the defect of the crimp boundary no longer existed. However, the thermal stability of the ZrO₂/stainless steel substrate under the CMS membrane preparation condition remained to be evaluated in the future. Due to this unexpected difficulty with the SS substrates, our project focus has been placed on the other commercial substrate, ceramic membranes.

One of the technical barriers for ceramic membranes is their scale-up potential. The conventional ceramic membranes/modules originally developed for liquid phase applications are costly and not suitable for high temperature applications. Thus, our project focus here has been the development of a ceramic membrane/module, which is economical and suitable for high temperature applications proposed under this project (200-300°C). Further, to prepare for the field test planned in the future, we have focused on (i) full-scale membrane production, (ii) full-scale module design and fabrication, and (iii) membrane performance stability testing under harsh field environment. A significant number (i.e., 98) of full-scale membrane tubes have been produced with an on-spec ratio of >76% during this first production trial. Also, we have verified our membrane functional performance and material stability with a hydrocracker purge gas at a refinery pilot testing facility. No change in membrane performance was noted over the >100 hrs of testing conducted in the presence of >30% H₂S, >5,000 ppm NH₃ (estimated), and heavy hydrocarbons on the order of 25%. The excellent stability of these membranes opens the door for the use of our membrane in the WGS environment with significantly reduced pretreatment burden.

We also initiated the fabrication of a prototype ceramic membrane module which could be (i) qualified for the proposed application temperature, and (ii) cost acceptable for large scale applications. An innovative full-scale module has been designed, which can potentially deliver >20 to 30 m²/module, suitable for large-scale applications, such as hydrogen production and power generation from coal. A prototype ceramic membrane bundle (3" diameter and 35"L) has been prepared, which passes the temperature stability requirement. It also meets the low end of the burst pressure requirement, i.e., 500-750 psi. With additional modifications, we are confident that the ceramic module we have conceived can be operated up to 1,500 psi.

Single stage water-gas-shift at a low temperature (WGS-LTS) via a membrane reactor (MR) has been studied through both mathematical simulation and experimental verification. Using the kinetic parameters experimentally obtained by us, we were able to validate the mathematical

model via the bench-top experimental results. Although the thermodynamic conversion of CO could be as high as ~90% at the LTS condition, our proposed MR yields a reactor size that is 10 to >55% smaller than the comparable conventional reactor for a CO conversion of 80 to 90%. In addition, the CO contaminant level in the hydrogen produced via MR ranges from 1,000 to 4,000 ppm vs 40,000 to >70,000 ppm via the conventional reactor. Or a nearly complete conversion of CO, i.e., >99%, can be achieved with our proposed WGS-LTS-MR. The advantages of the reduced WGS reactor size and the reduced CO contaminant level by the proposed MR provide an excellent opportunity for intensification of the hydrogen production process.

Pre- and post-treatment requirement for our proposed WGS-MR process has been defined. To avoid the hot gas clean-up (HGCU) requirement, the target temperature for the feed to the WGS-MR was set at 250°C. Thus, our proposed process permits the recovery of as much heat as possible from the gasifier off-gas via HRSG to maximize the overall power generation efficiency. Also, particulate removal can be accomplished at this low temperature with existing technology. The amount of water addition to the gasifier off-gas is limited to near the stoichiometric requirement. The loss in the WGS reaction efficiency, however, can be compensated for with the use of the proposed WGS-MR. Since (i) our membrane has demonstrated an excellent sulfur resistance at the proposed reaction temperature, and (ii) H₂S and other sulfur removal contaminants can be rejected by our hydrogen selective CMS membrane, no sulfur removal pre-treatment is required for the WGS-MR using a sulfur resistant catalyst, i.e., Co/MoS₂ catalyst. Thus, the pretreatment requirement in our proposed WGS-MR process can be streamlined to particulate removal only. No post treatment is required for hydrogen production for power generation or as chemicals for sale. Since the delivery of CO at <<10 ppm is not practical with our technology, post treatment with preferential oxidation (PROX) for the elimination of trace CO is necessary to prepare H₂ for PEM fuel cell applications. Since the CO contaminant level from our WGS-MR is 20-30 ppm, PROX can be implemented economically and reliably. Finally, hydrogen product separation is integrated into the WGS reactor; thus, no separate hydrogen separation step is required. The CO₂-rich stream reject stream from the membrane is available at high pressure and can be sent for sequestration.

Our process simulation on the WGS-MR based upon the suggested pre- and post-treatment has demonstrated that a nearly complete CO conversion (i.e., 99+%) can be accomplished. We estimate that ~90% of the hydrogen produced from the H₂+CO in the coal gasifier off-gas can be recovered via our proposed WGS-MR process. The produced H₂ purity level ranges from 80 to 92% for membrane H₂/CO₂ selectivities of 10 and 25, respectively. If a H₂ purity of 95% is required, the hydrogen recovery ratio will drop to ~80% for the membrane with H₂/CO₂=25. No cost minimization has been taken into consideration presently. In summary, with the use of our proposed CMS membrane reactor (MR) for WGS, the pre- and post-treatment requirement has been streamlined significantly. In addition, our proposed MR offers a nearly complete conversion of CO; thus, minimum or no post treatment is required to meet the CO contaminant spec for hydrogen products. Finally the thermal management required to deal with the WGS reaction exotherm can be integrated into our proposed WGS-MR reactor.

In short, in addition to the improvement of the WGS reaction efficiency, a membrane reactor (MR) for the coal gasifier off-gas can reduce the capital and operating cost significantly for the pre- and post-treatment via process intensification before, during and after the WGS reaction.

Using the economics published in the literature as the base case, our proposed WGS-MR with the sulfide catalyst can deliver the production economics comparable to existing hydrogen production cost from methane steam reforming. More importantly, our proposed process scheme does not rely on the development of the high temperature advanced membrane technology to justify the production economics as proposed in the literature. Preparation of the proposed hydrogen selective CMS membrane for field testing is recommended as the next step.

3. EXPERIMENTAL

3.1. Preparation of CMS Membrane on Commercial Stainless Steel Substrate

SEM was performed on the cross section of the stainless steel substrate deposited with ZrO₂ provided by Pall Corp. Bubble point was performed for the substrates received recently. The ZrO₂/SS substrate was deposited with the CMS membrane following the same protocol we have used throughout this project. This CMS/ZrO₂/SS membrane was then characterized with the SEM, the bubble point, and gas permeation.

3.2. Full Scale Membrane and Module Preparation

Since the commercial stainless steel substrate did not produce the desirable performance of the CMS membrane as discussed in Sec. 4.1, our project has used the CMS/ceramic membranes for the WGS/membrane reactor study while our supplier performed improvement of its stainless steel substrate in parallel.

Membrane Preparation... The full-scale membranes were prepared according to the protocol we developed previously. Once prepared, the membrane permeances were determined at 120°C in terms of He, H₂, and N₂ permeances. Nitrogen was used as a surrogate gas for CO. In addition, we packaged the individual tubes together as a bundle using ceramic potting material. The bundle was used for burst pressure evaluation.

Permeance and Selectivity... Our membrane manufacturing development made significant progress under this project. Based upon the performance data on these full scale membranes, H₂ permeance = 4 m³/m²/hr/bar at 250°C (projected from the data at 120°C shown in Figure 5) and H₂/CO = 100 appears achievable. Thus, these performance data were used in our simulation in this section.

Field Test Under Harsh Environment... While our CMS membrane will be tested eventually at a coal based utility plant, the membrane developed from this project was field tested at a refinery pilot test facility for hydrogen recovery from a refinery waste stream. This stream provided an opportunity to evaluate the membrane stability operated under a harsh industrial environment, such as the presence of sulfur, ammonia and heavy hydrocarbons, which are commonly encountered in coal gasification applications.

Membrane Challenge Test... Finally our hydrogen selective membrane was subject to a challenge test at the end of this field test. The membrane was exposed to dead-end gas separation (i.e., exposed to the enriched contaminants) for about 17 hours in the field. The permeance was recorded before the challenge test, at the end of the dead-end test, and after the regeneration to determine the degree of permeance poison and its restoration.

Fabrication of Modules for Large Scale Applications... A multiple tube element (3" diameter and 35"L) has been successfully fabricated as a prototype unit to demonstrate our proposed concept. Its configuration is similar to our existing commercial membrane elements for liquid

phase applications. Major modification here is to replace the epoxy potting of the tube bundle with the high temperature ceramic potting; thus, the bundle element can take the temperature of >500-600°C. Two different designs were conceived based upon this bundle concept: shell-and-tube heat exchanger-like and candle filter-like. In the shell-and-tube design the element can be mounted on two ends to the housing. In the candle filter design, the element is mounted on one-end only while the other end is sealed, mimicking existing candle filters used for particulates removal.

3.3. Mathematical Modeling of Water Gas Shift Reaction via Membrane Reactor

Mathematical Model, Kinetic Parameters and Feed Compositions... A mathematical model has been developed based upon the material balance coupled with the reaction rate equations. The model, once developed, was solved numerically via the finite difference method. A steady state condition with concentration profile along the axial direction of the reactor is assumed here. The feed composition is represented by CO:H₂:CO₂:H₂O = 1.00:0.70:0.33:1.10. The water content was calculated based upon 1.1 times of the stoichiometric requirement for the complete conversion of CO present. This H₂O to CO ratio, i.e., 1.1, is deemed to be minimal requirement for WGS. According to our calculations, assuming that the off-gas is available at ~1,200°C, quenching the reaction with water to the 1.1:1 ratio would yield a stream temperature of ~600°C. Hence, additional cooling is necessary to chill the stream to the LTS range of ~200°C and can be accomplished via indirect cooling. The indirect cooling allows one to recover the heat for other purposes. The advantage of the indirect cooling at a lower temperature is the use of less exotic heat exchanger material. From the reaction kinetic standpoint, the use of the minimum steam: CO ratio here (versus 3:1 in the conventional reactor) is justified since the improved efficiency of the proposed MR compensates for the rate loss.

Experimental Verification of Mathematical Model for WGS-MR... During, Year II and III, a lab scale CMS membrane reactor with 0.35cm ID, 0.45cm OD, and 10" L was selected for this study. This CMS membrane was characterized with both single gas and mixed gas at the target reactor temperature, 250°C and 50 psig.

The membrane was packed with the Cu/ZnO catalyst for CO conversion via WGS reaction. Feed composition and the reactor configuration and its operating condition are detailed below.

Feed Composition			Operating Condition	
	Ratio	Mol Fraction		
CO	1	0.16	Feed Pressure	3 atm
CO ₂	0	0.00	Permeate Press	1 atm
H ₂ O	1.1	0.18	Temperature	225-250C
H ₂	4	0.66	Sweep ratio	0.1
N ₂	0	0.00	Wc	30 g
			Surface Area	0.0028 m ²

The experiment was performed at several selected W/F's to compare the predicted vs experimental CO conversion. In addition, during Yr II, we have performed the two different levels of the sweep ratio to compare its effect on conversion and CO impurity level using a different membrane.

Effect of Operating Variables on WGS-MR-LTS... Using the mathematical model developed previously, we have performed sensitivity analysis to determine the effect of each key operating variable.

3.4. Process Simulation for Coal Gasifier Off-gas

Using the mathematical model developed and verified above, we performed the optimization study on the proposed WGS-MR. Although no cost optimization was attempted here, we have configured a process scheme, which could streamline the hydrogen production via WGS-MR. The pre-treatment and post-treatment requirements were thus determined. Then a mathematical simulation was performed for WGS-MR under this proposed streamlined scheme. In addition, sensitivity analysis was performed to determine the effect of the H₂/CO₂ selectivity on the hydrogen purity. To eliminate the sulfur removal pretreatment requirement, Co/MoS₂ catalyst was employed in this optimization study.

3.5. Potential Process Schemes Available in Literature for Hydrogen Production from Coal Gasification Process.

The seven options identified in the paper published by Stiegel and Armezan [Ref. 3] for producing hydrogen from coal were used as the basis to benchmark ours vs existing and emerging hydrogen production processes. The seven cases are listed below:

- Case 1 Conventional Coal to H₂ (without CO₂ Recovery):
GE (ChevronTexaco) quench gasifier/WGS/Low-Temp. Gas Cleaning/Gas Turbine/Steam Turbine
- Case 2 Conventional Coal to H₂ (with conventional PSA CO₂ Recovery/Sequestration):
Single Train, GE (ChevronTexaco) quench gasifier/WGS/Low-Temp. Gas Cleaning/ Gas Turbine/Steam Turbine/Sequestration
- Case 3 Conventional Coal to H₂ (with Membrane CO₂ Recovery/Sequestration):
Single Train, ConocoPhillips Advanced E-gas gasifier/WGS/High-Temp. Gas Cleaning/Gas Turbine/Steam Turbine
- Case 4 Advanced Coal to H₂/Power (without CO₂ Recovery)
Two train, ConocoPhillips Advanced E-gas gasifier /WGS/Low-Temp. Gas Cleaning/No CO₂ Removal/Gas Turbine/Steam Turbine
- Case 5 Advanced Coal to H₂ (with conventional PSA CO₂ Recovery/Sequestration)
Two train, ConocoPhillips Advanced E-gas gasifier /WGS/Low-Temp. Gas Cleaning/Gas Turbine/Steam Turbine
- Case 6 Advanced Coal to H₂ (with conventional PSA CO₂ Recovery/Sequestration)

Two train, ConocoPhillips Advanced E-gas gasifier/High-Temp. Gas Cleanup/WGS/SOFC/GasTurbine/Steam Turbine

Case 7

Advanced Coal to H₂ (with membrane CO₂ Recovery/Sequestration)

Two train, ConocoPhillips Advanced E-gas gasifier /High-Temp. Gas Cleanup (HGCU)/WGS/SOFC/Gas Turbine/Steam Turbine.

Only the cases involved in the use of the membrane were evaluated against ours. Since the production economics for these 7 cases was compared against the existing hydrogen production via methane steam reforming, by comparing ours against these cases, our production economics can be evaluated against the existing hydrogen production cost.

4. RESULTS AND DISCUSSION

4.1. Preparation of CMS Membrane on Stainless Steel Substrate

Permeance and Selectivity of CMS/SS Membranes... During Yr I of this project, we received several samples of the first generation stainless steel substrate provided by our supplier, Pall Corp. The stainless steel substrate was deposited with ZrO_2 to reduce its pore size to 0.1 micron range by the supplier. For us to deposit the CMS membrane, microporous Al_2O_3 thin film was deposited on top of this substrate to further reduce its pore size to the range comparable to the ceramic substrate we have used throughout our study.

This substrate with ZrO_2 and Al_2O_3 deposition was then used for the deposition of the CMS membrane. It was found that the CMS membranes thus produced show much lower selectivity of H_2 over other gases as shown in Table 1. It should be noted that the CMS/SS membrane quality became unacceptable when calcined at the intermediate and higher temperatures although these are the temperature we prefer to produce a CMS membrane with a high selectivity. For instance, H_2/N_2 of 39 and 98 at $220^\circ C$ were obtained for the CMS/Ceramic membranes calcined at the intermediate and high temperatures. The selectivity for H_2/CH_4 is much higher. However, the best selectivity we have obtained for the CMS/SS membrane is ~ 17 for H_2/N_2 and H_2/CH_4 at $220^\circ C$. Evidently the lower selectivity of CMS/SS is partially attributed to the lack of the thermal stability of the membrane when calcined at the intermediate and the higher temperature.

Table 1 Comparison of Gas Permeation for CMS Membranes Deposited on Stainless Steel vs Ceramic Substrate.

Part ID	Substrate	Firing Temp.	H_2 Permeance [m ³ /m ² /hr/bar]	H_2/N_2 200°C	H_2/CH_4 200°C	H_2/C_2 200°C
DZp-18	Pall S.S.	Low	1.8	17	16.8	45
NN-02	M&P Ceramic	Intermediate	1.6	39	155	>500
DZ-216	M&P Ceramic	High	1.0	98	166	>500

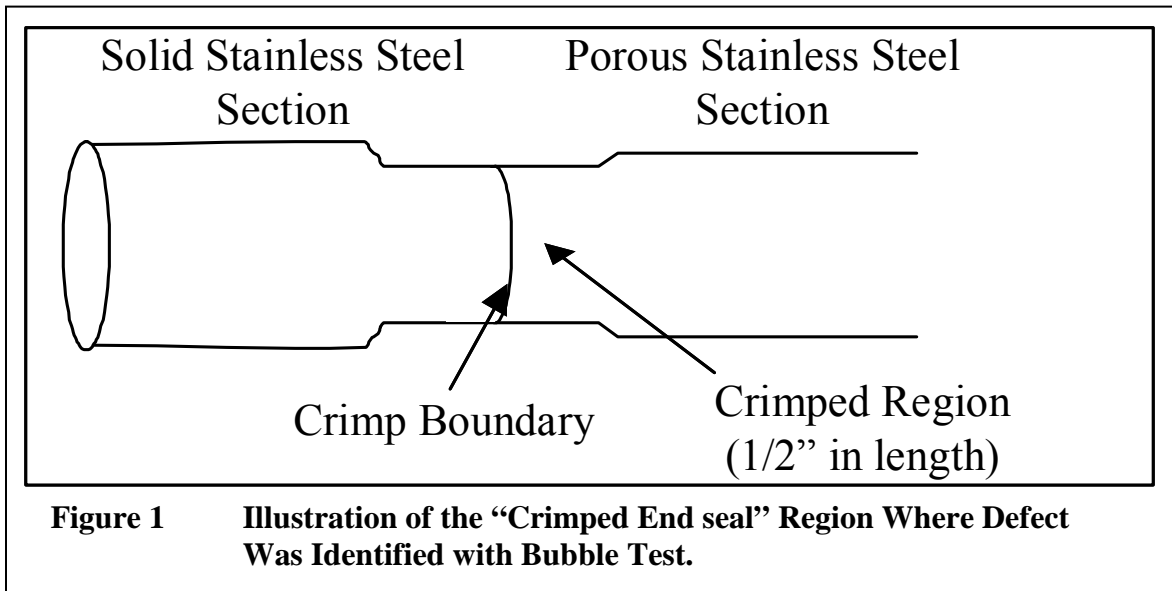
Morphological Characterization of CMS/SS Membranes... The CMS/SS membranes prepared above were characterized morphologically with the bubble point method for the purpose of identifying defects of the membranes. Although this method does not provide the quantitative information on the number of defects, it does provide an overview on the quality of the membrane layer as summarized in Table 2. Out of the 14 parts we have prepared, we found that the CMS/SS membranes calcined at the low temperature deliver about 50% successful rate, i.e., no obvious bubbles were identified. No successful tubes were identified for those calcined at the intermediate temperature. Further, most of the defects were found from the crimp end where the porous stainless steel was welded to the non-pervious stainless steel as end seals. Nearly all tubes calcined at the intermediate temperature show this type of defects. The other type of defects is

the delamination of the CMS layer at the center of the membrane section. The defects are further elucidated in the next section.

Table 2 Qualitative Description of Defects Observed on CMS Membranes Deposited on Stainless Steel Substrate

Firing Temp	# of Parts	%Successful	# of Crimp Leak	# of Center/Delam.
Low	8	50	2	4
Intermediate1	2	0	2	1
Intermediate2	4	0	4	3

Two types of defects were found as indicated in the above section. The first type defect is located at the crimp boundary between the solid stainless steel section and the porous stainless steel section as described in the schematic in Figure 1. The second type defect is resulted from the intermediate layer delamination as presented in the SEM pictures in Figure 2. Firing temperatures required to produce highly H₂ selective membranes result in delamination of the intermediate ZrO₂ layer. Based upon the diagnosis above, we believe that the end seal defects are most likely present in the stainless steel substrate, while the delamination is resulted from the lack of the thermal stability of the stainless steel/ZrO₂ substrate under the temperature/atmosphere required for the preparation of the CMS substrate.



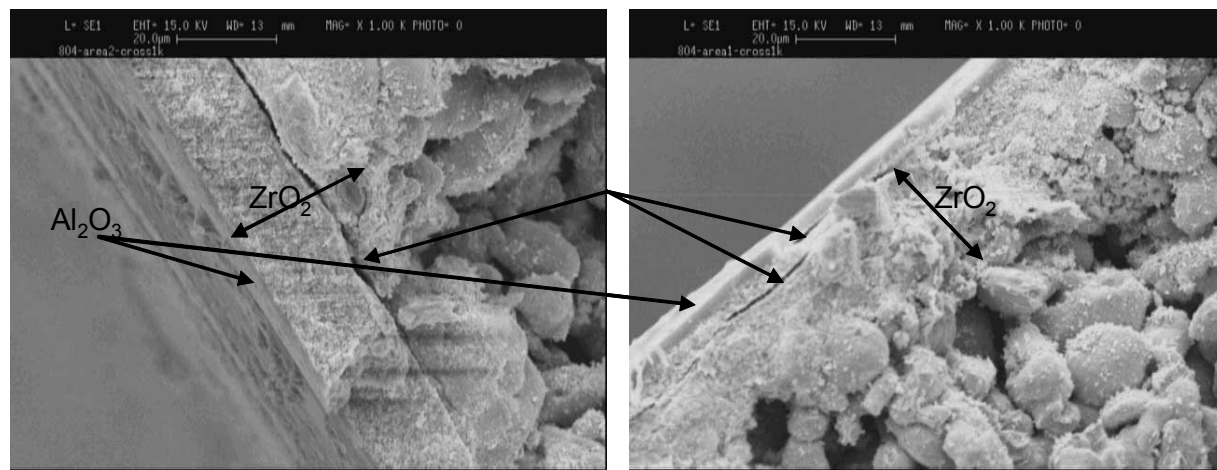


Figure 2 SEM Photomicrographs of the Cross Section of Inside Tube Surface of ZrO₂/stainless steel substrate including ZrO₂ layer and M&P Al₂O₃ layer.

Characterization of Stainless Steel Substrate Received Recently... Recently we have received the 2nd generation of the ZrO₂/SS substrate provided by Pall Corp with the improved end seals and other features. Thus, our CMS on SS substrate activity was resumed. Thus far, we have performed the SEM morphological characterization of the cross section of the membrane and the leak check of the end seals. Figure 3 presents the cross section of the 2nd generation of ZrO₂/SS substrate. It appears that the ZrO₂ layer with 25 micron thickness was deposited on the stainless steel substrate. Moreover, the top surface of the ZrO₂ appears very smooth. Bubble point was performed on one of the samples, Pall Id-"MP&T-

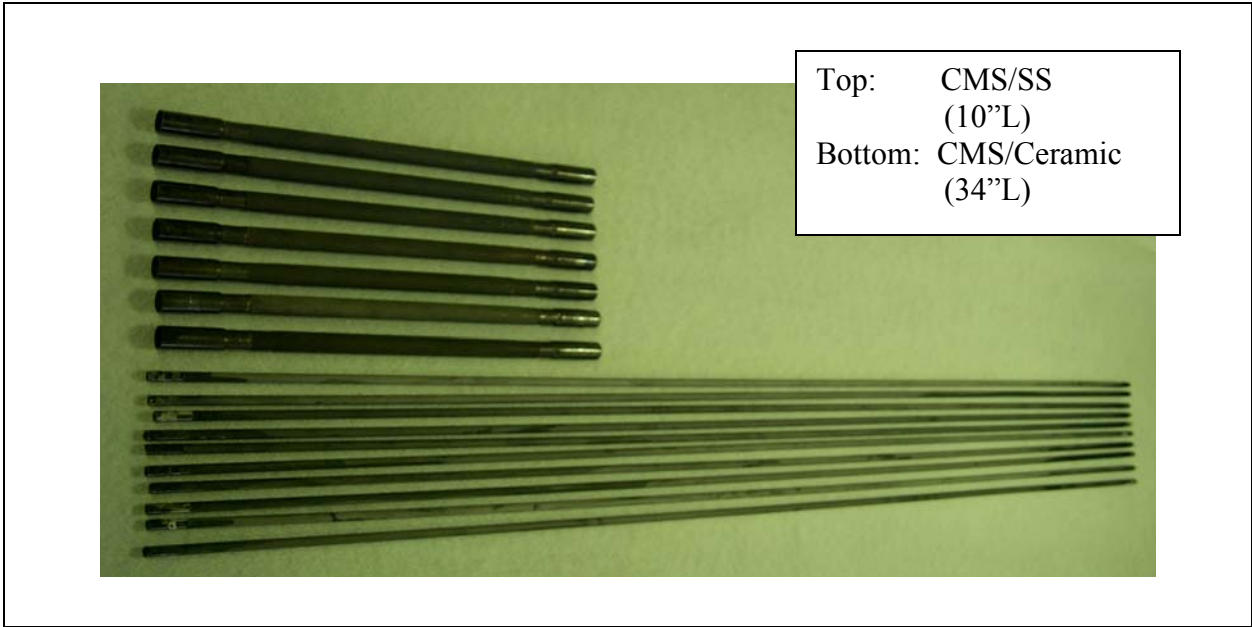
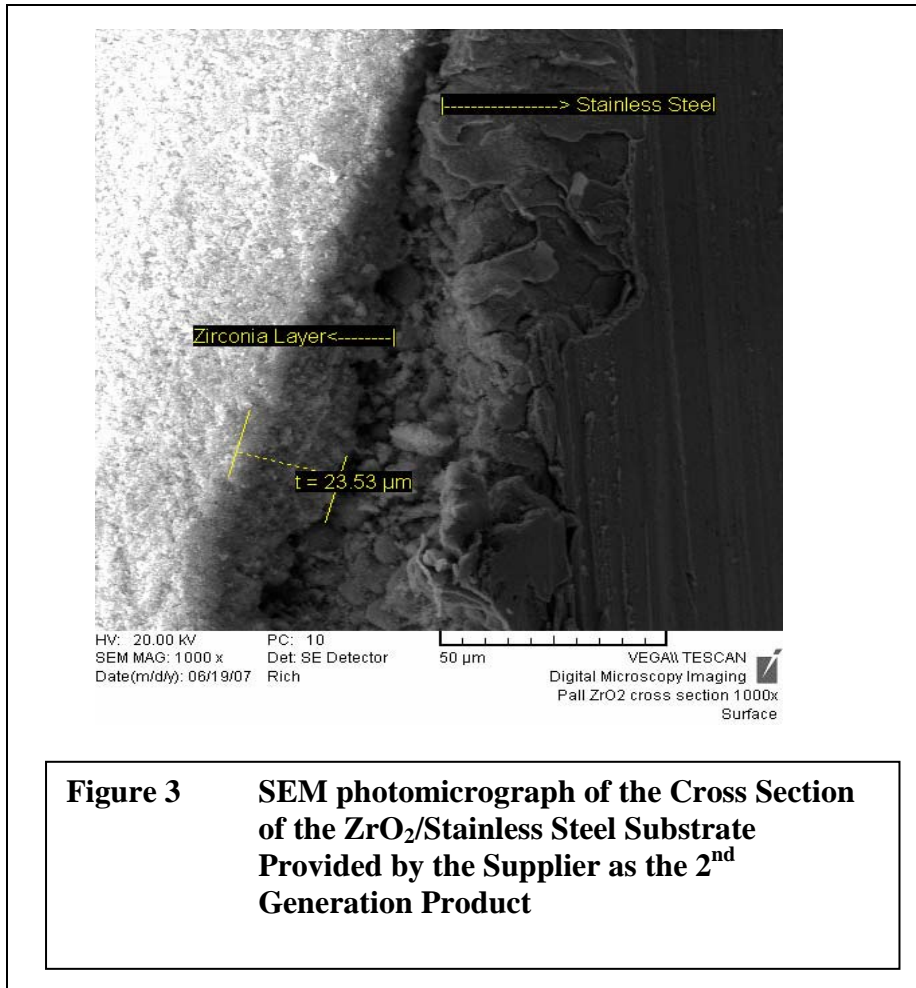


Figure 4 Picture of CMS Membrane Deposited on SS and Ceramic Tubes

032707-4". No foaming/breakthrough was observed at 24 psi of IPA. Obviously, the welds/endseals looked good for this sample. The permeances at room temperature are 143 and 288 $\text{m}^3/\text{m}^2/\text{hr}/\text{bar}$ for He and N_2 respectively. In summary, based upon our limited characterization result, it appears that defect of the end seals has been corrected for the 2nd generation ZrO_2/SS substrate. More samples will be characterized to obtain the statistically significant result. In addition, the thermal stability of these substrates were tested during the remaining period of the project. Our goal here is to collect enough characterization result to confirm the suitability of the ZrO_2/SS substrate for the deposition of the CMS membranes. No CMS membrane deposition activity was attempted due to the approaching to the end of this project.

4.2. Full Scale Membrane and Module Production

Quantities Produced and On-Spec Ratio... A total of 98 membrane tubes have been produced thus far. We set our spec at a H_2 permeance of $>0.35 \text{ m}^3/\text{m}^2/\text{hr}$ and H_2/N_2 selectivity of >50 selectivity at 120°C . This would translate into a H_2 permeance of $>0.5 \text{ m}^3/\text{m}^2/\text{hr}/\text{bar}$ and H_2/N_2 selectivity of >75 at the target operating temperature of 250°C . About 23 out of 98 tubes failed to meet this spec during the first production trial, which leads to $>75\%$ on-spec ratio. Please refer to Figure 5 and Table 3 for details.

Full-Scale Module Fabrication... One of the major challenges for ceramic based membranes is its scale up potential. During this reporting period, we have come out with a flexible design, which allows us to fabricate membrane modules with $>30 \text{ m}^2/\text{module}$ without using exotic engineering or materials. This would qualify the ceramic membrane and module for mega-scale applications, such as the proposed application, which usually requires several hundred square meters. With the availability of our innovative module design, ceramic membranes no longer suffer this scale-up disadvantage. Due to the proprietary nature of the design, no details are disclosed here.

Table 3 Characterization of Full-scale Hydrogen Selective Membrane (30”L) Produced During this Project Period

Tube #	Temp [C]	Permeance [m3/m2/hr/bar]		Selectivity		Fail to meet Spec.*
		He	H2	He/N2	H2/N2	
113	120	0.188	0.524	19	53	
114	120	0.306	0.765	32	80	
128	120	0.753	1.390	39	72	
129	120	0.382	0.974	20	51	
130	120	0.278	0.649	42	98	
132	120	0.523	1.068	47	96	
135	120	0.899	2.055	35	80	
137	120	0.454	0.856	87	164	
140	120	0.303	0.598	73	144	
141	120	0.279	0.728	59	154	
143	120	0.557	1.346	24	58	
145	120	0.293	0.760	27	70	
147	120	0.271	0.690	33	84	
148	120	0.548	1.370	34	85	
153	120	0.319	0.775	28	68	
156	120	0.220	0.436	88	175	
163	120	0.244	0.397	56	91	
164	120	0.204	0.345	28	47	x
168	120	0.132	0.157	43	51	x
169	120	0.177	0.253	150	214	x
171	120	0.118	0.146	38	47	x
175	120	0.225	0.500	68	152	
177	120	0.278	0.666	31	73	
178	120	0.259	0.604	21	49	x
180	120	0.684	1.683	28	70	
182	120	0.413	0.897	19	40	
183	120	0.203	0.371	178	324	
184	120	0.306	0.638	73	151	
185	120	0.246	0.604	30	74	
187	120	0.142	0.266	25	46	x
188	120	0.544	1.265	28	64	
190	120	0.399	0.977	44	109	
196	120	0.370	0.763	79	163	
197	120	0.204	0.353	237	409	
198	120	0.679	1.531	25	56	
200	120	0.678	1.356	30	60	
201	120	0.147	0.254	307	532	x
202	120	0.699	1.625	18	42	x
203	120	0.318	0.641	112	225	
204	120	0.170	0.308	119	215	x
205	120	0.323	0.690	30	64	
206	120	0.416	0.707	59	100	
207	120	0.425	0.773	54	99	
208	120	0.241	0.444	31	58	
210	120	0.310	0.637	91	187	
211	120	0.302	0.659	73	160	
214	120	0.297	0.523	214	377	
215	120	0.232	0.355	75	114	
216	120	0.239	0.349	122	178	
218	120	0.253	0.389	150	230	
219	120	0.234	0.347	41	61	
220	120	0.203	0.285	155	217	x
221	120	0.236	0.359	57	86	
223	120	0.246	0.480	24	46	
226	120	0.151	0.282	43	80	x
227	120	0.200	0.320	178	285	x
228	120	0.367	0.697	26	50	
229	120	0.218	0.321	125	183	

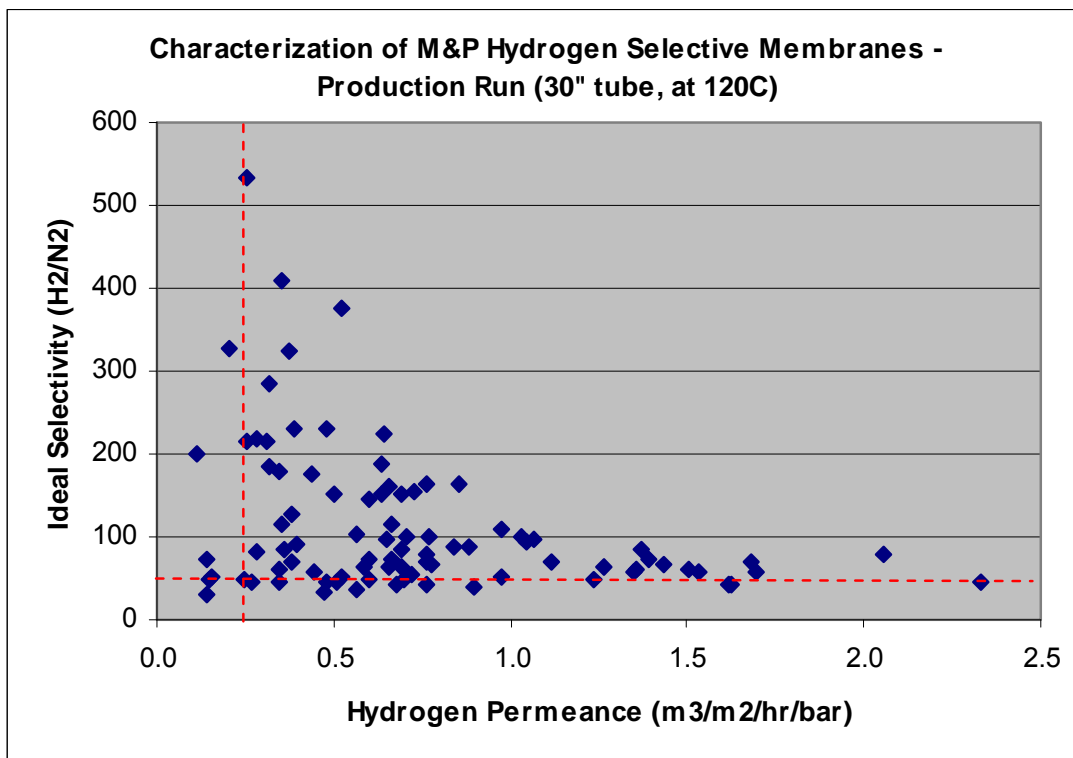
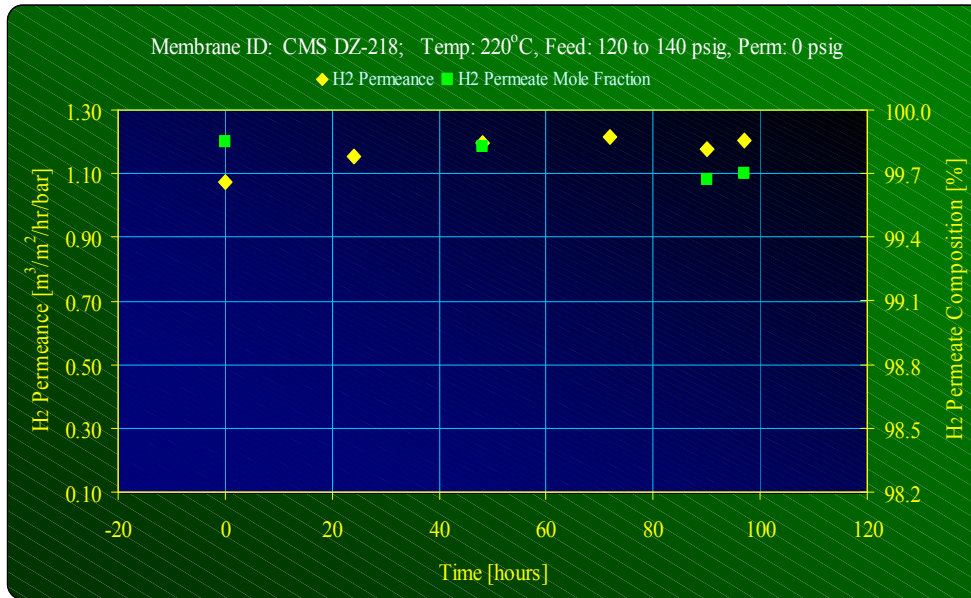


Figure 5. H₂ permeance vs. Selectivity of Full Scale Membrane Tubes Prepared During this Project Period.

Membrane Performance Stability in Presence of Concentrated H₂S... The field test results generated at the refinery pilot test facility are summarized in Figure 7. At 220°C and 10 bar, a stable hydrogen permeance of 1.1 m³/m²/hr/bar was obtained throughout the test period of about 120 hrs. Hydrogen purity was enriched from ~90% to 99.9% with the hydrogen recovery ratio of 85 to 92%. In addition, the H₂S concentration was reduced from 5.2% in the feed to ≤0.16% in the permeate. More importantly, no membrane permeance degradation was observed under this concentrated H₂S environment.

Membrane Regeneration after Challenge Test... The aggressive “dead-head” (no reject flow) challenge test reduced the permeance substantially; however, our regeneration restored the original permeance as presented in Table 4. Hydrogen permeance of 1.27 m³/m²/hr/bar and the selectivity of ~75 for hydrogen over nitrogen at 220°C were obtained before the challenge test. The dead head challenge test was conducted for 17 hours so that the contaminant levels far exceeded those in the standard run, including >>30% H₂S and heavy hydrocarbons. As a result, the membrane was poisoned and its permeance was reduced by ~50% to 0.62 m³/m²/hr/bar. However, this permeance loss was restored via our proprietary regeneration technique to nearly

the original level, i.e., 1.26 m³/m²/hr/bar and the selectivity of 67. Based upon the results from the poison study in the field and its regeneration, we believe that our CMS membrane can be regenerated in case the membrane is accidentally poisoned.



At time = 3 hours					At time = 100 hours				
Gas	Composition [%]			H ₂ /Slow Selectivity	Gas	Composition [%]			H ₂ /Slow Selectivity
	Feed	Reject	Permeate			Feed	Reject	Permeate	
H ₂ S	5.2	32.0	0.03	163	H ₂ S	4.8	24.5	0.16	74
H ₂	89.9	38.9	99.88	1	H ₂	90.8	50.6	99.70	1
C ₁	2.1	12.2	0.08	123	C ₁	1.9	9.9	0.06	123
C ₂	0.88	5.4	0.01	~600	C ₂	0.81	4.2	0.01	~600
C ₃₊	1.88	11.6	ND	>1,000	C ₃₊	1.66	10.7	ND	>1,000
Stage Cut			85%		Stage Cut			80%	
H₂ Recovery			92%		H₂ Recovery			85%	

Figure 6 Gas Stream Compositions and Stage Cut and H₂ Recovery for the VGO Hydrocracker Pilot Test

Table 4 Degradation of the CMS Membrane Challenged by the Dead-end Operation and the Restoration of the Original Permeance via Regeneration.

Membrane Regeneration		
Pure Component Permeance and Selectivity		
Test Conditions: 220°C @ ~120 psig		
Test Phase	H₂ [m³/m²/hr/bar]	H₂/N₂ [-]
Before Hydrocracker Testing	1.27	75
After Hydrocracker Testing	1.22	ND
After Dead Head Hydrocracker Challenge Test >> ~17 hrs w/NO Reject Flow (100% Stage Cut) >> Permeate flow falls from ~450 to ~3 cc/min	0.62	53
After Regeneration	1.26	67

Fabrication of Modules for Large Scale Applications... For the heat exchanger design, fluid can be fed to either the shell or tube side. In the candle filter design; however, fluid can only be fed into the shell side while the permeate can be collected from the exit of the tube side. This latter design offers the advantage of separating the ceramic element expansion/contraction from the steel housing expansion/contraction as a result of temperature change. Thus, no mismatch would incur. The disadvantage of the candle filter is that no permeate side purge can be implemented. Since our application temperature is at 200-300°C, we believe that the mismatch between the housing and the element could be manageable. Thus, we will continue the development of both designs. The burst pressure test was also conducted in this month for the

single tube as well as the element. The burst pressure for the single tube was tested up to >1500 psi from the outside of the tube without rupture; thus, we believe that the individual tube strength is more than adequate for the proposed application. The burst pressure of the candle filter element (3") was 500-750 psi. The failure was resulted from the pressure exerting on the tube sheet. Based upon our proposed process scheme, the pressure drop across the membrane would be in the range of 500 to 1500psi. Although we can increase the tube sheet thickness to enhance the burst pressure as an option; the tube sheet is currently under redesign to accommodate the burst pressure of >1500 psi as an ultimate solution.

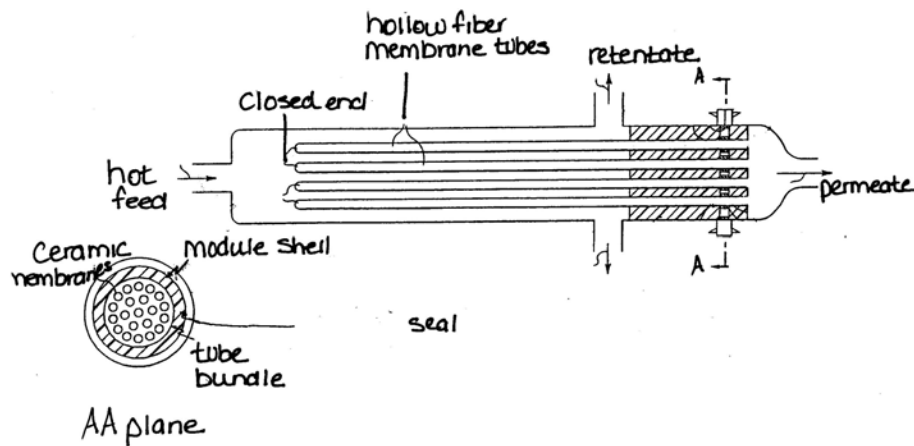


Figure 7. Candle Filter Ceramic Membrane Bundle and Module (bottom) and Patented High Temperature Packing/Seal Design (top) and a Single Element Pilot Scale Module (middle).

4.3. Mathematical Modeling of Water Gas Shift Reaction via Membrane Reactor

Mathematical Model, Kinetic Parameters and Feed Composition... The mathematical model (see Appendix I) has been developed during this reporting period. To verify its accuracy, a material balance check was performed numerically. The results presented in Appendix II validate the model. This model, along with the kinetic parameters obtained experimentally, has been employed for comparison between the packed bed and the proposed membrane reactor for a single stage WGS-LTS reaction.

For all the calculations performed here we utilized the kinetic equations for WGS, described as follows [Ref. 1.]

$$r = A \cdot \exp(-E_a / RT) \cdot \frac{P_{CO} \cdot P_{H_2O}^{1.4}}{P_{CO_2}^{0.7} \cdot P_{H_2}^{0.9}} \frac{1}{P_t^{0.4}} (1 - \beta)$$
$$\beta = \frac{1}{K_g} \frac{(P_{CO_2} \cdot P_{H_2})}{(P_{CO} \cdot P_{H_2O})}$$
$$K_g = \frac{P_{CO_2} \cdot P_{H_2}}{P_{CO} \cdot P_{H_2O}}$$

A is the preexponential factor, E_a is the apparent activation energy, P_i is the partial pressure of component i , P_t is the total pressure, β is the approach to equilibrium, and K_g is the equilibrium constant for the water-gas shift reaction. The activation energy, E_a , listed in the reference is $E_a = 86.5$ (kJ/mol). The experimental E_a obtained by our study during this period is $E_a = 114.2$ (kJ/mol). Details of the experimental results are listed in Table 1 and Figure 1 below. The preexponential factor, A , obtained based upon our experimental E_a is $A = 1.77 \times 10^{11}$ (mol/g-hr-bar^{0.4})

Table 5. Experimental Results for Kinetic Parameter Determination

Composition	CO : H ₂ : H ₂ O = 1.0 : 4.0 : 2.5					
Pressure(psig)	52.5		50		50	
Temperature(C)	205		225		250	
Weight of Catalyst(g)	10		30		30	
Kinetic data	W/Fo CO (g*hr/mol)	CO Conversion(%)	W/Fo CO (g*hr/mol)	CO Conversion(%)	W/Fo CO (g*hr/mol)	CO Conversion(%)
	1.56E+02	77.96	4.67E+02	96.52	4.67E+02	96.63
	7.78E+01	68.47	2.33E+02	95.23	2.33E+02	95.21
	5.19E+01	61.66	1.56E+02	92.22	1.56E+02	92.94
	3.89E+01	50.93	1.17E+02	88.19	1.17E+02	88.43
	3.11E+01	47.96	9.33E+01	79.38	9.33E+01	86.35
	2.59E+01	38.48	7.78E+01	71.78	7.78E+01	77.86
Equilibrium Conversion of CO(%)	98.30		97.54		96.27	

$k = k_0 \cdot \exp(-E/RT)$			
T(C)	205	225	250
T(K)	478.15	498.15	523.15
R(J/ mol*K)	8.314	8.314	8.314
k	5.39E-02	2.21E-01	6.46E-01

ln (k)	-2.92E+00	-1.51E+00	-4.37E-01
1/RT	2.52E-04	2.41E-04	2.30E-04

intercept (= ln (k ₀))	25.90
slope (= -E)	-114218.6

k ₀ g-mol/(g cat*hr*bar ^{0.4})	1.77E+11
E (J/mol)	114218.6
E (KJ/mol)	114.22

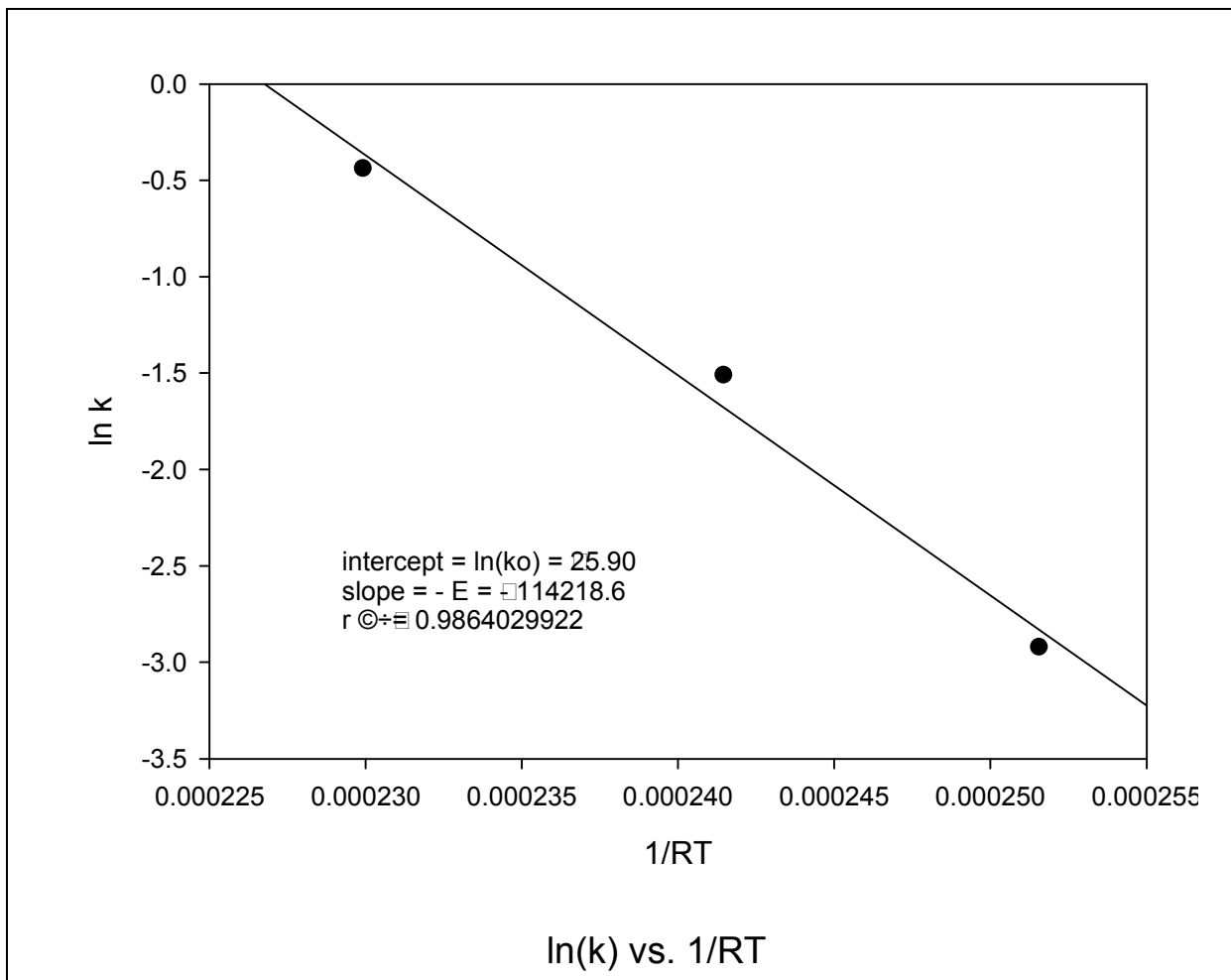


Figure 8 Experimental determination of E_a and A based upon $\ln(k)$ vs. $1/RT$

The kinetic parameters, obtained for the Sud-Chemie catalyst used in this study, are different from that reported in the literature as shown above. As expected the MR performance predictions used ours vs the literature's are significantly different. However, the performance trend and the comparative difference between the membrane reactor (MR) and the packed fixed-bed reactor (PFC) are quite similar as shown in Table 2. Throughout this study, we employed the kinetic parameters obtained from our experimental study. It is believed that the conclusions generated with our own kinetic parameters would be applicable to other cases.

Table 6 Membrane Reactor Performance Prediction based upon Ours vs. Literature Kinetic Parameters

Case A. Using the kinetic parameters from the literature

$k = 1.52 \text{ E}8 \text{ (gmole/(gr catal.hr.bar}^{0.4})$

$E_a = 86500 \text{ (J/mol)}$

Xe	W/FCO(g*hr/mol CO) required to reach 95% of equilibrium conversion at PFR						
	PFR	1X H2		5X H2		10X H2	
		MR-co	MR-counter	MR-co	MR-counter	MR-co	MR-counter
0.899	34.0	26.0	32.4	18.2	20.1	14.2	14.7

Xe	W/FCO(g*hr/mol CO) required to reach 90% of equilibrium conversion at PFR						
	PFR	1X H2		5X H2		10X H2	
		MR-co	MR-counter	MR-co	MR-counter	MR-co	MR-counter
0.899	19.5	16.9	18.7	12.8	14.1	10.4	11.1

Case B. Using the kinetic parameter we obtained experimentally

$k = 1.77 \text{ E}11 \text{ (gmole/(gr catal.hr.bar}^{0.4})$

$E_a = 114218.6 \text{ (J/mol)}$

Xe	W/FCO(g*hr/mol CO) required to reach 95% of equilibrium conversion at PFR						
	PFR	1X H2		5X H2		10X H2	
		MR-co	MR-counter	MR-co	MR-counter	MR-co	MR-counter
0.899	23.6	17.5	19.9	13.0	14.2	10.2	10.7

Xe	W/FCO(g*hr/mol CO) required to reach 90% of equilibrium conversion at PFR						
	PFR	1X H2		5X H2		10X H2	
		MR-co	MR-counter	MR-co	MR-counter	MR-co	MR-counter
0.899	12.9	11.2	11.8	9	9.7	7.5	7.9

Experimental Verification of Mathematical Model... CO conversions vs W/F at 250°C for the feed specified above are presented in Figure 4. Also shown in the figure is the CO conversion based upon the thermodynamic calculation. Permeances for each component were experimentally determined: 1.12, 0.066, 0.163, 1.55 m³/m²/hr/bar for H₂, CO, CO₂ and H₂O respectively. With these physical and rate parameters, the CO conversion vs W/F predicted by the mathematical model developed in this study is presented in Figure 4. The MR shows about 10% enhancement over the PFR at this operating condition. About 90 and 91% conversion were obtained at W/F= 350 and 400 respectively. These experimental results correlate well with the prediction shown in Figure 4.

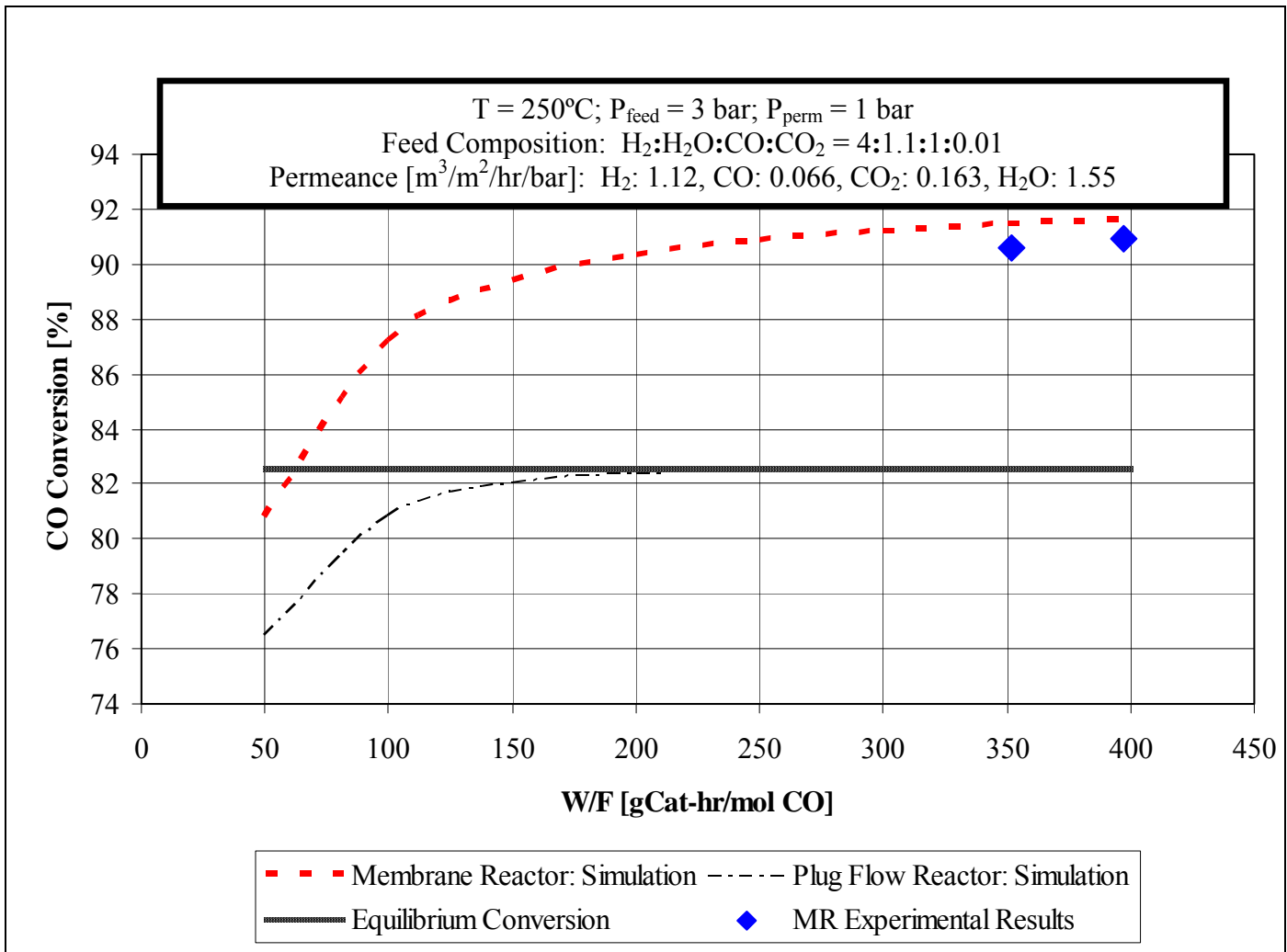


Figure 9 LTS-WGS via Our CMS-Based Membrane Reactor: Experimental vs Simulation Results

Additional experimental data was generated with a 2nd membrane reactor in the end of Year II, particularly in the range of W/F=50 to 200, where the CO conversion is more sensitive to the change of W/F. The experimental and predicted results are presented in Figures 2 and 3. The mathematical model can predict the conversion and the effect of sweep ratio reasonably well for the feed composition suggested for the WGS-MR. In the next section, we evaluated effects of some key parameters on the performance of the proposed WGS-MR.

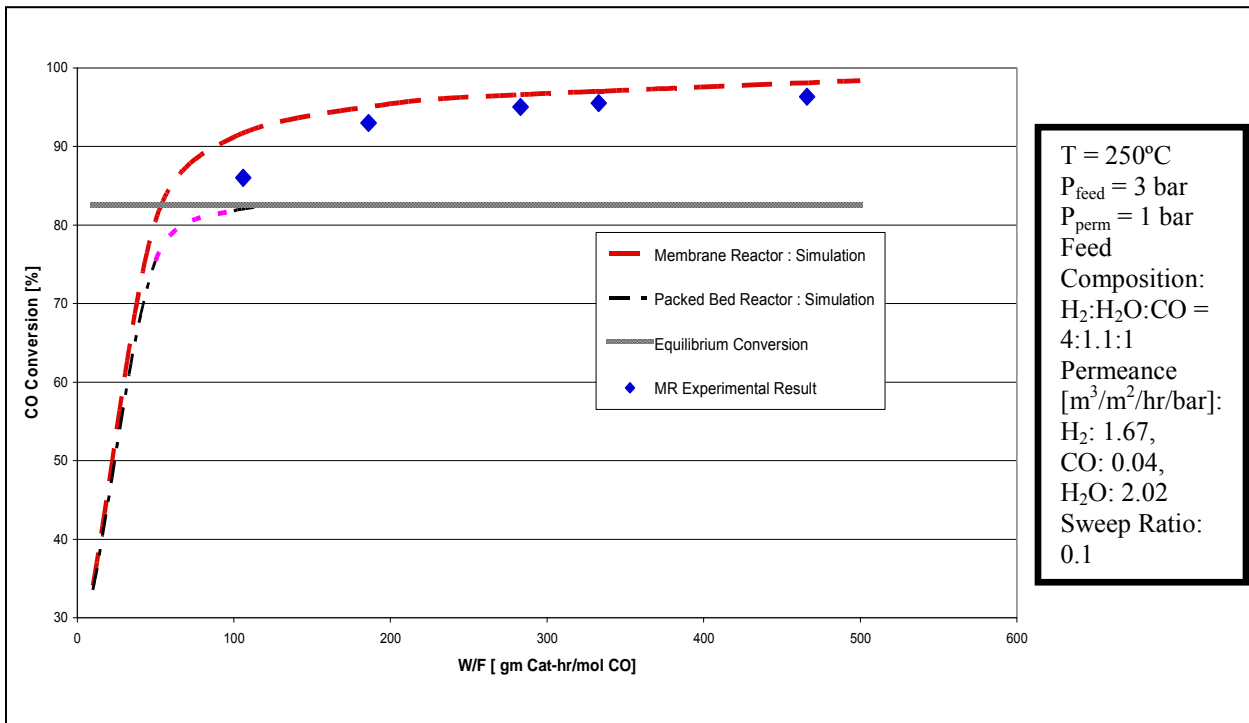


Figure 10 Experimental vs Predicted CO Conversion using a CMS Membrane as a Reactor.

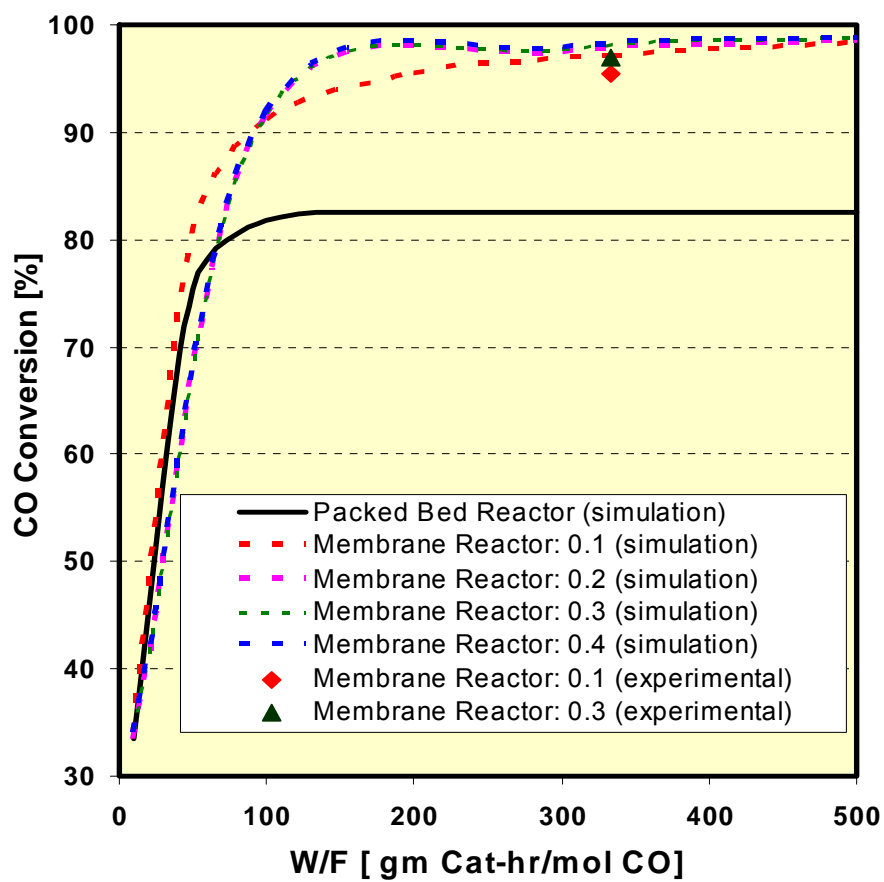


Figure 11
Effect of Sweep Ratio (as a fraction of the feed flow rate) on the CO Conversion: Experimental vs Predicted. The feed condition used is the same as the one used for Figure 10.

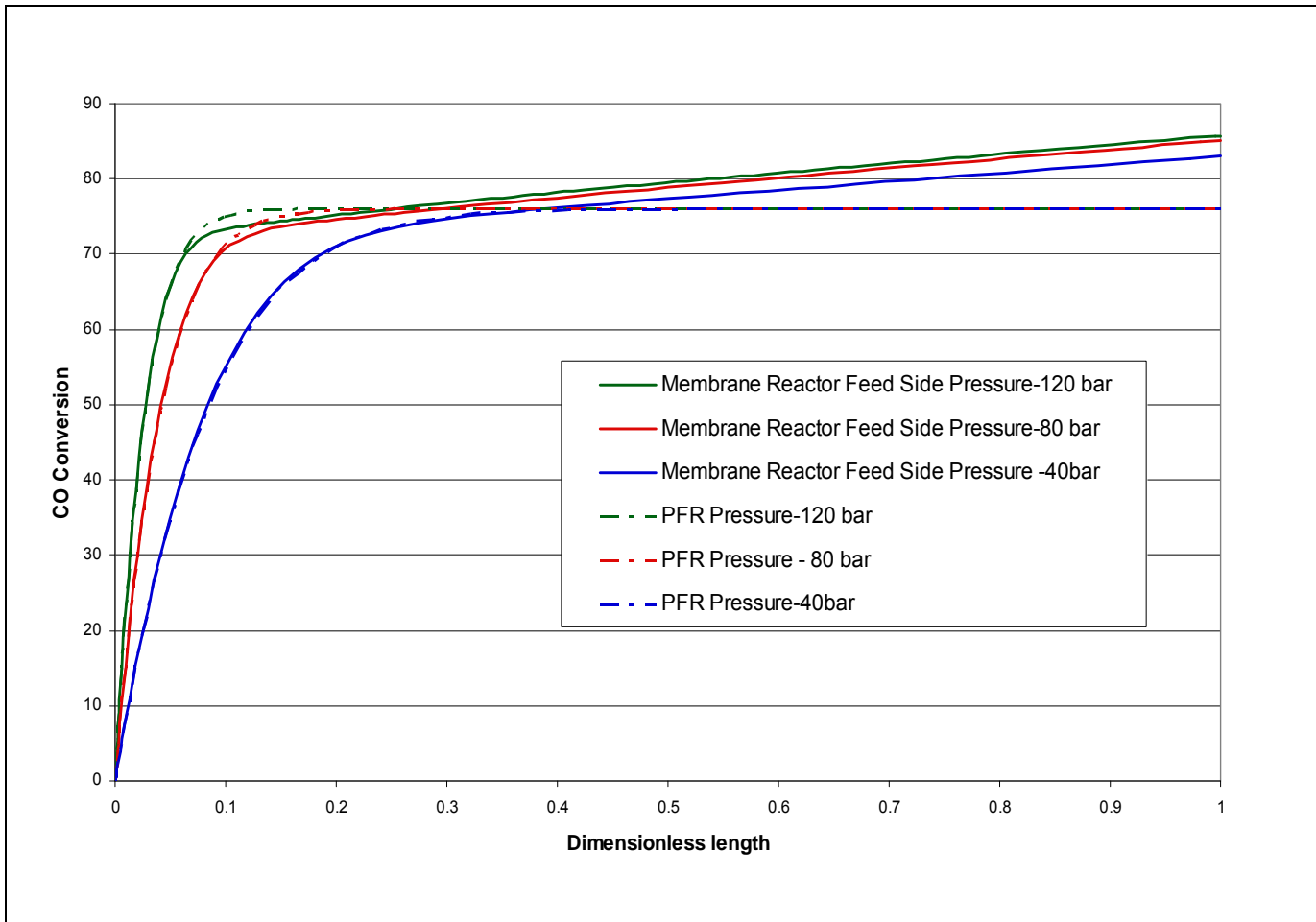


Figure 12 Effect of Feed Pressure on the CO Conversion using a CMS-WGS-MR (the feed pressure as indicated, the rest of the condition is presented in text as the base case)

4.4. Effect of Operating Variables on WGS-MR Performance

Using the mathematical model verified with experimental data, we have performed simulation study to investigate the effects of key operating parameters as follows:

CO Conversion Ratio... CO conversion is one of the performance criteria for our proposed process. In this subsection, we evaluate the effect of key operating parameters, including W/F, feed pressure and sweep ratio, on the CO conversion. The effect of feed pressure on the CO conversion is presented in Figure 4. The range of the pressure for this study is 40 to 120 bar.

The lower pressure represents the off-gas pressure obtained from the BGL gasifier, while the upper end, 120 bar, represents the off-gas from the Texaco oxygen blown gasifier. The pressure has a very slight effect on the degree of CO conversion as shown in Figure 4. The effect of W/F on the CO conversion is presented in Figure 5. When the W/F increases from 0.5 to 1.5, the CO conversion improves significantly. Since the conversion above the equilibrium is dependent upon the rate of the product removal, the higher W/F provides a sufficient time for the reactor to remove a significant quantity of the product, hydrogen. Thus, we believe that W/F effect is most likely resulted from the increase in the membrane surface area because the reaction kinetics under the selected operating condition, i.e., high pressure, is very fast as observed for the packed bed in the figure. The permeation rate vs reaction rate will be selected in the future for optimization study. Figure 6 presents the effect of the sweep ratio. As the effect of pressure, the sweep ratio effect is very modest on the degree of conversion. In conclusion, using the base case presented above, our simulation indicates that the W/F has the profound effect on the degree of conversion. Further, our analysis shows that this effect is most likely resulted from the increase in the membrane surface area. The permeation rate vs the reaction rate will be chosen for our optimization study in the future.

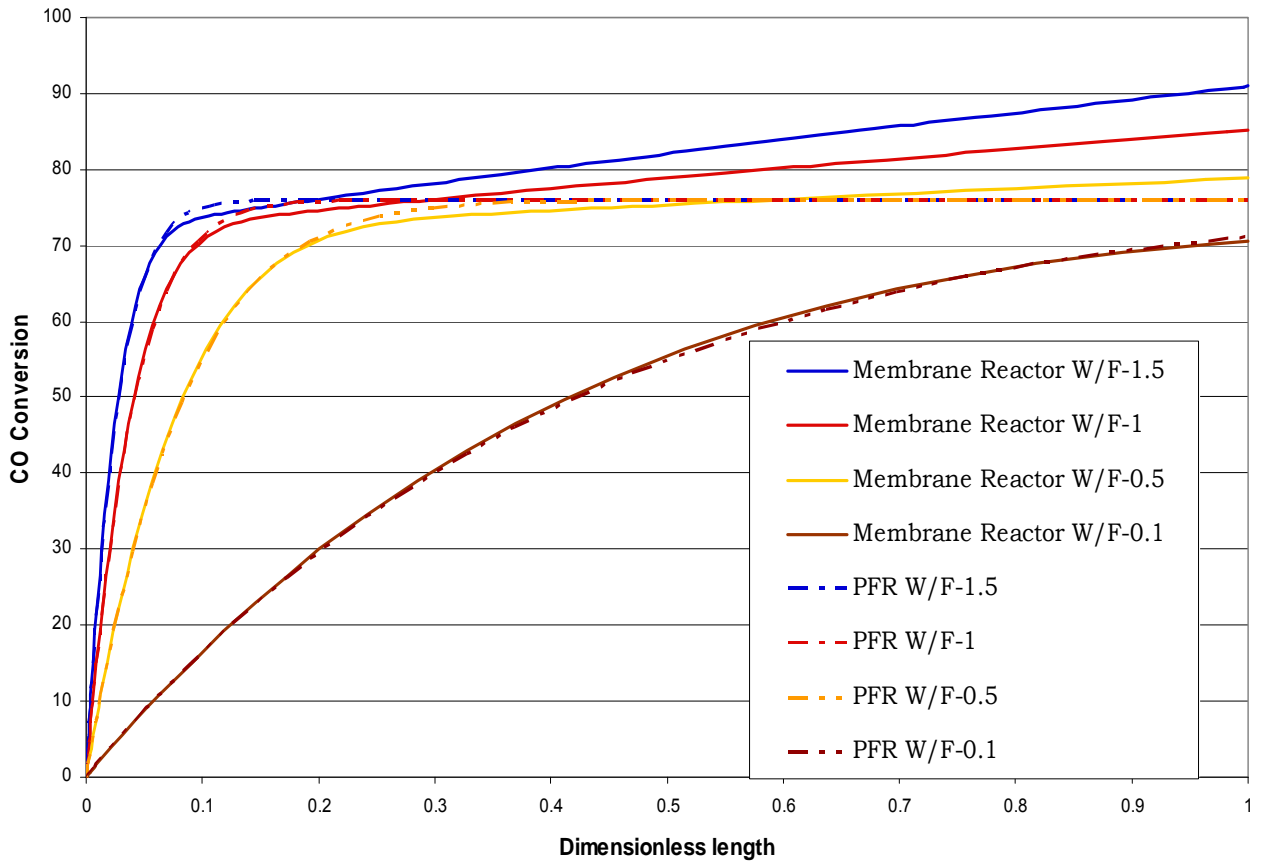


Figure 13 Effect of W/F on the CO Conversion (the W/F used as noted, the rest of the operating condition is presented in the text as the base case)

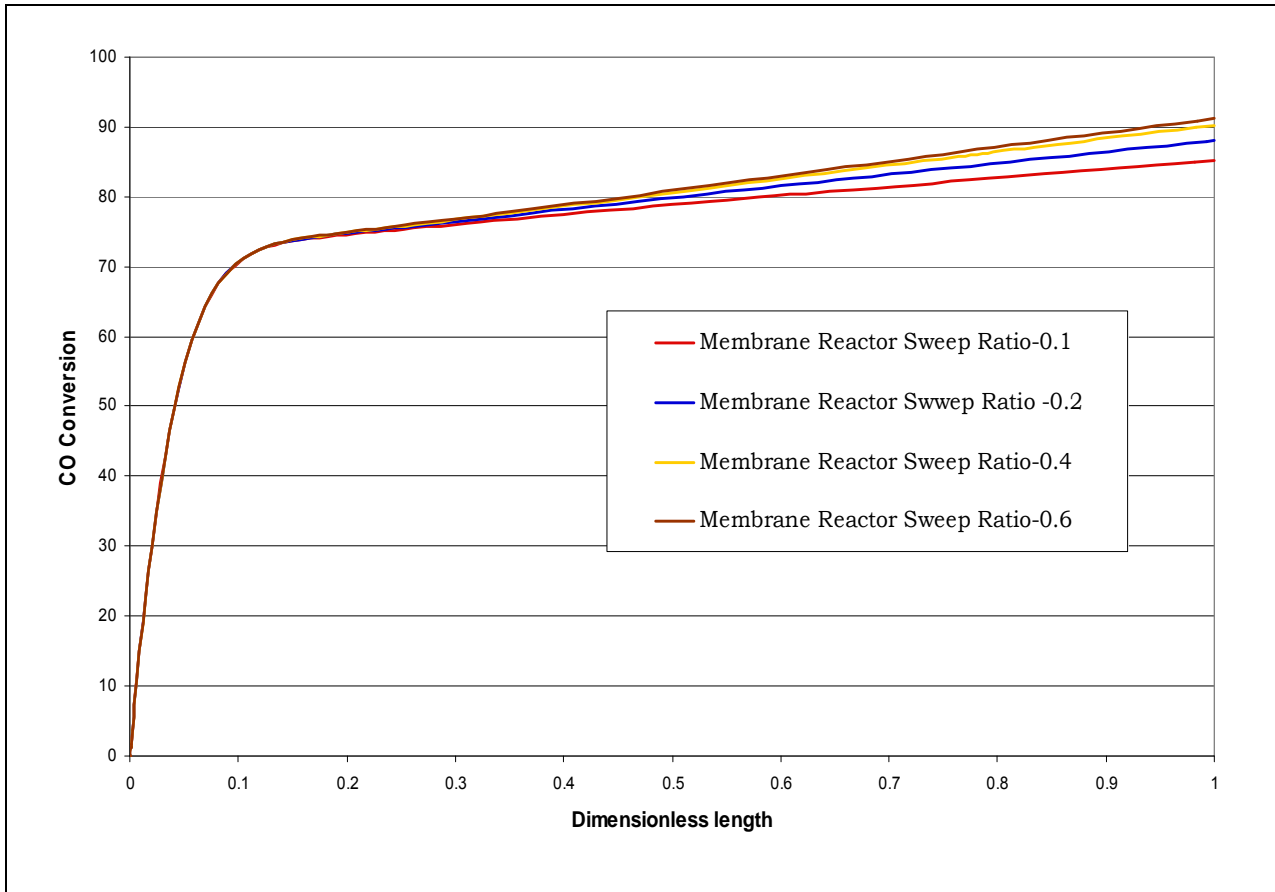


Figure 14 Effect of Sweep Ratio on the CO Conversion (sweep ratio as a fraction of the feed stream as noted, the rest of the condition is presented in the text as the base case)

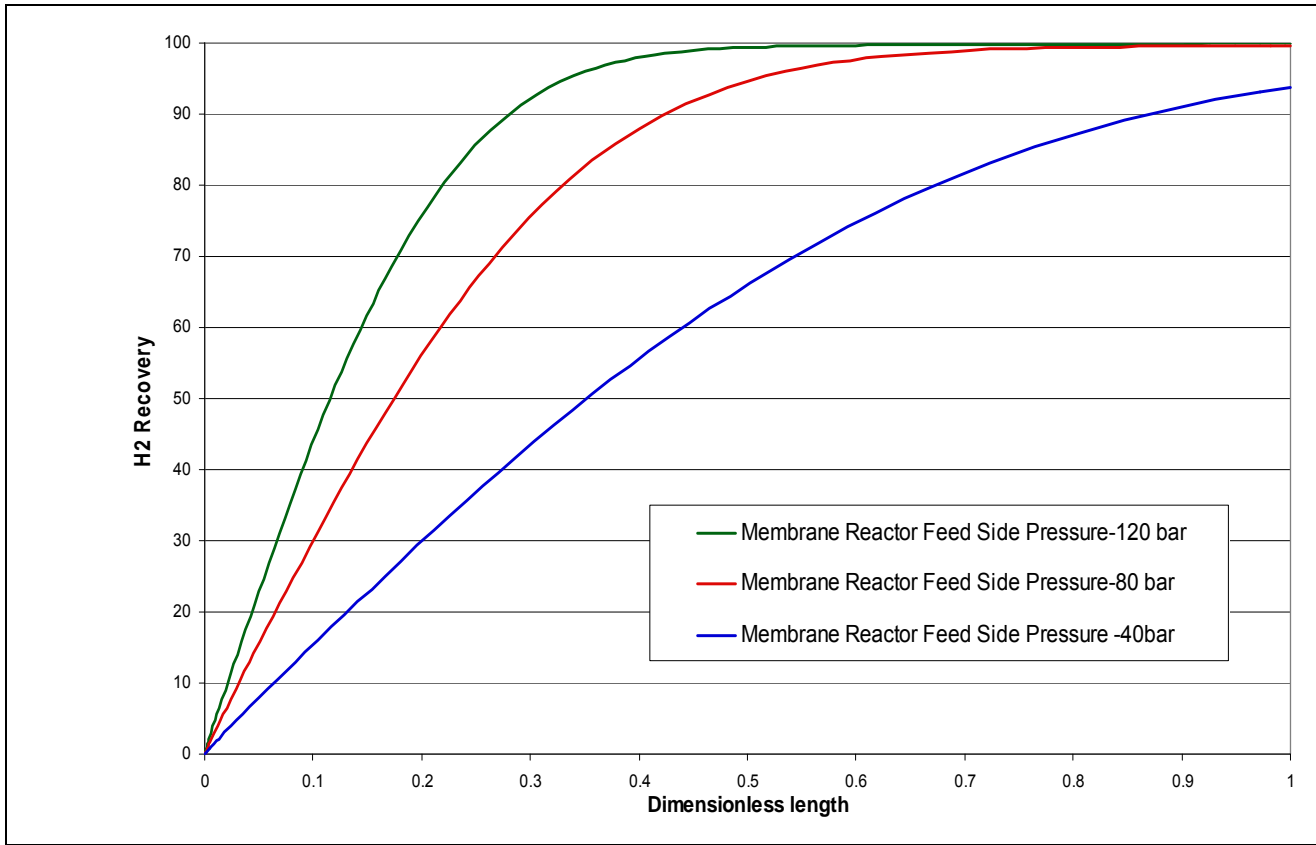


Figure 15 Effect of Feed pressure on the Hydrogen Recovery Ratio (the feed pressures as noted, the rest of the conditions are presented in the text as the base case).

Hydrogen Recovery Ratio... A membrane reactor offers the advantage of integrating the reaction and product separation into a single unit. Thus, it is very important for us to select an operating variable which can recover as much hydrogen as possible. Again we have chosen the feed pressure, W/F and the sweep ratio to evaluate their effect on the hydrogen recovery ratio. As expected the higher the feed pressure, the higher the recovery ratio is. According to the base case selected above, the system pressure >80 bar can deliver a nearly complete recovery of hydrogen. When the system pressure is at 40 bar, an increase in the membrane surface area is necessary in order to achieve a high degree of hydrogen recovery. The W/F effect is presented in Figure 8. As expected, the W/F effect in effect can be translated in the effect of the membrane surface area. Thus, the higher the W/F is, the more efficient the hydrogen recovery is. According to our simulation, W/F at 1 or above is sufficient to deliver a complete hydrogen recovery. Finally the sweep ratio effect is presented in Figure 8, its effect on the hydrogen recovery is insignificant. In conclusion, the hydrogen recovery appears not a dominating performance criterion for the base case selected. It appears that a high degree of hydrogen recovery can be accomplished within the operating parameters we selected. During the optimization study, the

CO version, not the degree of hydrogen recovery, was selected as a primary performance criterion.

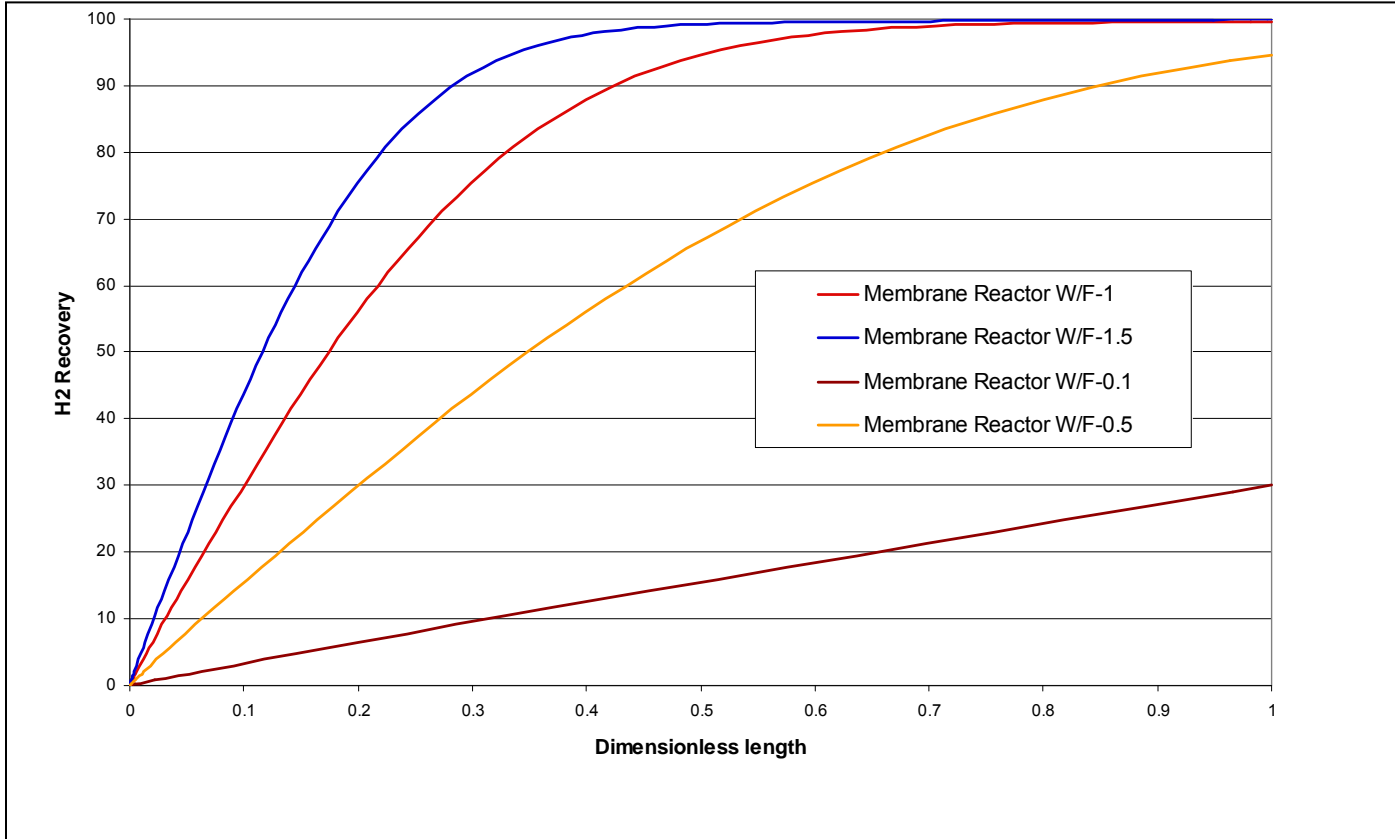


Figure 16 Effect of W/F on Hydrogen Recovery Ratio (the W/F used as noted, the rest of the conditions are presented in the text as the base case)

CO Impurity Concentration... The CO impurity is considered as an important performance criterion, in particular for fuel cell applications. Figure 8 presents the CO concentration as a function of the feed pressure. It appears that the feed pressure has a significant effect on the CO concentration. At a higher feed pressure, i.e., 120 bar, the CO impurity level could reach as high as 5,000 ppm although this level is still ten times less than that from the packed bed. About 1,000 ppm can be achieved for the feed pressure at 40 bar. The simulation results indicate that the CO permeation could be more efficient at the high feed pressure. Thus, the high CO impurities level at 120 bar is most likely resulted from the leak of the CO during the initial stage of the reactor. Thus our optimization study should focus on the optimization of the reaction rate vs permeation rate; thus, the product conversion can be maximized and the impurity permeation could be kept at a minimum. According to the hydrogen recovery ratio vs reactor length in Figure 10, a nearly 100% hydrogen recovery is accomplished at the reactor length (dimensionless) $\ll 1$. Thus, the CO impurities could be reduced to about 1,000 ppm or less when the reactor is optimized.

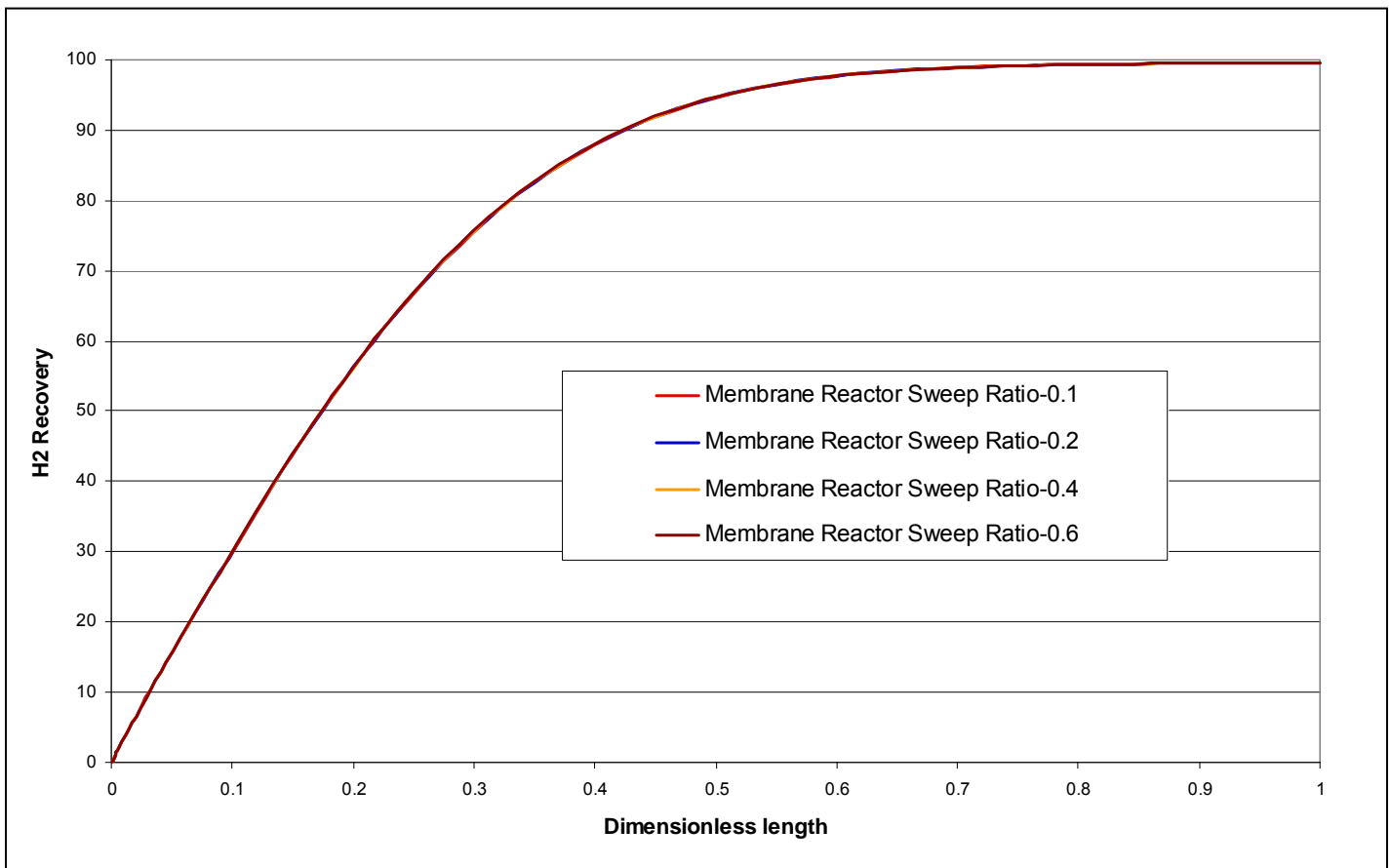


Figure 17 Effect of Sweep Ratio on Hydrogen Recovery Ratio (the sweep ratio used as indicated, the rest of the conditions are presented in the text as the base case).

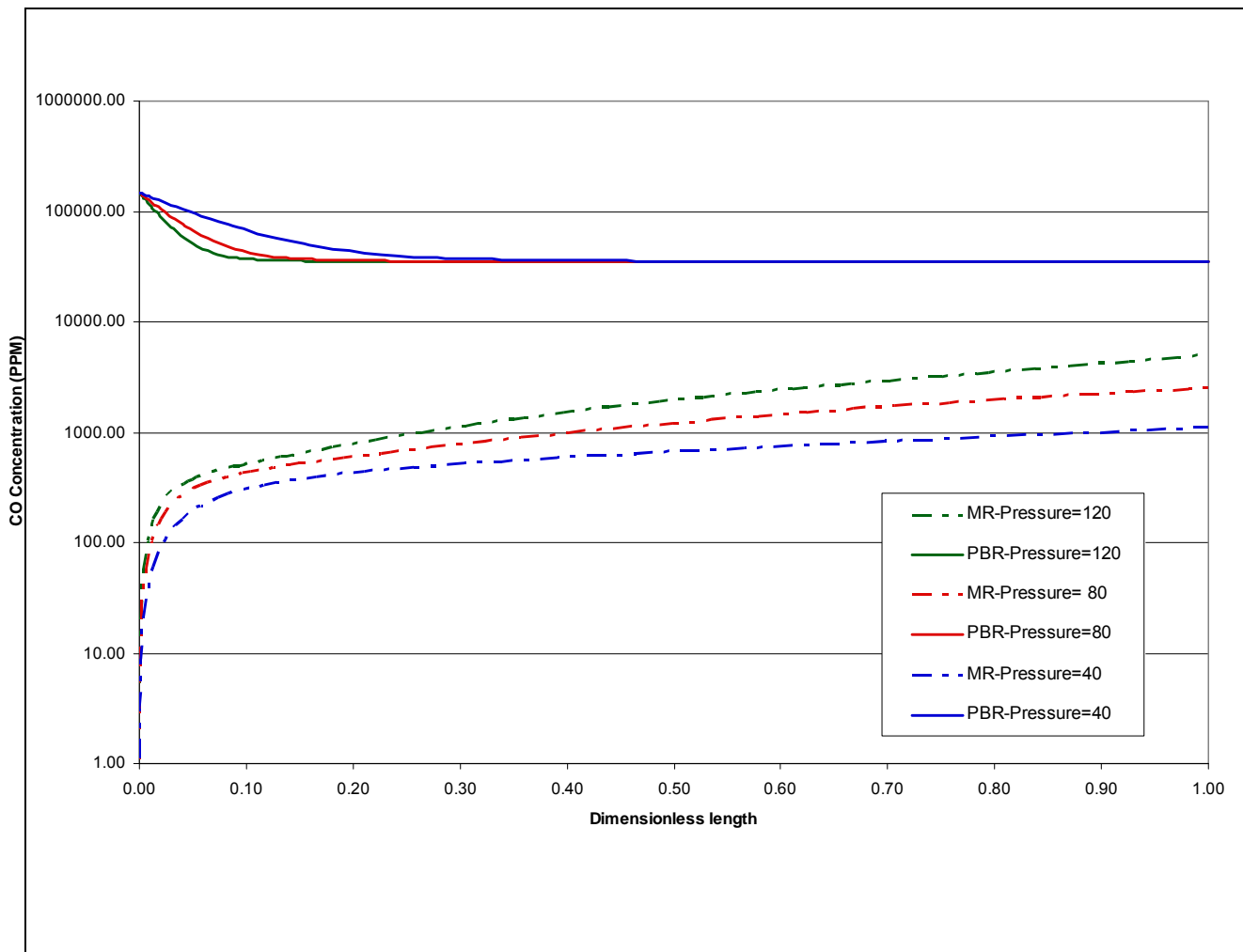


Figure 18 Effect of Feed Pressure on the CO Impurity Level in the Hydrogen Recovered (the feed pressure as noted, the rest of the conditions are presented in the text as the base case).

Optimization Study... A preliminary optimization study based upon the above experience has been performed to get some idea about the performance of the WGS-MR under the proposed scheme. It appears that a nearly complete CO conversion and ~95% hydrogen recovery can be achieved with the CO impurity level at 3500 ppm for the feed side pressure at 40 bar as shown in Figure 11. The CO impurity level can be reduced to 1500 ppm, however, the recovery ratio is reduced to ~70%. This simulation study should be treated very preliminary since the reaction kinetics of the catalyst has not been verified at such a high pressure. More comprehensive optimization study will be performed in future to focus on the reduction of the CO impurity level with a reasonable hydrogen recovery ratio.

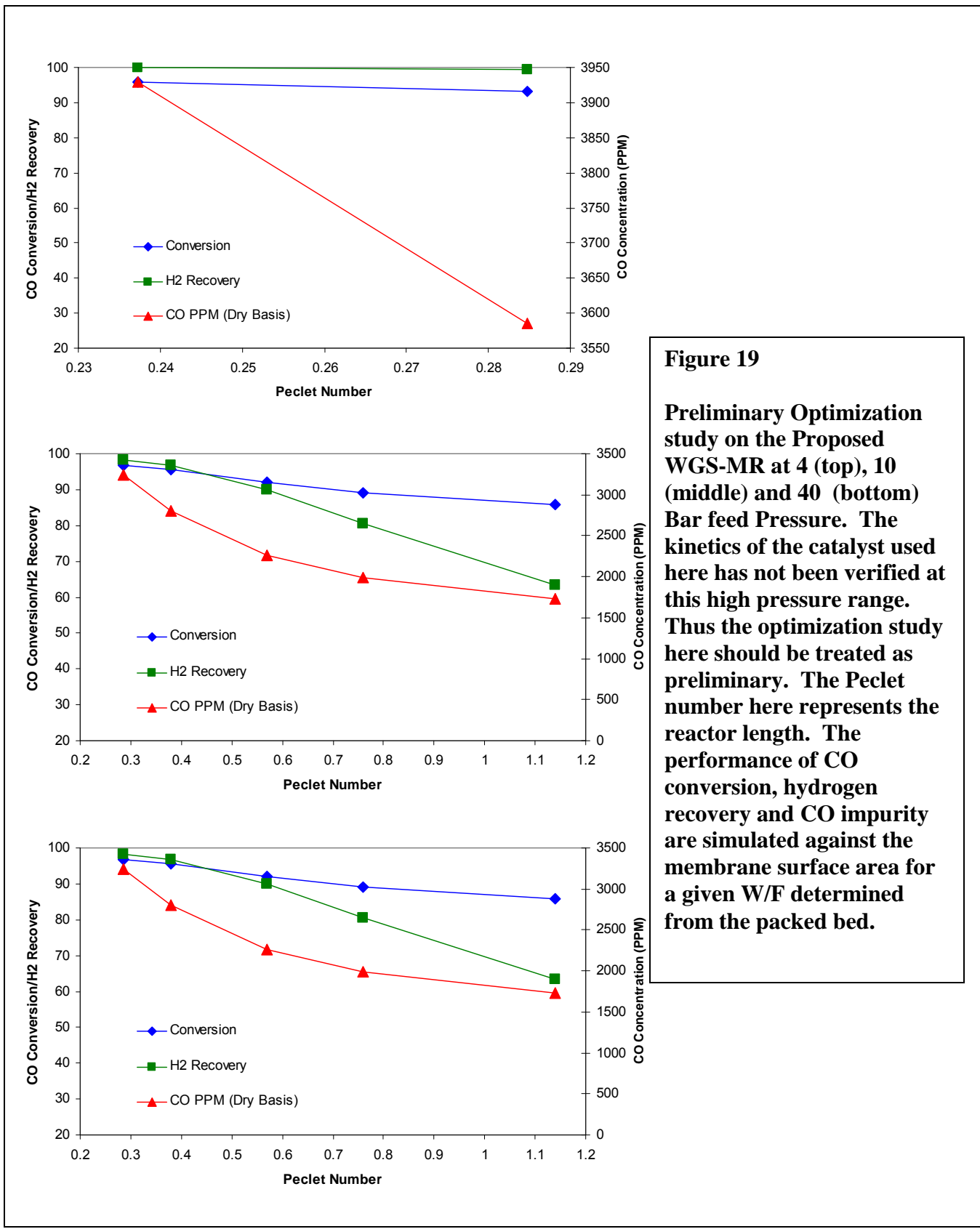


Figure 19
Preliminary Optimization study on the Proposed WGS-MR at 4 (top), 10 (middle) and 40 (bottom) Bar feed Pressure. The kinetics of the catalyst used here has not been verified at this high pressure range. Thus the optimization study here should be treated as preliminary. The Peclet number here represents the reactor length. The performance of CO conversion, hydrogen recovery and CO impurity are simulated against the membrane surface area for a given W/F determined from the packed bed.

In summary, our mathematical simulation for the single stage LTS-WGS operation with MR demonstrates its unique advantage in achieving high CO conversion in a reactor volume that is 10 to >55% less than the PFR requirement. In addition, the CO level is low at 1,000 to 4,000 ppm and can be readily post-treated with existing polishing technologies, such as PROX or methanation. In comparison, the PFR cannot deliver the CO contaminant at a level low enough for further treatment by the PROX or methanation; an additional unit operation to separate CO contaminant from hydrogen is necessary.

(number in this summary statement may not be consistent with the figures).

4.5. Process Simulation for Coal Gasifier Off-gas

Under this project, we also attempted to perform process simulation and optimization, focusing on the use of our CMS membrane for WGS-MR with the mathematical model developed and verified in this project. A comprehensive process optimization is beyond the scope of this project; however, an optimization around the WGS-MR would give us valuable information, specifically the relationship of hydrogen purity vs hydrogen recovery ratio with the unit operations which are streamlined with the use of our proposed WGS-MR.

Operating Conditions Selected for WGS-MR... Several unit operations involving the pre- and post-treatment are selected in order to minimize the variables involved in the optimization. They are listed below:

- The target temperature for the feed to the WGS-MR is set at a low temperature, e.g., 250°C.
- The amount of water addition to the gasifier off-gas is limited to near the stoichiometric requirement. Significant over-stoichiometric water addition has been practiced routinely to enhance the CO conversion. However, from the power generation standpoint, the water quench to the gasifier stream is essentially a loss in the power generation efficiency. In addition, dilution of reactants and products, which are unfavorable to WGS reaction and membrane permeation in most occasions. The WGS conversion efficiency under the stoichiometric environment could be discounted significantly; however, the use of WGS-MR can enhance the reaction efficiency to compensate for this loss in efficiency.
- WGS reaction in the presence of sulfur can be accomplished with the use of the Co/MoS₂ catalyst. This catalyst has been employed industrially for WGS in the presence of sulfur. Since our membrane has demonstrated an excellent sulfur resistance at our proposed reaction temperature, the reaction kinetics published in the literature [Ref. 2] for this sulfide catalyst is used here for simulation.

Further, our simulation strategy is based upon the principles below:

- It is our objective to achieve a nearly complete CO conversion with the proposed CMS-MR. Although conversion vs production cost may play an important role in an overall process optimization, no cost optimization has been taken into consideration. However,

a nearly complete CO conversion, i.e., >99%, can be achieved with the use of our CMS-MR.

- Since the delivery of CO to <<10 ppm ready for PEM fuel cell applications is not practical with our technology without using any post treatment, such as PROX. In our proposed process, the PROX is treated as essential post treatment to eliminate the CO contaminant level of 20-30 ppm. Thus, PROX can be implemented economically and reliably. Therefore, our optimization does not take into consideration of minimizing the CO contaminant level.

The results from simulation based upon the above operating conditions and the strategy are presented in the next section.

Simulation of Hydrogen Separator and WGS Membrane Reactor.... Our simulation here focuses on the unit operation of H₂ Separation/WGS under isothermal condition. Our goal is (i) to make sure that a nearly complete CO conversion and hydrogen recovery can be accomplished with the proposed membrane reactor and (ii) to prepare the mathematical model for simulating the proposed process once the input parameters become available from our future experimental study. Since no experimental study has been performed by us on the use of the sour shift catalyst, our simulation here was based upon the literature data available with modifications to suite our application condition. The membrane performance and the reaction kinetic parameters selected for this simulation is listed as follows:

Feed Composition

CO= 0.13
 CO₂= 0.27
 H₂O= 0.21
 H₂= 0.39
 N₂ = 0.01
 Pressure 80 bar
 Temperature 280°C

Permeances of the CMS membrane are listed as follows:

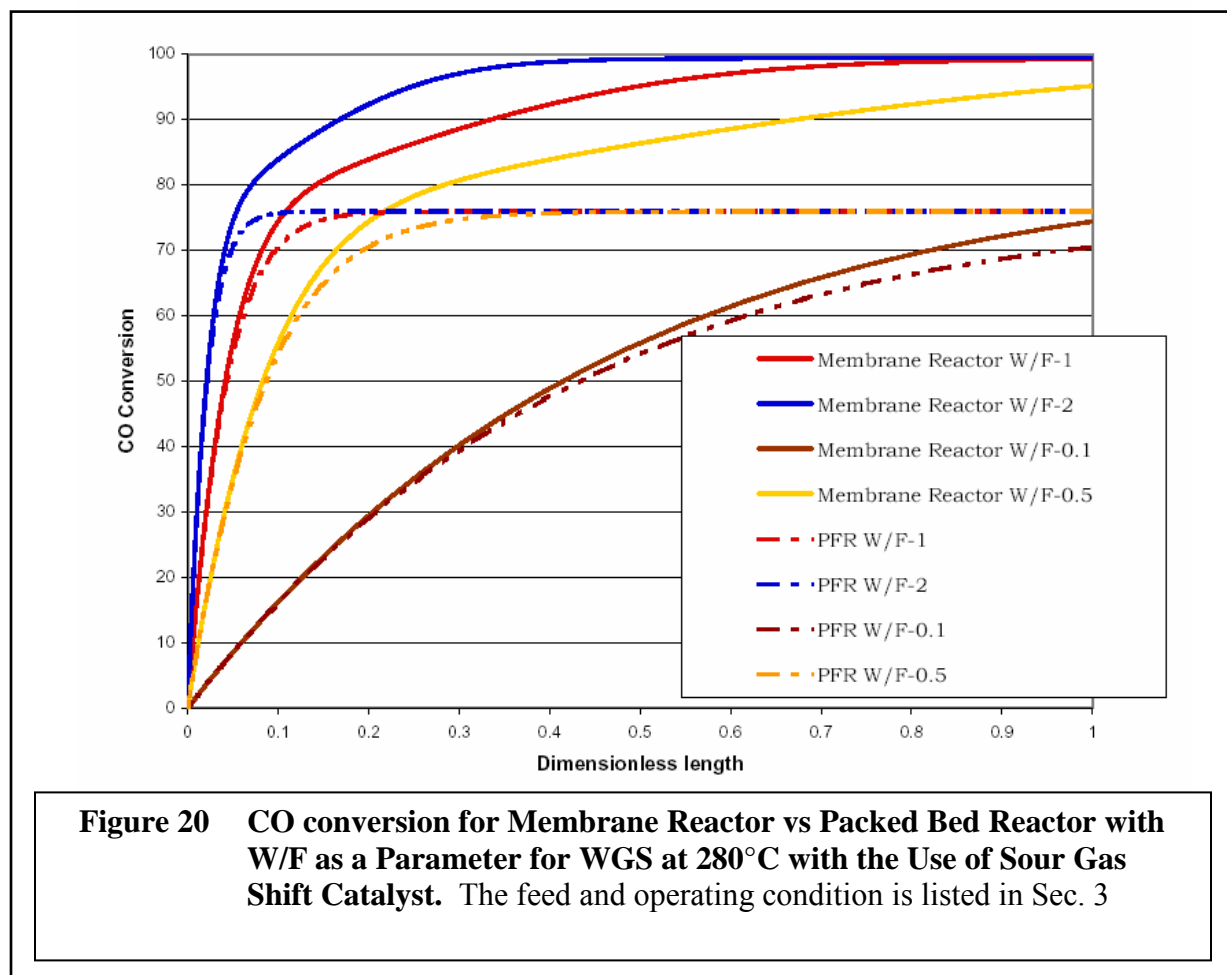
CO 0.033 m³/(m²-Hr-atm)
 CO₂ 0.25 m³/(m²-Hr-atm)
 H₂O 0.0898 m³/(m²-Hr-atm)
 H₂ 2.5 m³/(m²-Hr-atm)
 N₂ 0.033 m³/(m²-Hr-atm)

The sour gas shift catalyst, i.e., Co/MoS₂, is used in this simulation,

Rate Expression = $k \cdot (1 - \beta) \cdot P_{CO}^{0.8} \cdot P_{H_2O}^{0.29} \cdot P_{CO_2}^{-0.07}$
 Reaction rate constant [gmole/(gr-catal.sec.atm^{0.4})] $k = k_0 \cdot \exp(-5950 / (R \cdot (T + 273)))$
 Preexponential factor [gmole/(gr-catal.sec.bar^{0.4})] $k_0 = 6.0$

Our simulation (Figure 2) shows that the membrane reactor can convert CO nearly completely as opposed to ~75% conversion of the CO, i.e., about 3% residual CO in the exit, by the packed

reactor under the condition simulated, i.e., 280°C and H₂/CO ratio = 1.6. The packed bed reaches equilibrium rather quickly, about 0.1 to 0.3 bed length, indicating that the catalyst reaction kinetic parameters chosen can deliver a very fast reaction at this condition. The W/F studied here ranges from 0.1 to 2. As expected, when the W/F is very small, such as W/F=0.1, the reactor is not sized enough to achieve a complete completion even for the MR. However, when the W/F increases to 0.5 and above, a nearly complete conversion is observed for the packed bed. Again, the simulation will be revised after the experimentally determined catalytic kinetic parameters become available to us. Nevertheless, the simulation here clearly demonstrates that the CO conversion can be nearly complete using the MR due to the removal of hydrogen product to overcome the limitation imposed by the equilibrium.



Hydrogen recovery is also preformed to show whether the membrane surface area used for the WGS reactor is sufficient to recover the hydrogen produced. It appears that when W/F=1 and above, a nearly total recovery of hydrogen produced by the membrane is possible as shown in Figure 3. For the W/F<1, an additional hydrogen membrane area may be required for the recovery of hydrogen. The effect of feed pressure on CO conversion is presented in Figure 4. When the feed side pressure increases, in addition to the enhancement of the reaction rate by the

feed pressure according to the reaction kinetics, the permeate flux is also enhanced significantly. Thus, it is expected that the membrane reactor performance is enhanced with the feed pressure increase. Figure 4 shows the CO conversion vs feed pressure for $W/F=1$. The conversion is enhanced as the feed pressure increases from 40 to 120bar, representing the pressure range of existing coal gasifier technologies. The effect of pressure on hydrogen recovery is also simulated in Figure 5. As expected, more hydrogen is recovered with the shorter bed when the feed pressure is higher. Finally the residual CO concentration in the product is simulated for both membrane and packed bed reactor. Since the packed bed reactor reaches equilibrium at $\sim 75\%$ conversion, the residual CO concentration in the product is about 35,000 ppm CO on the dry basis as shown in Figure 6. On the other hand, the membrane reactor can deliver the concentration at ~ 800 ppm CO in the final hydrogen product as a result of the enhanced conversion and the separation by the membrane. In this study, no optimization has been performed. Thus, the actual level of CO in the membrane reactor could be lower.

Figure 21 Hydrogen Recovery in the Membrane Reactor with W/F as a Parameter.

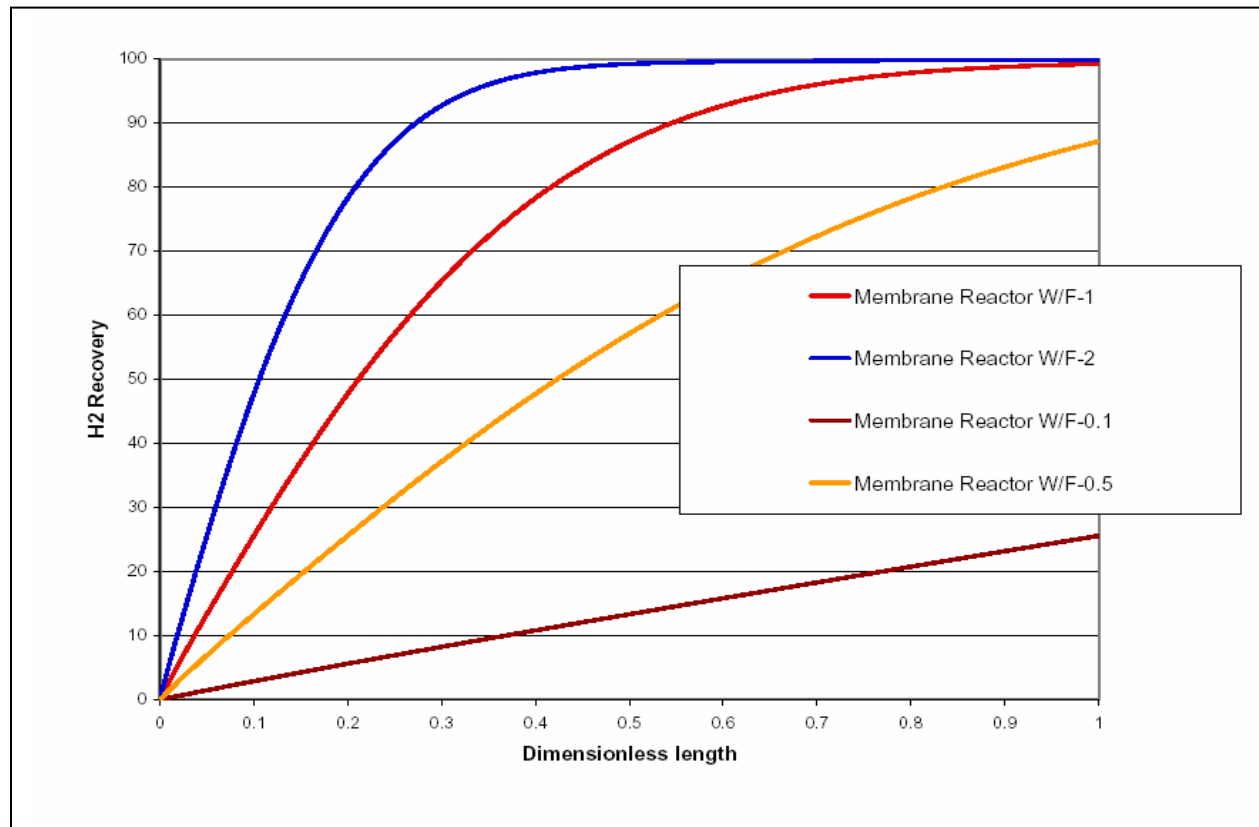


Figure 21 Hydrogen Recovery in the Membrane Reactor with W/F as a Parameter.

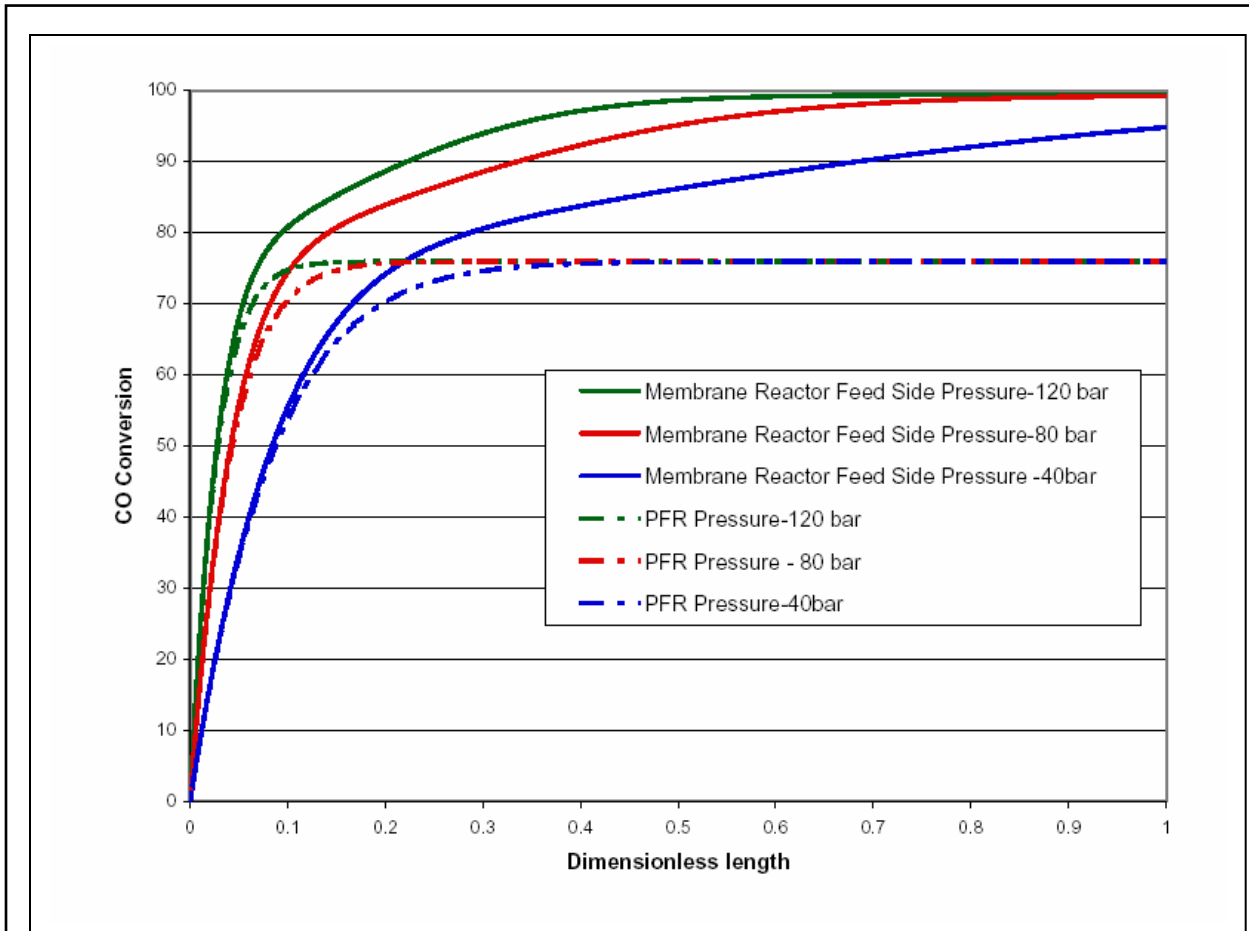


Figure 22 CO Conversion in a Membrane Reactor with Feed Pressure as a Parameter. The feed and operating condition is listed in Sec. 3.

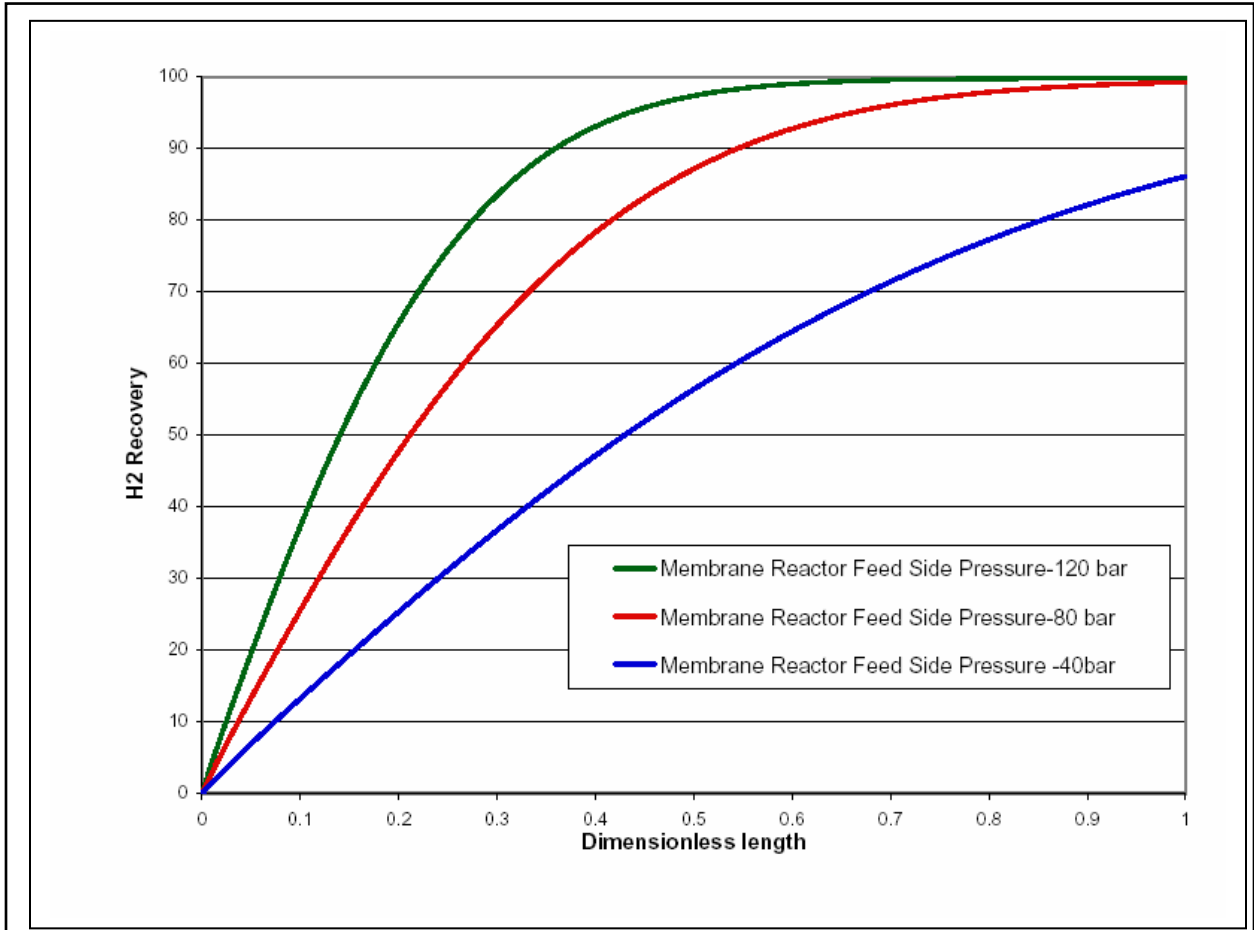
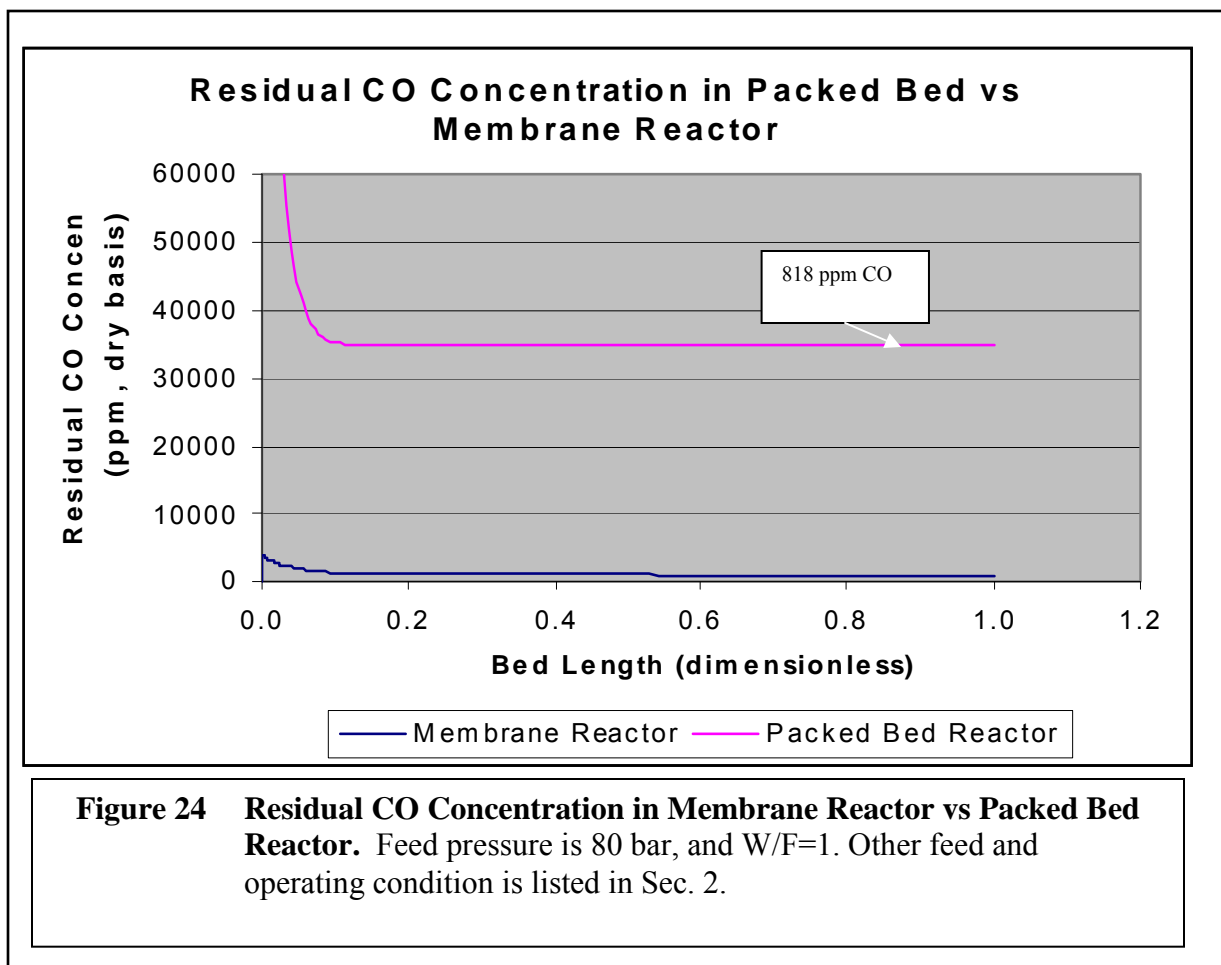


Figure 23 Hydrogen Recovery in a Membrane Reactor with the Feed Side Pressure as a Parameter. The rest of the operating condition is listed in Sec. 3



In summary, our simulation has demonstrated the advantage of the membrane reactor to achieve a nearly complete conversion of CO using Co/Mo-sulfide catalyst for the process we proposed without the pretreatment for sulfur removal. Experimental study is planned in the future to obtain the catalyst kinetic parameters and the CO conversion to verify the mathematical prediction.

Effect of Hydrogen Purity on Hydrogen Recovery Ratio... A relationship for hydrogen purity and its CO contaminant vs % hydrogen recovered is established here to demonstrate the trade-off relationship.

H₂ FROM COAL VIA CMS-WGS MEMBRANE REACTOR

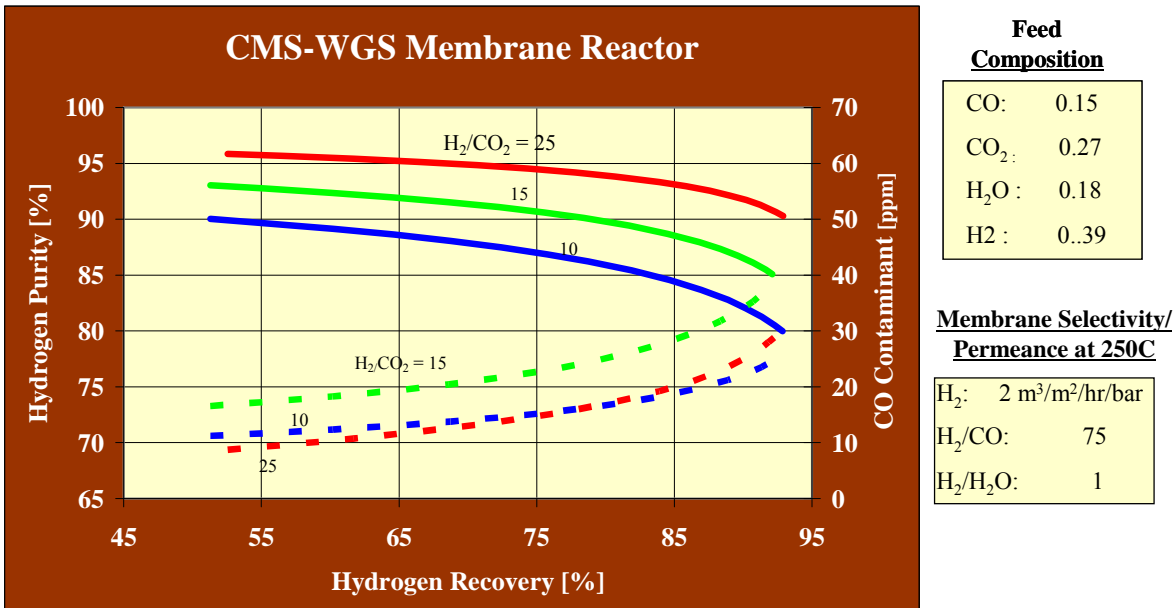
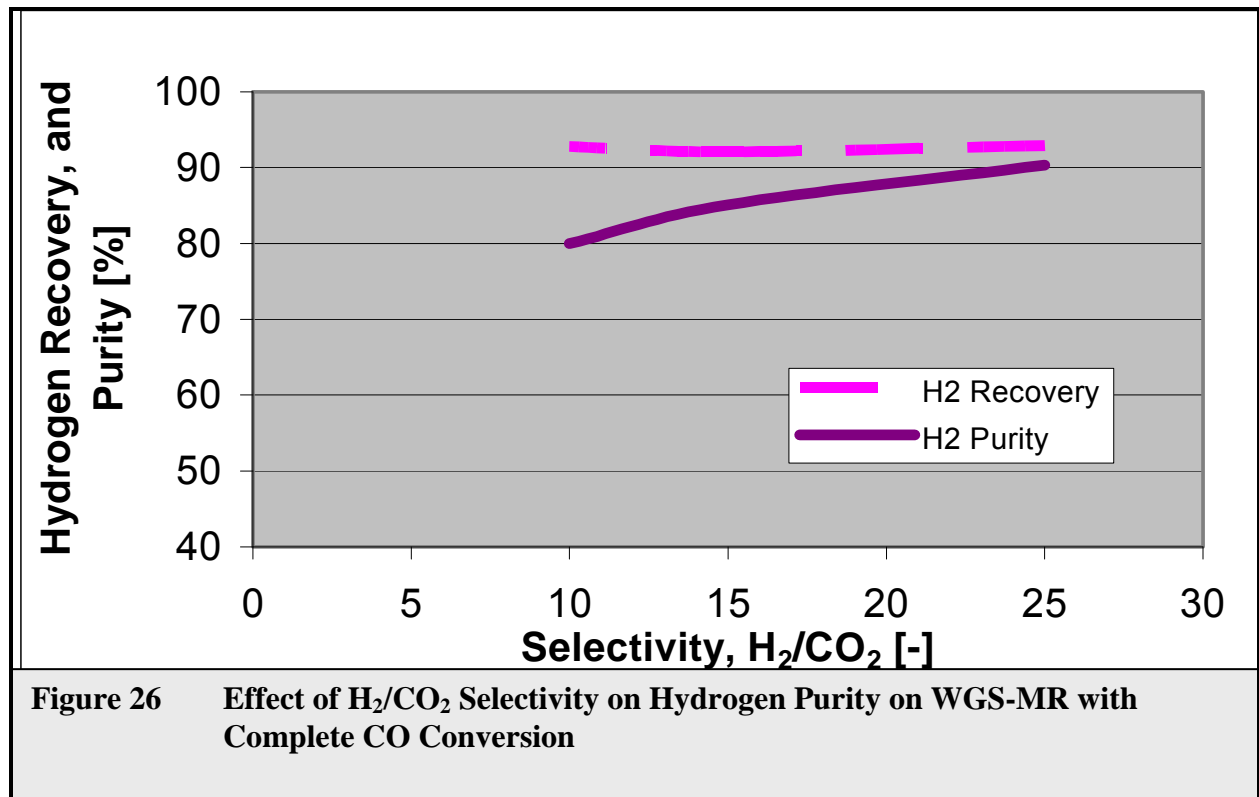


Figure 25 Hydrogen Purity and CO Contaminant Level for the WGS-MR with A Nearly Complete Conversion of CO and the Use of Nearly Stoichiometric H₂O/CO Ratio.

Hydrogen purity and CO contaminant level vs % hydrogen recovered is presented in Figure 6 for the membrane with hydrogen permeance of 2 m³/m²/hr/bar and the selectivity of H₂/CO=75. In comparison with the membrane property employed in Sec. 4.2 for verification, the hydrogen permeance used here is lower while the selectivity is higher. As indicated in Sec. 4.2, a membrane with a higher hydrogen permeance was selected to maximize the hydrogen recovery ratio with the lab scale reactor we used there. Thus, a lower hydrogen permeance with a higher selectivity used here is in-line with the properties of the CMS membranes we have produced thus far. In addition, our typical H₂/CO₂ selectivities range from <5 to >25 at this temperature are selected, depending upon the hydrogen permeance required. For hydrogen permeance of 2 m³/m²/hr/bar, a H₂/CO₂=10 is considered as our base case. A typical coal gasifier off-gas composition was adopted here (see Figure 6). The H₂O/CO ratio used in this simulation is 1.2.

For the selectivity of H₂/CO₂=10, our simulation shows that the hydrogen purity of 80% and CO contaminant of 25 ppm can be produced at 90% hydrogen recovered. To enhance the purity to 90% the recovered ratio diminishes to ~55%. Thus, it is not practical to enhance the hydrogen

purity using the membrane with $H_2/CO_2=10$. Since majority of impurity is CO_2 , to enhance the purity can be most effectively accomplished with the use of the membrane with a higher H_2/CO_2 , we perform some sensitivity analysis on the variation of H_2/CO_2 on the hydrogen purity vs hydrogen recovered. The hydrogen purity can be enhanced to 92% with the 90% hydrogen recovered. Its corresponding CO contaminant level is ~ 30 ppm. On the other hand, if the hydrogen recovered of 80% is acceptable, hydrogen purity approaches 95%. Figure 7 presents the effect of H_2/CO_2 selectivity on hydrogen purity at the recovery ratio of 92%. The purity will increase from 80 to 90% with the H_2/CO_2 selectivity increase from 10 to 25. In summary, 90% hydrogen produced from the H_2+CO in the feed can be recovered via our proposed WGS-MR process. Its purity level ranges from 80 to 92% depending upon the H_2/CO_2 ratio. If the purity of 95% is required, the hydrogen recovery ratio will drop to 80% level for the membrane with $H_2/CO_2=25$.



Management of Proposed Single Stage LTS... The exothermic WGS reaction could cause the reactor temperature to rise significantly. To protect the catalyst, an effective thermal management is essential. In the past, the WGS reaction was primarily implemented in the steam reformed stream containing 7 to 10% CO . Thus the temperature rise is not as severe as the WGS for the coal gasifier off-gas, which contains $>30\%$ CO . To accomplish the process intensification objective, instead of using the conventional multiple inter-stage cooler, we have developed an elegant solution to integrate the thermal management into the membrane reactor.

An innovative membrane was also developed to accomplish this objective. Due to the proprietary nature of this innovative thermal management approach, no detailed discussion is made here.

4.6. Benchmarking against Other Hydrogen Production Processes

The seven cases of the hydrogen production from coal presented in the literature have been based here for benchmarking against our proposed process. The major process features discussed in these cases are summarized below:

Table 7 Processes for Hydrogen Production from Coal discussed in the Literature [Ref. 3]

Technology Maturity	Case #	Thermal Efficiency (%)	Capital Cost [\$MM]	RSP* of H ₂ [\$/MM Btu]	CO ₂ Sequestration	Gas Clean-up	H ₂ /CO ₂ Separations
Existing Technology	1	63.8	367	6.83	no	low	PSA
	2	59	416	8.18	yes	low	PSA
Advanced Technology	3	75.5	425	5.89	yes	high	Membrane
	4	62.4	455	5.42	no	Low (??)	PSA
	5	56.5	475	5.64	yes	Low (??)	PSA
Futuristic Technology	6	64.5	517	2.79	yes	high	PSA
	7	65.2	509	2.40	yes	high	Membrane

*RSP: required sale price

The two cases utilizing membrane technologies, Case #3&7, are detailed below:

Table 8 Process Features of Two Cases (Cases #3 & 7) involving the use of Membranes

	Membrane Type	Temp. °C	Pressure Drop	Recovered Component	Reject Component	Energy Recovery	CO ₂ Disposal
Case 3	Ceramic	600	100 psi	H ₂	Combusted (O ₂)	HRSG	Compression
Case 7	Advanced	600	Not specified	CO ₂	H ₂	SOFC	Compression

In this report we focus on the ceramic membrane used in Case #3; no advanced membrane as in Case #7 of futuristic technology is taken into consideration. The detail of the process scheme for Case #3 is presented below:

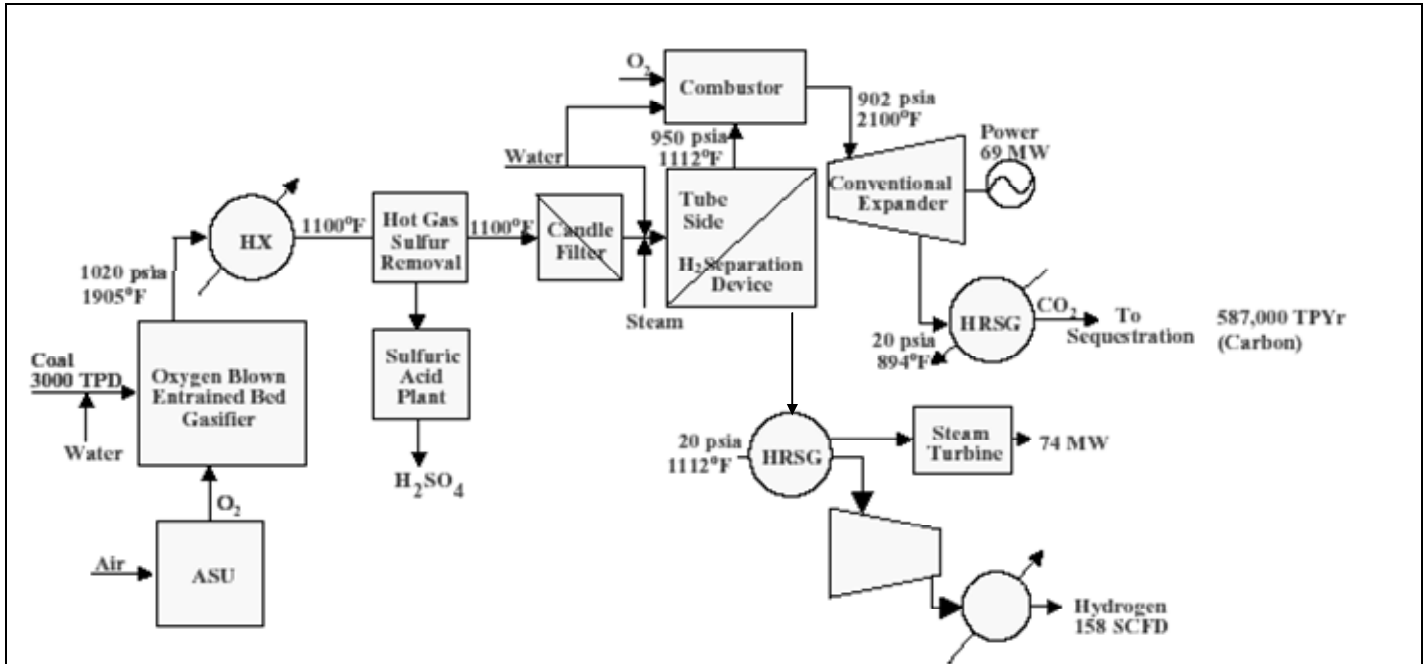


Fig. 4. Production of hydrogen using advanced gasifier, gas cleaning, and membrane technologies (Case 3).

•Table and Figure are adapted from the reference by Stiegel, G. J., and M. Ramezan, "Hydrogen from coal gasification; An economical pathway to a sustainable energy future", *International J. of Coal Geology*, 65, 173(2006).

Media and Process Tech Inc.

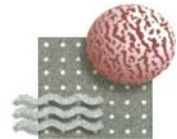


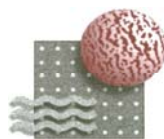
Figure 27 Production of Hydrogen using Advanced Gasifier, Gas Cleaning, and Membrane Technologies (Case #3)

The production economics from the existing coal gasification process and the Case #3 is summarized in the table below against the existing commercial hydrogen production via methane steam reforming:

Table 9 Economic Analysis for Hydrogen from Existing and Advanced Coal Based Process vs from Steam Methane Reforming

<div style="text-align: center; background-color: #800000; color: white; padding: 5px;"> Economic Analysis <i>Hydrogen from Existing and Advanced Coal Based Process vs from Steam Methane Reforming</i> </div>								
Technology Maturity		Case # cited in Ref. 1	Thermal Efficiency (%)	Capital Cost [\$MM]	RSP* of H ₂ [\$/MM Btu]	CO ₂ Sequestration	Gas Cleanup Temperature	H ₂ /CO ₂ Separations
Existing Technology	Coal Gasification	1	63.8	367	6.83	no	low	PSA
	Coal Gasification	2	59	416	8.18	Yes	Low	PSA
	Steam methane Reforming				4.60	no	Not applicable	PSA
	Steam methane Reforming				5.70	yes	Not applicable	PSA
Advanced Technology	Membrane based, proposed in Ref. 1	3	75.5	425	5.89	yes	high	Membrane

*RSP: required sale price



Media and Process Tech Inc.

Evidently the existing processes are not economically competitive against the natural gas reforming process (based upon the RSP vs current hydrogen production cost) if the CO₂ sequestration is essential for the process. CO₂ sequestration adds \$1.40/MM Btu H₂ to the conventional technology, i.e., from \$6.80 to 8.20/MM Btu (Case #1 and 2) as estimated in this reference. This increased price is considered not favorable in comparison with hydrogen produced from natural gas costing \$4.60 and 5.70/MM Btu without and with CO₂ sequestration listed in this publication. To become competitive, the advanced technology (Case #3) is suggested to include a hot gas cleanup (HGCU) and high temperature hydrogen separative membrane (600°C). With the efficiency improved by the high temperature operation and the

avoidance of the scrubber operation can then off set the cost increase of the CO₂ sequestration and becomes competitive, i.e., \$5.89 vs \$5.70 of the proposed vs existing steam methane reforming respectively. Following the same vein of the process concept presented in Case #3, we examined our membrane reactor technology with the specific focus on the reduction of the pre-treatment requirement and the maturity of the membrane and its associate technologies, which is discussed in the next section.

Use of Our Proposed CMS Membrane-based Process for Case #3... The objective of our project is to follow a similar strategy adopted y Case #3 as addressed in Ref. #3. Instead of the high temperature ceramic membrane (e.g., ionic conductive membranes), however, we use our membrane technology, which is readily available or near commercialization stage for our proposed process condition. Specifically the features of our proposed process include:

- Elimination of the hot gas clean up (HGCU) via the use of our sulfur resistant CMS membrane. HGCU technology, although very efficient, remains to be developed and demonstrated.
- Elimination of the amine scrubber as the process proposed in the Case #3.
- Instead of the high temperature membrane operation in Case #3, our CMS membrane can be operated at 150 to 300°C, which faces much less challenge in terms of the hardware design.
- Sour gas shift (SGS) can be used to accomplish the water gas shift reaction without the pre-treatment of sulfur removal at a high temperature. Hot gas clean-up (HGCU) could be very efficient for sulfur removal; however, the technology remains to be developed and demonstrated.
- To recover the heat generation from the WGS to improve power generation efficiency, our 1st stage WGS reaction will be a single bed conventional packed bed with post heat-exchanger to recuperate the energy, while the 2nd stage via the CMS membrane can be operated with in-situ thermal management to achieve a nearly total conversion of CO. Thus, a nearly complete conversion of CO can be accomplished with a simple and compact system.

The CO₂ sequestration can be accomplished via the two options:

- If H₂S can be disposed along with CO₂, then, the hydrogen/electricity co-production and CO₂ sequestration can be accomplished without sulfur removal. A proprietary process for CO₂ and H₂S removal and then preparation of CO₂ for sequestration is currently under development by us.
- If H₂S cannot be disposed along with CO₂ sequestration for environmental reasons, we can insert a scrubber after hydrogen removal. Thus, the scrubber size and cost can be reduced significantly since the stream size after hydrogen removal is much reduced.

A process scheme based upon Case #3 incorporating the above features has been prepared for the use of our proposed WGS/CMS-MR as presented below:

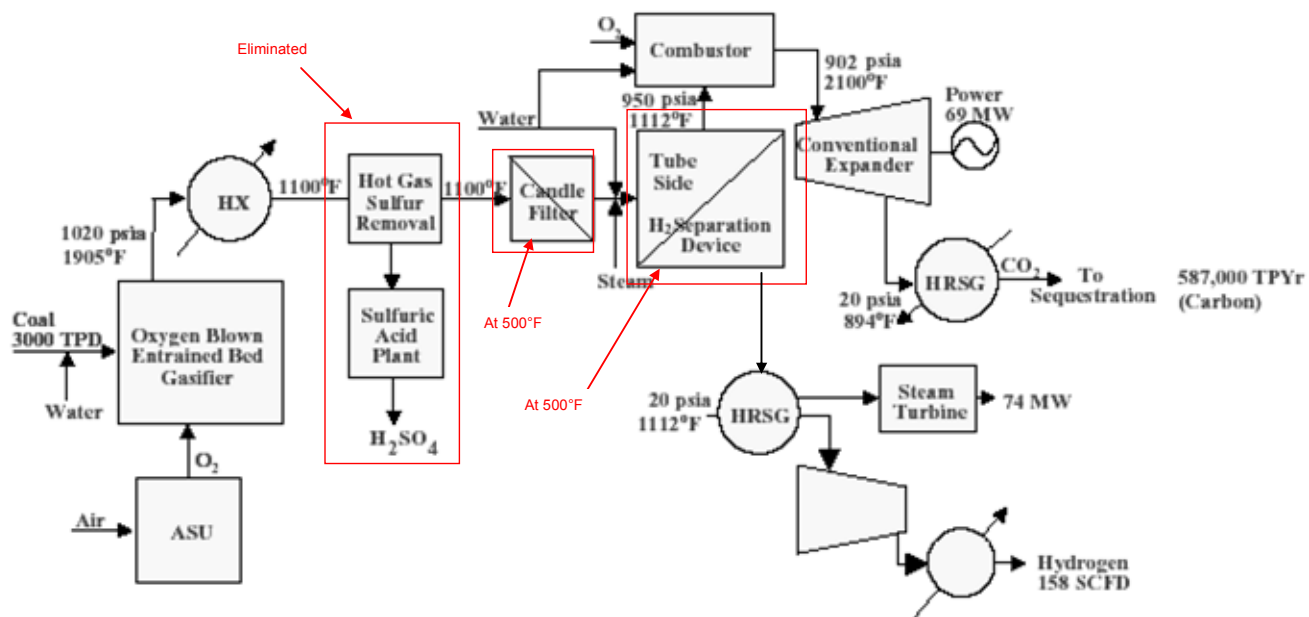


Fig. 4. Production of hydrogen using advanced gasifier, gas cleaning, and membrane technologies (Case 3).

•Table and Figure are adapted from the reference by Stiegel, G. J., and M. Ramezan, "Hydrogen from coal gasification; An economical pathway to a sustainable energy future", International J. of Coal Geology, 65, 173(2006).

Media and Process Tech Inc.

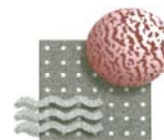
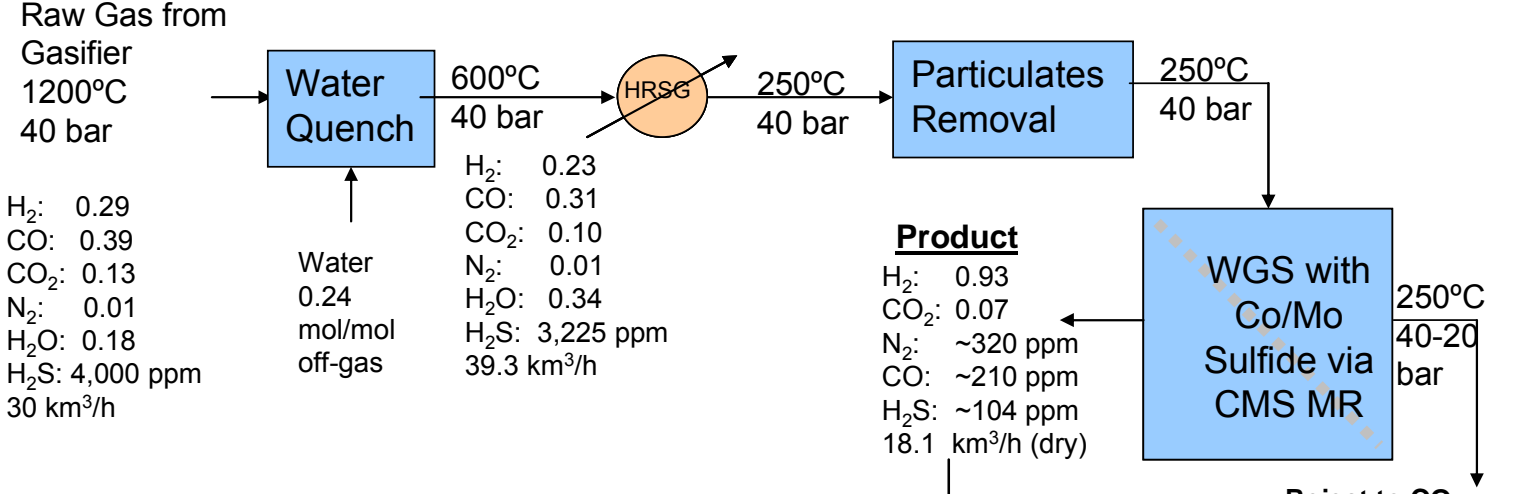


Figure 28 Production of Hydrogen based upon Case #3 Incorporating Process Features offered by our Proposed WGS/CMS-MR (indicated in red).

Hydrogen Production from Coal
 No Sulfur Removal Pre-treatment for WGS, No Hot Gas Clean-up Requirement,
 Minimum Excess Water Addition and Use of Co/Mo WGS Catalyst

Based upon Carbon Molecular Sieve (CMS) H₂ Selective Membrane Technology



H₂: 0.29
 CO: 0.39
 CO₂: 0.13
 N₂: 0.01
 H₂O: 0.18
 H₂S: 4,000 ppm
 30 km³/h

Water
 0.24
 mol/mol
 off-gas

H₂: 0.23
 CO: 0.31
 CO₂: 0.10
 N₂: 0.01
 H₂O: 0.34
 H₂S: 3,225 ppm
 39.3 km³/h

Membrane Reactor Performance Summary

CO Conversion (%)	99%
H ₂ Recovered*	80%
H ₂ O/CO Ratio in the feed to WGS (minimum excess water addition)	1.1

• Additional H₂ recovery can be achieved through stream recycling.

To Power Generation or to Polishing Step for H₂S and CO Clean-up and CO₂ removal to achieve 99+% purity

Abbreviation
 WGS: water gas shift
 HRSG: heat recovery steam generator
 MR: membrane reactor

Media and Process Tech Inc.

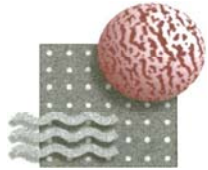


Figure 29 Overall Process Scheme for Hydrogen Production from Coal Gasifier Off-gas via WGS-MR with Our Hydrogen Selective CMS Membrane

An example of the proposed process is presented in Figure 5. With the above features in pre- and post-treatment and the reactor operation, we initiated the process simulation study for WGS-MR using the mathematical model developed to determine the steam sizes and their compositions.

Unique process features include:

1. Water quench is employed to lower the gasifier off-gas temperature to the level acceptable for HRSG (heat recovery steam generator). The amount of water added is controlled to the level sufficient for the water gas shift reaction (i.e., H_2O/CO ratio = ~ 1.4 in this case). Thus, the energy stored in the gasifier off-gas is not wasted for the sake of cooling or WGS. In addition, the sour gas shift catalyst is active at a high temperature; thus, the process does not rely upon the increased H_2O/CO ratio to achieve the conversion of CO. In short, the pre-treatment requires minimum steam addition; thus, the latent energy stored in the off-gas is not wasted as a result of cooling requirement.
2. The only gas cleanup requirement for this proposed process is particulates removal before entering the packed bed of the WGS. Under this proposed process, this removal can be implemented at 280°C right before the WGS. Thus, the conventional particulates removal technology can be applied. No hot gas cleanup technology (HGCU) is required.
3. WGS reaction by the Co-/Mo-sulfide catalyst (i.e., sour gas shift) was employed here. The first stage is a single stage, adiabatic WGS reaction with the conventional packed bed. Here we take the advantage of the extremely high reaction kinetics of WGS at the high CO concentration of the feed and the high temperature of the reactor. The use of the packed bed is expected to be simple and likely as efficient as the membrane reactor due to the extremely high reaction rate when the CO concentration is high at the high temperature (exit at the temperature near 900°F, the maximum allowable temperature). The less than desirable equilibrium conversion of CO at this high temperature can be compensated for by the use of the membrane reactor as a 2nd stage.
4. After the 1st stage WGS, a hydrogen separator is installed, which also functions as a WGS/MR. This reactor is operated as an isothermal reactor at $\sim 280^\circ\text{C}$ equipped with the in-situ thermal management. Thus, the membrane reactor can be operated in a simple and compact fashion, as opposed to the traditional MR (such as Pd based), whose thermal management technique remains to be resolved. The thermal management of the WGS/CMS-MR is our proprietary technology, which will be addressed separately.
5. Residual hydrogen, which cannot be removed by the membrane efficiently, will be further utilized in turbines after CO_2 and H_2S removal. A proprietary CO_2 removal process is currently under development by us in conjunction with our CMS membrane. If this

proprietary method is not applied, the conventional sour gas removal via scrubbing can be implemented here. Since the stream size is reduced to about 50% or less of the original size, the capital and operating costs using the conventional scrubber technology are much reduced. Also the concentrations of CO₂ and H₂S is higher, which may improve the removal efficiency.

Since the CMS membrane can be fabricated for high pressure applications, the hydrogen permeate can be maintained at a pressure high enough (>16 bar) for over-the-fence use without post compression. In summary, our proposed CMS-WGS/MR with the use of the sour shift gas catalyst offers an unparallel process opportunity to eliminate the HGCU. Instead, a mild temperature particulate removal is adequate for our proposed process. Thus, the pretreatment cost is reduced dramatically using the existing available technology. Also the steam addition to the reactor can be minimized since the WGS reaction can be enhanced with the membrane reactor to compensate for the lower steam to CO ratio. Based upon the economics performed for Case #3 (Table xxx), we believe that the proposed WGS/CMS-MR can meet the hydrogen production economics.

5. CONCLUSIONS

The conclusions drawn from this study are presented below:

Preparation of CMS Membranes on Stainless Steel (SS) Substrate

Our preliminary study on the deposition of the CMS membrane on stainless steel substrate concludes:

- The CMS membrane synthesis protocol we developed originally for the ceramic substrate was unfortunately not successful on the stainless steel substrate commercially available during Yr I. Our characterization results indicated two major sources of defects present in the stainless steel substrate, which contributed to the poor quality of the CMS membranes. They are (i) leaking from porous to non-porous transition (crimp) boundary at the endseal of the SS substrate, and (ii) the delamination of the ZrO₂ intermediate layer deposited on the stainless steel substrate (by the manufacturer) through the CMS membrane preparation.
- Near the end of the project period, a new batch of the SS substrate was received as the 2nd generation product from the supplier. Our characterization results confirmed that defects in the crimp boundary region no longer existed.

The thermal stability of the ZrO₂/SS substrate under the CMS membrane preparation condition remains to be re-evaluated in the future to determine the suitability of the ZrO₂/SS membrane as substrate for the preparation of the CMS membrane for hydrogen separation.

Preparation of Full Scale CMS Membranes and Modules

Our project focus has been placed on the use of our ceramic substrate. Major conclusions from the membrane and module preparation include:

- A significant number (i.e., 98) of full-scale membranes on ceramic substrates have been produced with an on-spec ratio of >76% during our first production trial. In addition, an innovative full-scale membrane module has been designed, which can potentially deliver >20 to 30 m²/module suitable for large-scale applications, such as power generation.
- Our CMS membrane functional performance and material stability were verified with a hydrocracker purge gas at a refinery pilot testing facility. No change in membrane performance was noted over the >100 hrs of testing conducted in the presence of >30% H₂S, >5,000 ppm NH₃ (estimated), and heavy hydrocarbons on the order of 25%. The excellent stability of these membranes under harsh environment opens the door for the use of our membrane in the WGS environment with the significantly reduced pretreatment requirement.
- Further, the membrane tested under this harsh environment was purposely poisoned by the contaminants present at the end of the test. This fouled membrane was regenerated

nearly completely, indicating the regenerability and robust of our CMS membrane in case of inadvertent contamination in field operation.

- A prototype ceramic membrane bundle/element has been fabricated for full-scale applications. With the replacement of the existing epoxy potting of our commercial product with the high temperature ceramic potting, the element can now be used at temperature $>500-600^{\circ}\text{C}$. Two bundle designs have been under preparation: heat exchanger-like and the candle filter-like. For the proposed applications at $200-300^{\circ}\text{C}$, both designs are considered suitable.
- The burst pressure has been performed for the single element and bundle. The single element can take the pressure $>1,500$ psi without burst. The bundle prepared during this period delivers the burst pressure at 500-750 psi. Although this pressure drop may be adequate for our proposed application, we are confident that the bundle can be re-designed with the objective of reaching a burst pressure of $>1,500$ psi.

Based upon our success in the initial manufacturing trial, the membrane material stability test, and the prototype module fabrication, we recommend the preparation of the field test membrane/module as the next step.

Mathematical Modeling of Water Gas Shift (WGS) Reaction via Membrane Reactor (MR)

To evaluate the improvement in hydrogen production via our proposed WGS/MR, a mathematical model has been established. Our conclusions from this modeling study include:

- Single stage water-gas-shift at low temperature (WGS-LTS) via a membrane reactor (MR) was studied through both mathematical simulation and experimental verification in this project. Using the kinetic parameters experimentally obtained by us, we were able to establish a mathematical model for the proposed WGS-MR.
- A series of experimental studies has been performed to verify the mathematical model prediction for the feed simulating the coal gasifier off-gas. The experimental results at various W/F's agree well with those obtained from the mathematical prediction. In addition the effect of sweep ratio on the CO conversion was experimentally performed; the results are consistent with the predicted conversion. Thus, we believe that the mathematical model we have developed is adequate for the simulation required by this project.
- Although the thermodynamic conversion of CO could be as high as $\sim 90\%$ in the LTS range, our proposed MR yields a reactor size that is 10 to $>55\%$ smaller than the comparable conventional reactor for a CO conversion of 80 to 90%. In addition, the CO contaminant level in the hydrogen produced via MR ranges from 1,000 to 4,000 ppm vs 40,000 to $>70,000$ ppm via the conventional reactor. The advantages of the reduced WGS reactor size and the reduced CO contaminant level provide an excellent opportunity for intensification of the hydrogen production process by the proposed MR.

- The effect of several operating parameters, including feed pressure, W/F and the sweep ratio, on CO conversion, hydrogen recovery and CO impurity level have been studied comprehensively using the mathematical model. The W/F shows the most profound effect on the CO conversion and the CO impurity level. Further study indicates that the membrane surface area instead of the W/F is in effect the key parameter which impact the CO conversion and CO impurity level.
- A preliminary optimization study has been performed in this period based upon the key operating parameters determined above. Our result shows that at 40 bar feed pressure a nearly complete CO conversion and >95% hydrogen recovery can be achieved with a CO impurity level at ~3500 ppm. If the hydrogen recovery ratio can be lowered, the CO impurity level can be reduced further.

Our mathematical model was verified with experimental results. This model also proves to be adequate for the WGS/MR we proposed for hydrogen production from coal-based syngas. A comprehensive optimization study based upon this model is recommended in the future.

Process Simulation for Coal Gasifier Off-gas

Based upon the results obtained above, a process simulation study was conducted around the use of WGS/MR with our CMS membrane for hydrogen production from coal gasifier offgas at 250°C. Our simulation employed (i) a near stoichiometric steam/carbon ratio and (ii) the use of the reaction kinetics for the sulfided catalyst available commercially. Our mathematical simulation on WGS-MR based upon the suggested pre- and post-treatment has concluded that

- A nearly complete CO conversion (i.e., 99+%) with the proposed CMS-MR can be accomplished. No cost minimization has been taken into consideration.
- ~90% of the hydrogen produced from the H₂+CO in the coal gasifier off-gas can be recovered via our proposed WGS-MR process. Its purity level ranges from 80 to 92% depending upon the membrane H₂/CO₂ selectivity of 10 to 25, respectively. If a H₂ purity of 95% is required, the hydrogen recovery ratio will drop to 80% for the membrane with H₂/CO₂=25.

Our simulation using the literature reaction kinetics for the Co/MoS₂ catalyst demonstrate similar process advantages identified with the conventional Zn/Cu catalyst, which was experimentally verified under this project. Experimental verification on the use of the sulfide catalyst for the proposed WGS/MR is recommended.

Benchmarking against Other Hydrogen Production Processes from Coal

According to the literature [Ref. 3], a MR in conjunction with the coal gasification could potentially deliver an economically viable hydrogen production process from coal, i.e., its economics is comparable to the existing methane steam reforming. Our CMS-based MR can be utilized for this proposed process. More importantly, the WGS reaction can be accomplished at a mild temperature without HGCP using our CMS-based membrane. As a result, the pretreatment can be streamlined significantly. In comparison with other emerging processes, additional advantages below can be drawn for our proposed WGS/MR process:

- Minimum water addition to the gasifier off-gas is proposed via water quench. The amount of water added is controlled to the level sufficient for the water gas shift reaction (i.e., H_2O/CO ratio = ~ 1.4 in this case). Thus, the energy stored in the gasifier off-gas is not wasted for the sake of cooling for WGS. This minimum water addition becomes technically feasible as a result of the use of the membrane reactor we proposed.
- The only gas cleanup requirement for this proposed process is particulate removal. This removal can be implemented at 280°C right before the WGS. Thus, the conventional particulates removal technology can be applied. No hot gas cleanup technology (HGCU) is required.
- WGS reaction by the Co-/Mo-S₂ catalyst (i.e., sour gas shift catalyst) can be employed here. Our mathematical simulation demonstrates the technical feasibility of a nearly complete CO conversion with this catalyst.
- Using the economics published in the literature as the base case, our proposed WGS-MR with the sulfide catalyst can deliver production economics comparable to existing hydrogen production cost via methane steam reforming. More importantly, our proposed process scheme does not rely on the development of the high temperature advanced membrane technology to justify the production economics as proposed in the literature. Preparation of the proposed hydrogen selective CMS membrane for field testing is recommended as the next step.
- After the 1st stage WGS, a hydrogen separator will be installed, which also functions as a WGS/MR. This reactor will be operated as an isothermal reactor at $\sim 280^\circ\text{C}$ equipped with the in-situ thermal management. Thus, the membrane reactor can be operated in a simple and compact fashion, as opposed to the traditional MR (such as Pd based), whose thermal management technique remains to be resolved. The thermal management of the WGS/CMS-MR is our proprietary technology, which will be addressed separately.
- Residual hydrogen, which cannot be removed by the membrane efficiently, will be further utilized in turbines after CO₂ and H₂S removal. A proprietary CO₂ removal process is currently under development by us in conjunction with our CMS membrane.
- Since the CMS membrane can be fabricated for high pressure applications, the hydrogen permeate can be maintained at a pressure high enough (>16 bar) for over-the-fence use without post compression.
- Since the delivery of CO to $\ll 10$ ppm is not practical with our technology, it is not possible to deliver H₂ directly to a PEM fuel cell. In our proposed process, PROX is treated as essential post treatment for the production of hydrogen as PEM fuel cell feedstock. Since the CO contaminant level from our WGS-MR is 20-30 ppm, PROX can be implemented economically and reliably.

In short, in addition to the improvement of the WGS reaction efficiency, a membrane reactor (MR) for the coal gasifier off-gas can reduce the capital and operating cost significantly for the pre- and post-treatment via process intensification before, during and after the WGS reaction. Using the economics published in the literature as the base case, our proposed WGS-MR with the sulfide catalyst can deliver the production economics comparable to existing hydrogen production cost from methane steam reforming. More importantly, our proposed process scheme does not rely on the development of the high temperature advanced membrane technology to justify the production economics as proposed in the literature. Preparation of the proposed hydrogen selective CMS membrane for field testing is recommended as the next step.

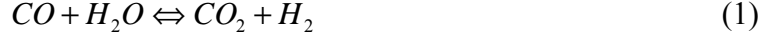
Literature Cited:

1. C. V. Ovesen, et. al. "A Microkinetic Analysis of the Water-Gas Shift Reaction under Industrial Conditions", *Journal of Catalysis* 158, 170-180 (1996)
2. Lund, C. R. F., "Effect of adding Co to MoS₂/Al₂O₃ upon the kinetics of the Water-Gas Shift", *I&EC Res.*, 35, 3067(1996).
3. Stiegel, G. J., and M. Ramezan, "Hydrogen from coal gasification: an economical pathway to a sustainable energy future", *International J. of Coal geology*, 65, 173(2006).

Acronyms

CMS	Carbon Molecular Sieve
Ea:	activation energy
HGCU:	hot gas clean up
HRSG:	heat recovery steam generator
LTS:	low temperature shift
M&P	Media and Process Technology, Inc
MR:	membrane reactor
PEM:	Proton exchange membrane
PFR:	packed fixed-bed reactor
PROX:	Preferential oxidation
SEM	Scanning Electro microscopic
SGS:	sour gas shift
SS:	stainless steel
W/F:	Ratio of catalyst dosage to feed rate
WGS:	water gas shift reaction

Appendix I Mathematical Model for Proposed Membrane Reactor for Water-Gas-Shift Reaction



$$r = k \frac{P_{CO} P_{H_2O}^{1.4}}{P_{H_2}^{0.9} P_{CO_2}^{0.7}} (1 - \beta) \frac{1}{P_t^{0.4}} \quad (2)$$

$$\beta = \frac{P_{CO_2} P_{H_2}}{K_e P_{H_2O} P_{CO}} \quad (3)$$

$$k = k_o \cdot \exp\left(-\frac{E_a}{RT}\right) \quad (4)$$

k_o is the preexponential factor, E_a is the apparent activation energy, P_j is the partial pressure of component j , P_t is the total pressure, β is the approach to equilibrium and K_g is the equilibrium constant for the water-gas shift reaction.

Mass transfer through the porous membrane is described by the following empirical equation:

$$F_j = U_j (P_j^F - P_j^P) \quad (5)$$

where F_j is the molar flux ($\text{mol}/\text{m}^2 \cdot \text{s}$), P_j^F the partial pressure of component j on the membrane feed side (bar), P_j^P the partial pressure of component j on the membrane permeate side (bar), and U_j the membrane permeance for component j ($\text{mol}/\text{m}^2 \cdot \text{bar} \cdot \text{s}$).

The mass balance on the feed side of the reactor packed with water gas shift reaction catalyst is described by the following equations for CO_2 , CO , H_2 , H_2O and an inert species (potentially used as a sweep gas or a blanketing agent; for catalytic water gas shift reaction, a practical sweep gas would be either steam or hydrogen, however):

$$\text{Feed side: } \frac{\partial n_j^F}{\partial z} = -\alpha_m U_j (P_j^F - P_j^P) + v_j A_c r^F \quad (6)$$

$$\text{Permeate side: } \frac{\partial n_j^P}{\partial z} = \alpha_m U_j (P_j^F - P_j^P) \quad (7)$$

$$j=1,2,\dots,n$$

$$\text{at } z = 0, \quad n_j = n_{j_o} \quad (8)$$

In eq. 6 and 7, n_j^F is the molar flow rate (mol/s) for species j on the feed side. n_j^P is the molar flow rate (mol/s) for species j on the permeate side, z is the reactor length variable (m), A_c the cross-sectional area available to flow for the reactor feed side (m^2), α_m the inner circumference

of the membrane (m), v_i the stoichiometric coefficient of component j and r^F the reaction rate expression.

The pressure drop in a packed bed can be calculated using the Ergun equation:

$$-\frac{dP^F}{dz} = 10^{-6} \frac{f (G^F)^2}{g_c d_p \rho^F} \quad (9)$$

$$\text{at } z = 0, \quad P^F = P_0^F \quad (10)$$

$$f = \left(\frac{1 - \varepsilon_v}{(\varepsilon_v)^3} \right) \left(1.75 + \frac{150(1 - \varepsilon_v)}{N_{Re}^F} \right) \quad (11)$$

$$N_{Re}^F < 500(1 - \varepsilon_v) \quad (12)$$

$$N_{Re}^F \equiv d_p G^F / \mu^F \quad (13)$$

where P^F is the feed-side pressure (bar), P_0^F the inlet feed-side pressure, μ^F the viscosity (Pa·s), d_p the particle diameter in the feed side (m), $G^F = \rho^F u^F$ the superficial mass flow velocity in the feed side (kg/m²·s), u^F the average velocity of the fluid, ρ^F the average density of the fluid (kg/m³), and g_c the gravity conversion factor equal to 1 in SI units.

The reactor conversion (based on CO, which is typically the limiting reagent) is defined by the following equation:

$$X_{CO} = \frac{n_{CO_0}^F - (n_{CO_{ex}}^F + n_{CO_{ex}}^P)}{n_{CO_0}^F} \quad (14)$$

where $n_{CO_0}^F$ is the inlet molar flow rate of CO and $n_{CO_{ex}}^F$ and $n_{CO_{ex}}^P$ are the CO molar flow rates at the exit of the reactor feed and permeate sides correspondingly (mol/s). The yield of product hydrogen, defined as the fraction of moles of CO fed into the reactor that have reacted to produce hydrogen, is given by the following equation:

$$Y_{H_2} = \frac{(n_{H_{2,ex}}^F - n_{H_{2,0}}^F) + (n_{H_{2,ex}}^P - n_{H_{2,0}}^P)}{n_{CO_0}^F} \quad (15)$$

where $n_{H_{2,ex}}^F$ and $n_{H_{2,ex}}^P$ are the hydrogen molar flow rates at the exit of respectively the reactor feed and permeate sides and $n_{H_{2,0}}^F$ and $n_{H_{2,0}}^P$ the H₂ molar flow rates potentially present at the inlet of the reactor feed and permeate sides (mol/s). $Y_{H_2} = 1$ when all of the CO has reacted completely to produce CO₂ and H₂.

Equations 1.7-1.10 can be written by defining the following variables and groups:

$$\begin{aligned}
n_o^F &= \sum_j n_{jo}^F; n_o^P = \sum_j n_{jo}^P; n^F = n_o^F \sum_j x_j^F; n^P = n_o^P \sum_j x_j^P \\
x_j^F &\equiv \frac{n_j^F}{n_o^F}; x_j^P \equiv \frac{n_j^P}{n_o^P} \\
y_j^F &= \frac{n_j^F}{n^F} = \frac{x_j^F}{\sum_j x_j^F}; y_j^P = \frac{n_j^P}{n^P} = \frac{x_j^P}{\sum_j x_j^P} \\
\Psi^F &\equiv \frac{P^F}{P_o^F}; \Psi^P \equiv \frac{P^P}{P_o^P}; \xi \equiv \frac{z}{L}; Pe_j^F \equiv \frac{n_o^F}{\alpha_m U_j P_o^F L}; Da \equiv \frac{A_c L}{n_o^F} \\
P_j^F &= y_j^F \cdot P^F = \frac{x_j^F}{\sum_j x_j^F} P_o^F \Psi^F; P_j^P = y_j^P \cdot P^P = \frac{x_j^P}{\sum_j x_j^P} P_o^P \Psi^P \\
MW_{ave}^F &= \frac{\sum_j x_j^F MW_j}{\sum_j x_j^F} \\
\rho^F &= \frac{P^F MW_{ave}^F}{RT} = \frac{P_o^F \Psi^F \sum_j x_j^F MW_j}{RT \sum_j x_j^F} \\
u^F &= \frac{Q^F}{A^F} = \frac{n_o^F RT}{P^F A^F} = \frac{n_o^F RT \sum_j x_j^F}{P_o^F \Psi^F A^F} \\
G^F &= \rho^F u^F = \frac{n_o^F \sum_j (x_j^F MW_j)}{A^F} \tag{16}
\end{aligned}$$

The equations equivalent to eqs 1.7-1.10 are

$$-\frac{d\Psi^F}{d\xi} = \frac{L}{P_o^F} \frac{f^F (G_m^F)^2}{g_c d_P^F \rho^F} \tag{17}$$

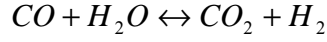
$$\text{Feed side: } \frac{dx_j^F}{d\xi} = -\frac{1}{Pe_j^F} \left(\frac{x_j^F}{\sum_j x_j^F} \Psi^F - \frac{x_j^P}{\sum_j x_j^P} \Psi^P \right) + v_j Da \cdot r^F \tag{18}$$

$$\text{Permeate side: } \frac{dx_j^P}{d\xi} = \frac{1}{Pe_j^F} \left(\frac{x_j^F}{\sum_j x_j^F} \Psi^F - \frac{x_j^P}{\sum_j x_j^P} \Psi^P \right) \tag{19}$$

$$\text{at } \xi = 0, \quad \Psi^F = 1, \quad \Psi^P = 1 \tag{20}$$

Appendix II: Material Balance of the Mathematical Model Developed in this Study.

Water gas shift reaction is as follows;



Mass balance for component CO along the reactor for counter-current flow system is as follows,

$$\frac{d(n_{CO}^F)}{dz} = \pi(R_o^2 - R_i^2) \cdot r_{CO} - 2\pi \cdot R_i \cdot K_{CO}(p_{CO}^F - p_{CO}^P) \quad (1) - \text{Feed side}$$

$$\frac{d(n_{CO}^P)}{dz} = -2\pi \cdot R_i \cdot K_{CO}(p_{CO}^F - p_{CO}^P) \quad (2) - \text{Permeate side}$$

From (1) and (2) we obtain

$$\frac{d(n_{CO}^F - n_{CO}^P)}{dz} = A_C \cdot r_{CO} \quad (3)$$

Where,

$$A_C \equiv \pi(R_o^2 - R_i^2)$$

Similarly, for component H₂O, CO₂ and H₂

$$\frac{d(n_{H_2O}^F - n_{H_2O}^P)}{dz} = A_C \cdot r_{H_2O} = A_C \cdot r_{CO} \quad (4)$$

$$\frac{d(n_{CO_2}^F - n_{CO_2}^P)}{dz} = A_C \cdot r_{CO_2} = -A_C \cdot r_{CO} \quad (5)$$

$$\frac{d(n_{H_2}^F - n_{H_2}^P)}{dz} = A_C \cdot r_{H_2} = -A_C \cdot r_{CO} \quad (6)$$

Add (3) and (5), we can get an equation with respect to C

$$r_{CO} + r_{CO_2} = A_C \cdot \frac{d(n_{CO}^F + n_{CO_2}^F - n_{CO}^P - n_{CO_2}^P)}{dz} = 0 \quad (7)$$

$$n_{CO}^F + n_{CO_2}^F - n_{CO}^P - n_{CO_2}^P = \text{const.} \quad (8)$$

Similarly, with respect to H

$$r_{H_2O} + r_{H_2} = 0 \quad (9)$$

$$n_{H_2O}^F + n_{H_2}^F - n_{H_2O}^P - n_{H_2}^P = \text{const.} \quad (10)$$

And O

$$r_{CO} + r_{H_2O} + 2r_{CO_2} = 0 \quad (11)$$

$$n_{CO}^F + n_{H_2O}^F + 2n_{CO_2}^F - n_{CO}^P - n_{H_2O}^P - 2n_{CO_2}^P = \text{const.} \quad (12)$$

Of course we don't need to make special forms such as (7), (9) and (11) because many expressions can be created. For example,

$$(3) + (6) = 0$$

$$(4) + (5) = 0$$

The following 5 graphs were obtained under the condition which is

Counter-current flow system

T = 250 °C, P_F = 3 atm, P_P = 1 atm, W/F_{CO} = 12.9(g-cat*hr/gmol CO)

Rich's base case

Note that the green lines in the following graphs are exactly same. (Figure 1, 2, 3 and 4)

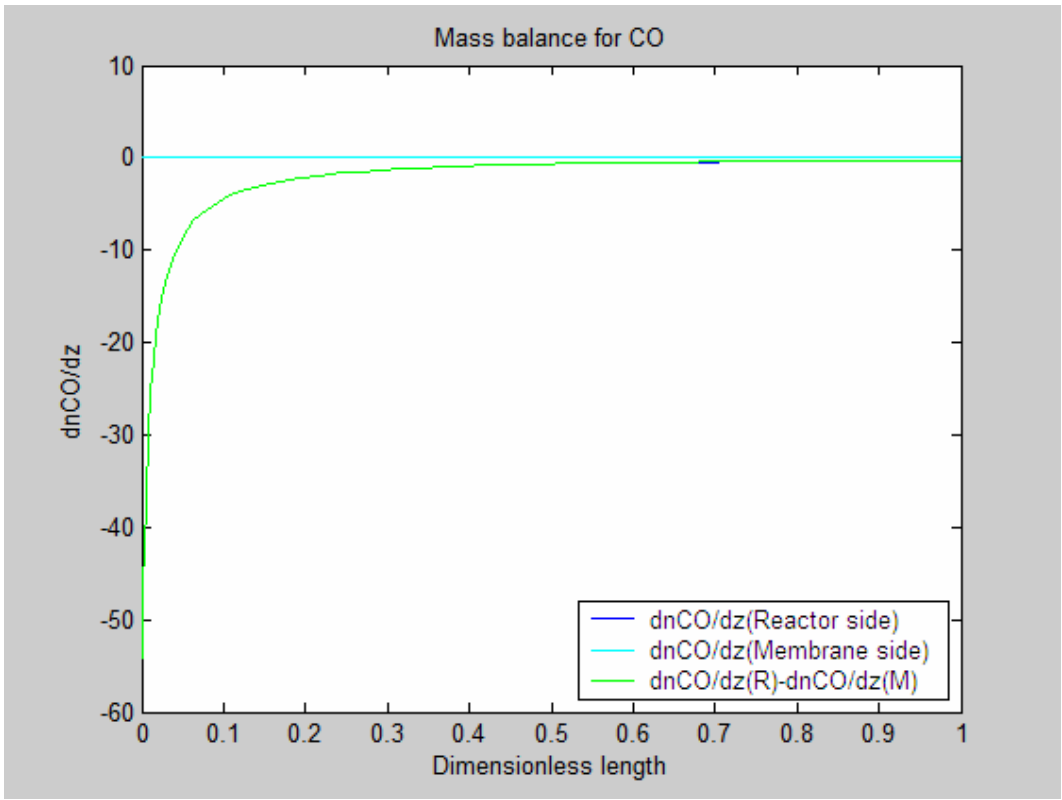


Figure 1 $\frac{dn_{CO}^F}{dz}$, $\frac{dn_{CO}^P}{dz}$, $\frac{dn_{CO}^F - dn_{CO}^P}{dz}$

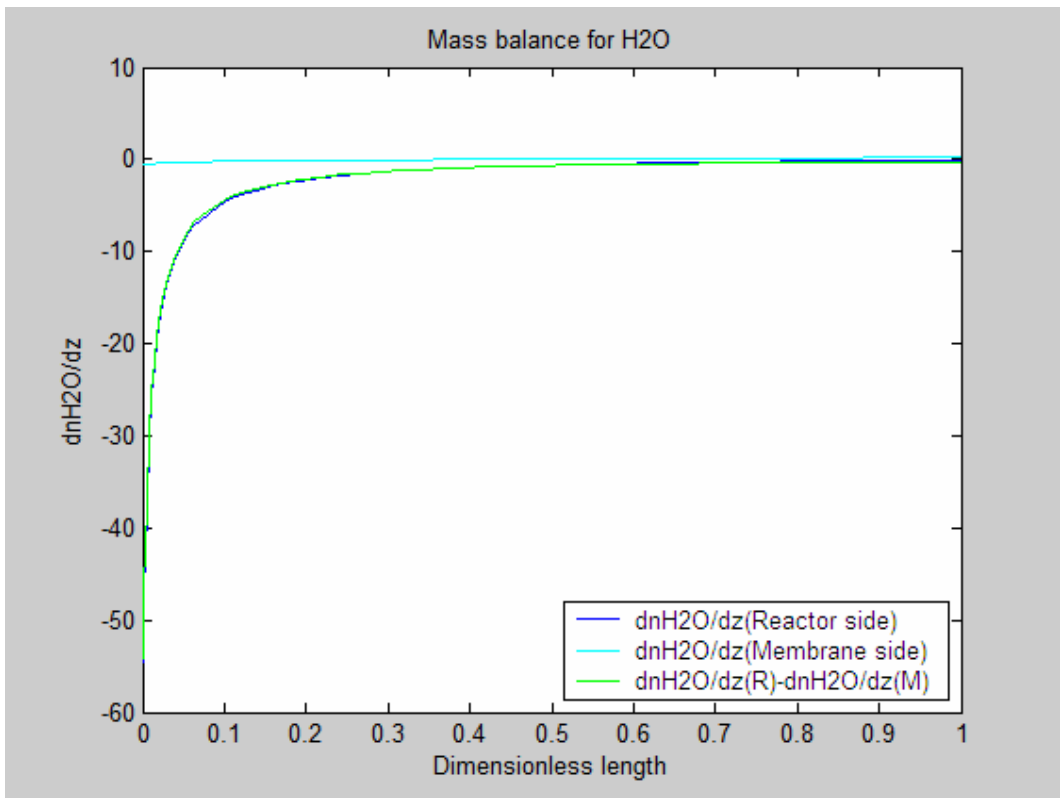


Figure 2 $\frac{dn_{H_2O}^F}{dz}$, $\frac{dn_{H_2O}^P}{dz}$, $\frac{dn_{H_2O}^F - dn_{H_2O}^P}{dz}$

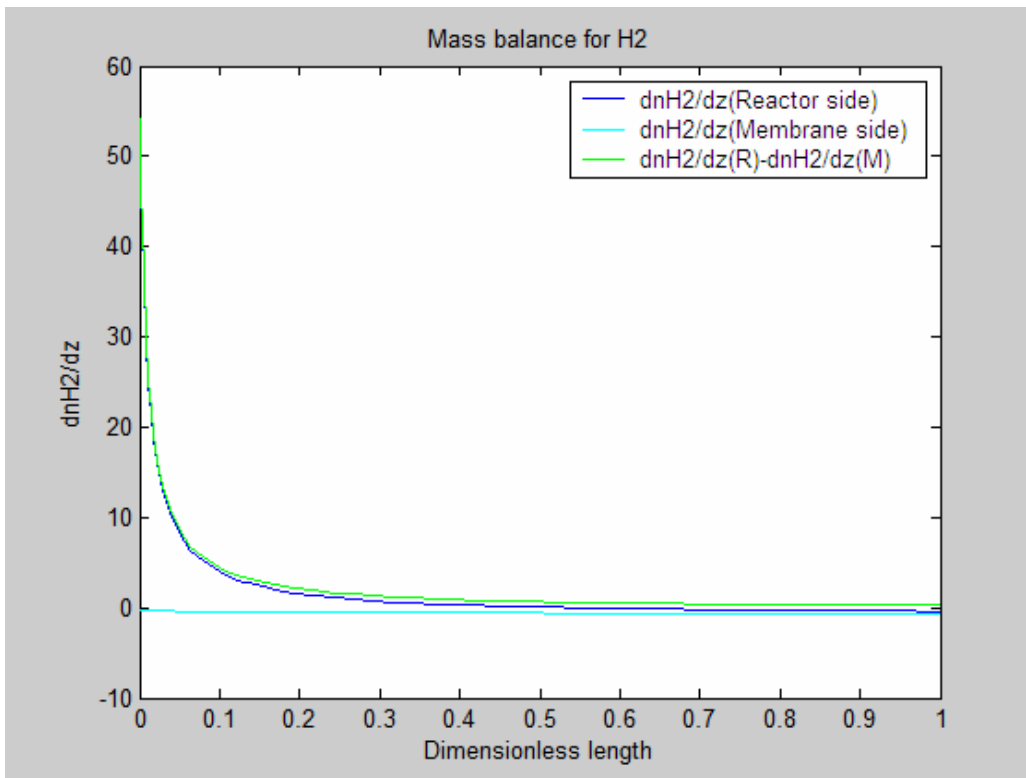


Figure 3 $\frac{dn_{H_2}^F}{dz}$, $\frac{dn_{H_2}^P}{dz}$, $\frac{dn_{H_2}^F - dn_{H_2}^P}{dz}$

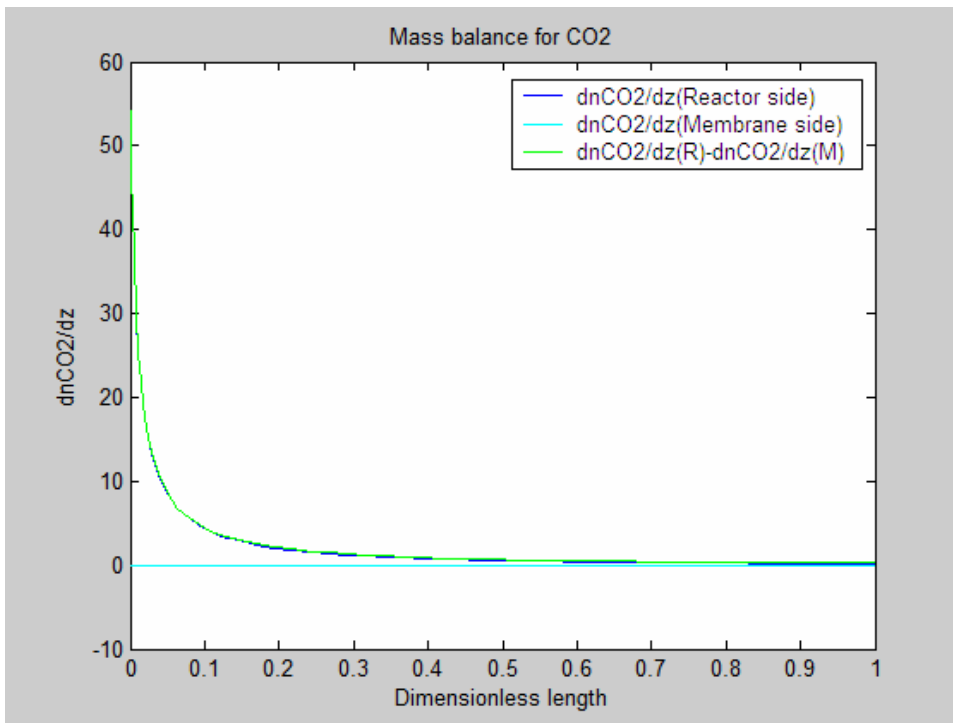


Figure 4 $\frac{dn_{CO_2}^F}{dz}$, $\frac{dn_{CO_2}^P}{dz}$, $\frac{dn_{CO_2}^F - dn_{CO_2}^P}{dz}$

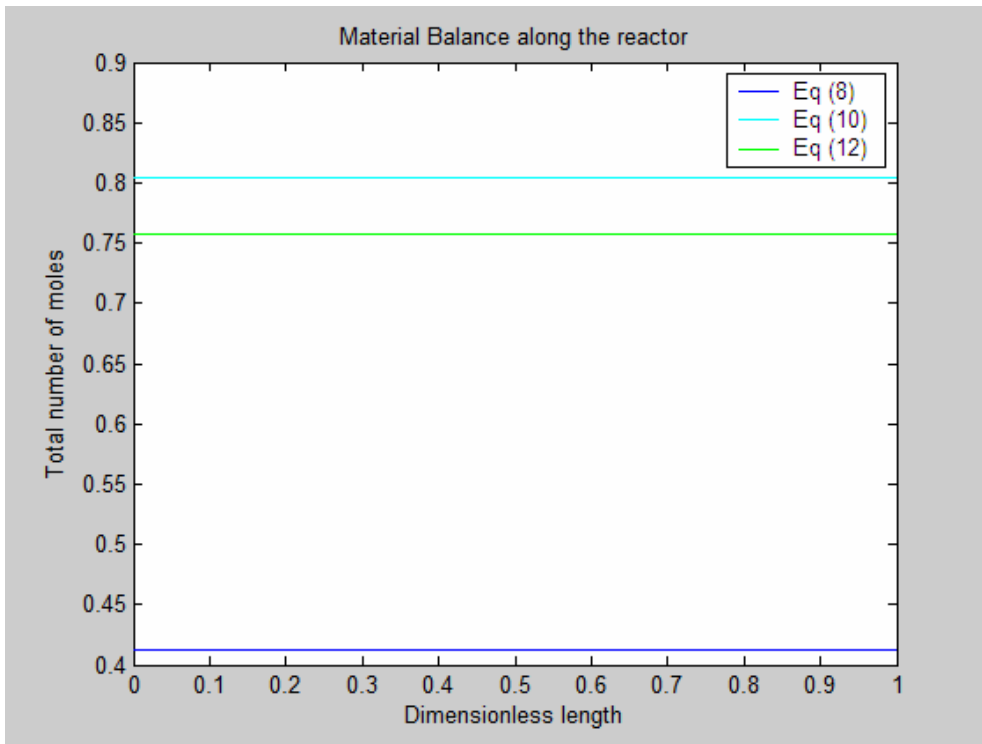


Figure 5 Eq. (8), (10) and (12)

In case of the co-current system, the sign for the permeate side must be changed. For example, if we get the mass balance for CO again, it goes

$$\frac{d(n_{CO}^F)}{dz} = A_C \cdot r_{CO} - 2\pi \cdot R_i \cdot K_{CO} (p_{CO}^F - p_{CO}^P) \quad (13) - \text{Feed side}$$

$$\frac{d(n_{CO}^P)}{dz} = 2\pi \cdot R_i \cdot K_{CO} (p_{CO}^F - p_{CO}^P) \quad (14) - \text{Permeate side}$$

From (1) and (2) we obtain

$$\frac{d(n_{CO}^F + n_{CO}^P)}{dz} = A_C \cdot r_{CO} \quad (15)$$

Similarly, for component H₂O, CO₂ and H₂

$$\frac{d(n_{H_2O}^F + n_{H_2O}^P)}{dz} = A_C \cdot r_{H_2O} = A_C \cdot r_{CO} \quad (16)$$

$$\frac{d(n_{CO_2}^F + n_{CO_2}^P)}{dz} = A_C \cdot r_{CO_2} = -A_C \cdot r_{CO} \quad (17)$$

$$\frac{d(n_{H_2}^F + n_{H_2}^P)}{dz} = A_C \cdot r_{H_2} = -A_C \cdot r_{CO} \quad (18)$$

Add (3) and (5), we can get an equation with respect to C

$$r_{CO} + r_{CO_2} = A_C \cdot \frac{d(n_{CO}^F + n_{CO_2}^F + n_{CO}^P + n_{CO_2}^P)}{dz} = 0 \quad (19)$$

$$n_{CO}^F + n_{CO_2}^F + n_{CO}^P + n_{CO_2}^P = \text{const.} \quad (20)$$

Similarly, with respect to H

$$r_{H_2O} + r_{H_2} = 0 \quad (21)$$

$$n_{H_2O}^F + n_{H_2}^F + n_{H_2O}^P + n_{H_2}^P = \text{const.} \quad (22)$$

And O

$$r_{CO} + r_{H_2O} + 2r_{CO_2} = 0 \quad (23)$$

$$n_{CO}^F + n_{H_2O}^F + 2n_{CO_2}^F + n_{CO}^P + n_{H_2O}^P + 2n_{CO_2}^P = const. \quad (24)$$

Now, the following 5 graphs were obtained under the same condition described above at co-current flow system.

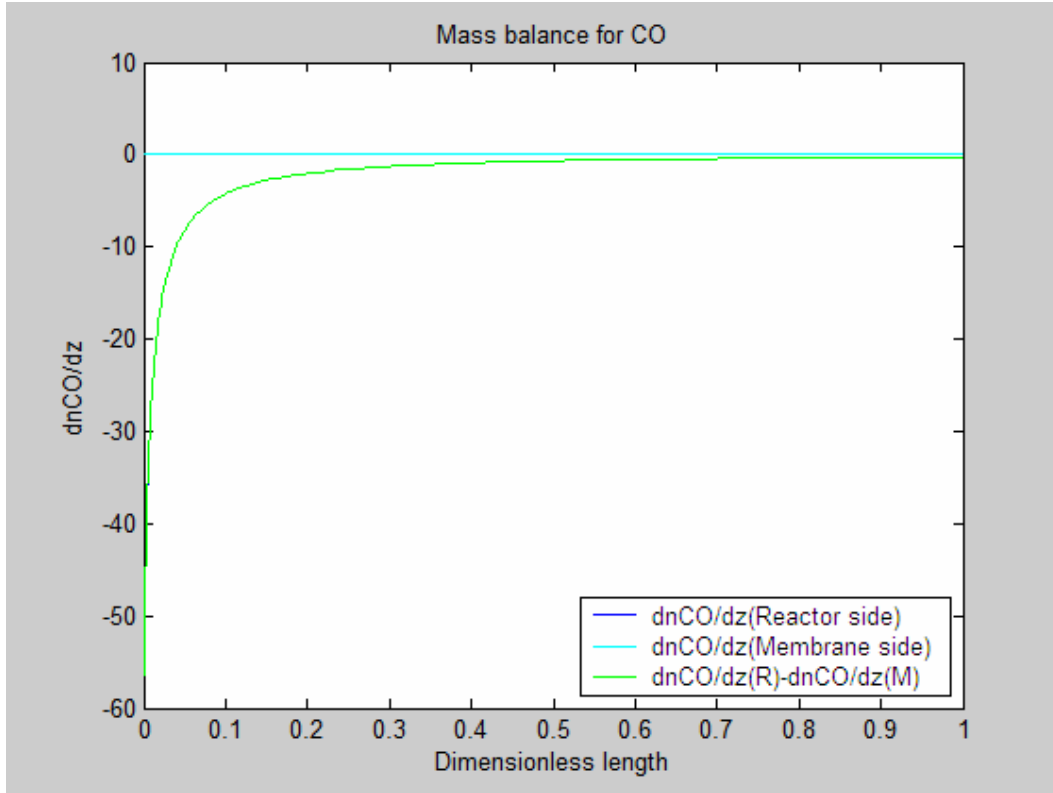


Figure 6 $\frac{dn_{CO}^F}{dz}$, $\frac{dn_{CO}^P}{dz}$, $\frac{dn_{CO}^F + dn_{CO}^P}{dz}$

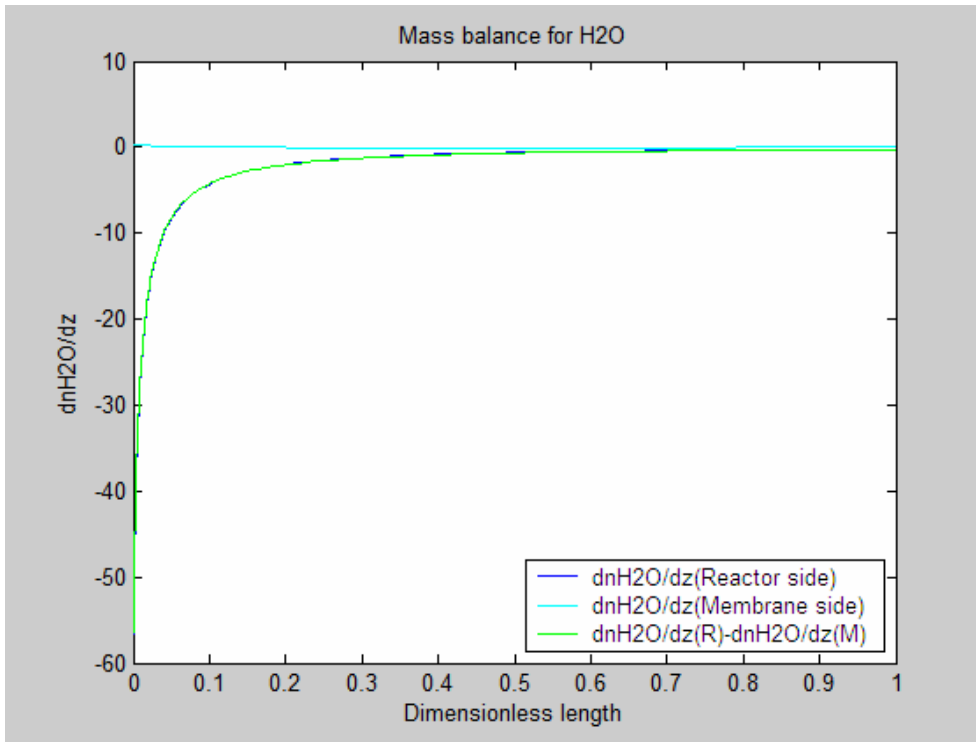


Figure 7 $\frac{dn_{H_2O}^F}{dz}$, $\frac{dn_{H_2O}^P}{dz}$, $\frac{dn_{H_2O}^F + dn_{H_2O}^P}{dz}$

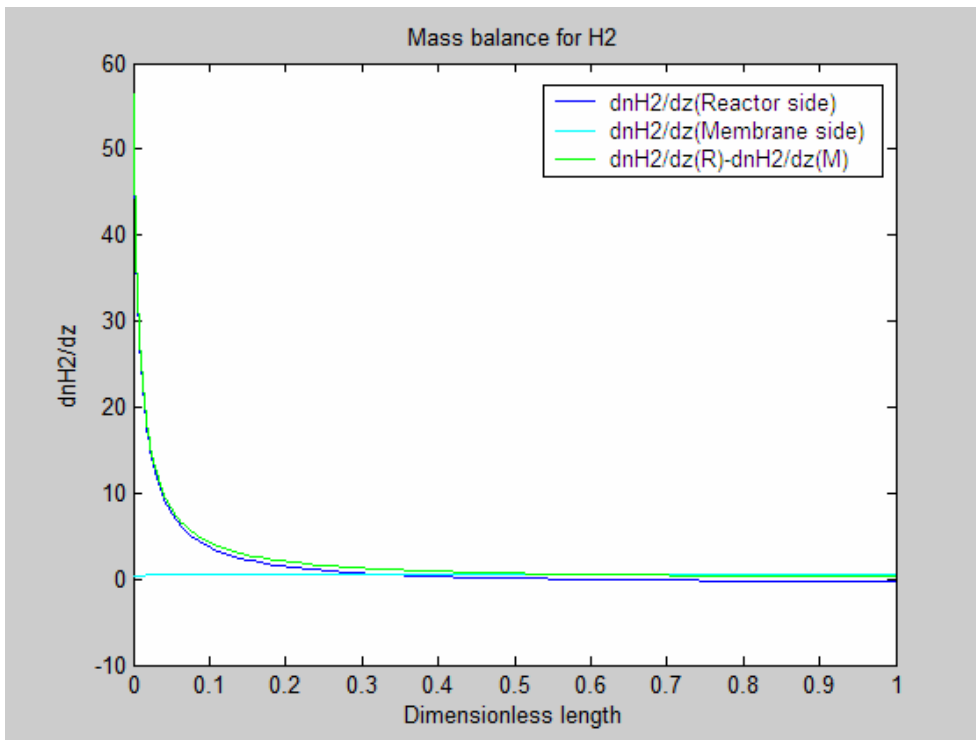


Figure 8 $\frac{dn_{H_2}^F}{dz}$, $\frac{dn_{H_2}^P}{dz}$, $\frac{dn_{H_2}^F + dn_{H_2}^P}{dz}$

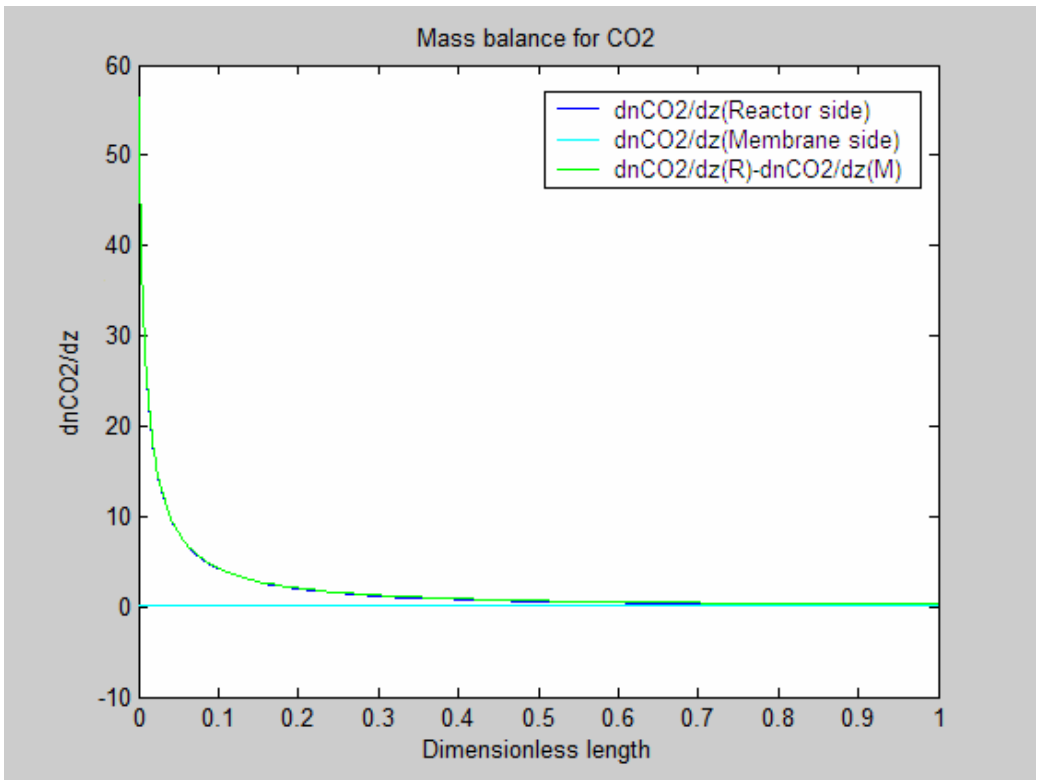


Figure 9 $\frac{dn_{CO_2}^F}{dz}$, $\frac{dn_{CO_2}^P}{dz}$, $\frac{dn_{CO_2}^F + dn_{CO_2}^P}{dz}$

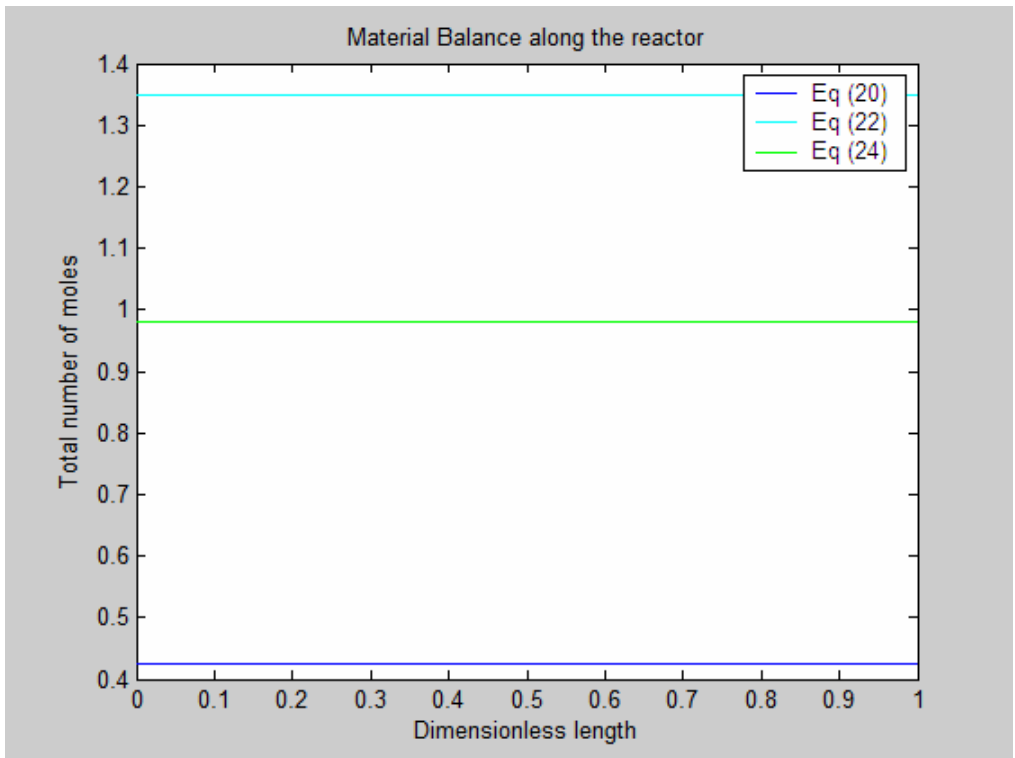


Figure 10 Eq. (20), (22) and (24)

